Norwegian University
of Life Sciences

Master's Thesis 2019 60 ECTS
Faculty of Science and Technology

Daily Temperature and Precipitation Variability in Scandinavia in a Large Ensemble Simulation

Nina Marianne Nyeng Waage
Environmental Physics and Renewable Energy

This thesis is dedicated to my sister.

Thank you for letting me wholeheartedly trust you.

Preface

Studying at the Norwegian University of Life Sciences has been a wonderful and enriching experience, which has made me grow both academically and personally. I am both sad and happy to say that this master thesis marks the end of my student era. The thesis is written for the Faculty of Science and Technology (REALTEK). The theme of the thesis is future changes to Scandinavian day-to-day variability in temperature and precipitation with global warming levels and the correlation to Arctic sea ice. I would like to humbly thank all my supervisors.

Bjørn Samset, thank you for being a role model and not being afraid to speak your mind in these critical times. Your enthusiasm for the climate is highly infectious and more people like you are truly needed. I am amazed by your unbelievably high capacity; both by how much knowledge you possess and how many activities you can fit inside your schedule.

Camilla Weum Stjern, thank you for all the fantastic feedback and help with coding. Thank you for showing me that being an adult does not necessarily mean putting away the pointless, yet joyful books and ideas. Thank you for showing me that growing up does not mean one has to fit inside a box, and even with a PhD, it is ok to be a kid a heart. You have made me hopeful for the future.

Arne Auen Grimenes, thank you for all our talks, both the easy as well as the deeper, life-altering ones. I am utterly impressed with how well you make people feel at ease. No wonder I am smiling every time I leave your office. Thank you for pushing me when I sorely needed it, as well as giving me the motivation to keep going. Thank you for believing in me, especially when I did not.

Last, but certainly not least, I want to thank my friends and family. You have been a crucial part of this process, and I thank you for giving me joy and laughter during stressful times. Linn, Guro and Sigrid, thank you for having the patience to read through my thesis.

Ås, 11. Desember 2019
Nina Marianne Nyeng Waage

Sammendrag

Ifølge den siste rapporten av IPCC, forventes det fremtidige endringer i både temperatur og nedbør på grunn av menneskeskapte, eller antropogene, klimaendringer. Det er også en høyere sannsynlighet for mer ekstremvær i form av tørke og mer intens nedbør. På grunn av mekanismer slik som Arktis amplifikasjon er regioner på høyere breddegrader, som Arktis og Skandinavia, spesielt sårbare. Her prosjekteres en økning av lufttemperaturer som er mye raskere enn resten av kloden. Hvis de antropogene endringene legges sammen med underliggende naturlig variabilitet kan sluttresultatet forsterkes eller reduseres kraftig. Forståelsen av hver enkelt komponent, hvordan de isolert påvirker vær og klima, i tillegg til den totale effekten er derfor kritisk. På grunn av individuelle interne prosesser, så vil det lokale daglige og sesongbaserte været ikke nødvendigvis gjenspeile de globale gjennomsnittlige verdiene. Disse lokale variasjonene kan dominere over store globale variasjoner og dermed skape kraftige anomalier som kan ha stor risiko.

Ved å benytte CESM1 Large Ensemble (30 medlemmer) og sannsynlighetstetthetsfunksjoner har denne studien analysert skandinavisk dag-til-dag variabilitet i temperatur og nedbør, hvordan den korrelerer med arktisk havis og hvordan variasjonen endres med økende globale temperaturer. Modellen ble kjørt for scenarier med historiske observasjoner og det såkalte scenariet RCP 8.5 for perioden 1920 til 2100. Vi har delt Skandinavia inn i tre regioner; nord, sentralt og sør. Ved økende global oppvarming fant vi et skifte mot høyere og mer ekstreme temperaturer i alle regioner. Spesielt Nord-Skandinavia anslås å oppleve en stor reduksjon i de kalde ytterpunktene. Vi fant mindre fremtidig temperaturvariabilitet i alle regioner med unntak av den sørskandinaviske sommeren som anslås å øke i variabilitet. Totalt sett ser vi en netto nedbørstigning og en større sannsynlighet for ekstrem nedbør i Skandinavia. Sør-Skandinavia er det eneste unntaket, med ingen endring i fremtidig nedbør i løpet av den boreale sommeren.

Vi fant ingen spesiell korrelasjon mellom variasjonen av havis på dag-til-dag variabiliteten i Skandinavia. En tydeligere korrelasjon kan ses mellom temperaturer i løpet av den skandinaviske vinteren (januar, februar og mars) og den følgende isutbredelsen i mars. Lave temperaturer gir økt havis og høyere temperaturer gir redusert havis. Videre har vi validert modellresultatet mot ERA5-reanalysen og funnet akseptabel overensstemmelse for den sentrale og sørlige regionen, men ikke like god for den nordlige regionen.

Abstract

According to the last assessment report from the Intergovernmental Panel on Climate Change, due to human-induced climate changes, alterations in future temperature and precipitation are expected, and we will have a higher likelihood of more extreme weather. As internal processes often dominate over global processes, the daily and seasonal weather on a local scale will not necessarily reflect the observed globally averaged changes. For example, regions in high latitudes such as the Arctic and Scandinavia are very vulnerable and experiences more rapid rises in surface air temperature due to processes such as Arctic amplification. Further, adding together anthropogenic changes with the underlying natural variability can amplify or reduce the total climatic impact. Understanding each component as well as how they influence weather and climate, is therefore of utmost importance.

By utilising the CESM1 Large Ensemble (30 ensemble members) and probability density functions, this thesis has analysed the Scandinavian day-to-day variability of temperature and precipitation, how it correlates to Arctic sea ice extent and how the variability changes with increasing global temperature. The model simulations were run with historical observations and the RCP 8.5 radiative forcing scenario, which corresponds to a high greenhouse gas emission pathway, for the period 1920 to 2100. We have separated Scandinavia into three regions; North, Central and South. With increasing global warming, we found a shift towards higher and more extreme temperatures in all regions. Northern Scandinavia, in particular, is projected to experience a substantial reduction in cold extremes. We also found less future temperature variability in all regions except for southern Scandinavian summer, which is projected to have an increase. Overall, we found a net precipitation rise and an escalation in the likelihood of extreme precipitation in Scandinavia, except for southern Scandinavia during the boreal summer, which have no change in future projection.

We found no particular correlation between sea ice variability in the day-to-day weather variability in Scandinavia. However, the Scandinavian winter (January, February and March) temperatures correlate with and influence the following March sea ice extent. Low temperatures give increased sea ice extent, and higher temperatures give reduced sea ice extent. Further, we validated the model result by using the ERA5 reanalysis and found an acceptable agreement for the central and southern region, but not as good for the northern region.

Contents

Abbreviations

Abbreviation	Meaning
AA	Arctic Amplification
AMOC	Atlantic Meridional Overturning Circulation
AO	Arctic Oscillation
CAM5	Community Atmosphere Model, version 5
CDS	Climate Data Store
CESM1	Community Earth System Model, version 1
CICE4	Community Ice CodE, version 4
CISM	Community Ice-Sheet Model
CMIP5	Coupled Model Intercomparison Project, version 5
CO_2	Carbon Dioxide
C2M	Community Land Model
ECMWF	European Centre for Medium-Range Weather Forecasts
ERA5	ECMWF ReAnalysis
GHG	Greenhouse gas
GMST	Global Mean Surface Temperature
IPCC	Intergovernmental Panel on Climate Change
LENS	Large Ensemble
NAC	North Atlantic Current
NAO	North Atlantic Oscillation
NOAA	National Oceanic and Atmospheric Administration
NwAC	Norwegian Atlantic Current
PDF	Probability Density Function
piControl	Preindustrial Control
POP2	Parallel Ocean Program, version 2
RCP	Representative Concentration Pathway
SAT	Surface Atmospheric Temperature
SLP	Sea Level Pressure
SST	Sea Surface Temperature

1 Introduction

The Earth's climate is continually changing due to natural processes and more recently, human influence. Climate is a result of a long-term average of the much more chaotic and instant daily weather. Both weather and climate are an outcome of a highly dynamic system which consists of a multitude of different components and processes, each affecting one another in complex ways. Changing one part will have consequences and repercussions throughout the system, and will leading to fluctuations between climate states. As shown in Figure 1.1, the climate on Earth evolves continuously in response to both external forcing and internal feedbacks. These changes are referred to as natural changes, such as the ocean circulations, atmospheric circulations, volcanoes and the solar cycle.

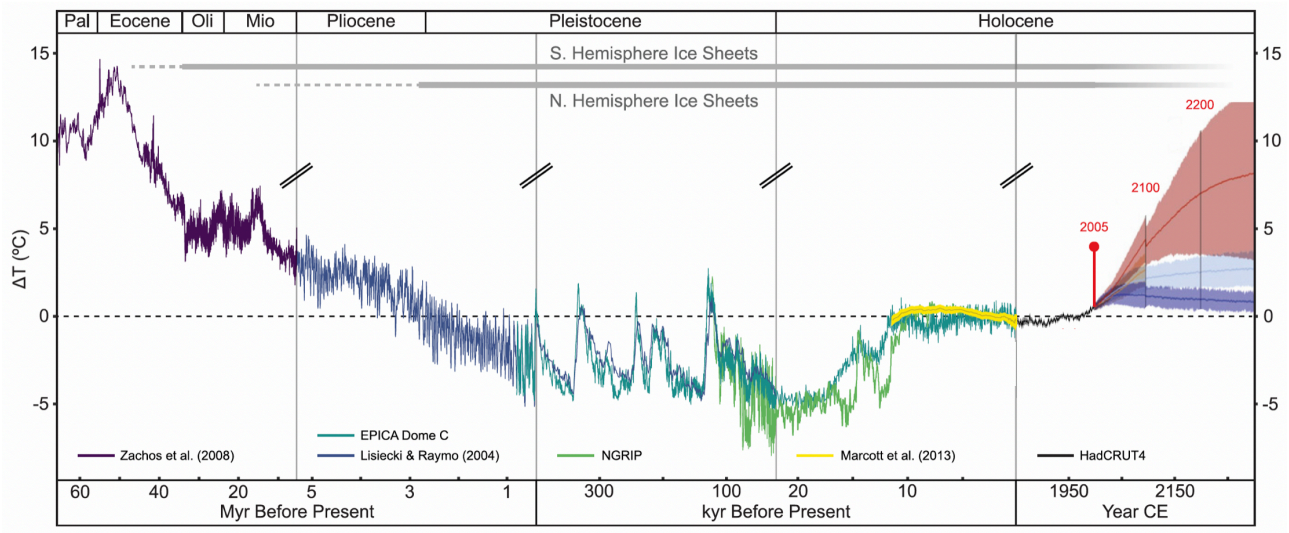

Figure 1.1 *The fluctuating temperature anomalies for the past 65 Million years, from the Paleocene to the recent and projected warming trend. Temperature anomalies are relative to the 1961–1990 global means and are composed from five proxy-based reconstructions, modern observations, as well as future temperature projections for four emissions pathways, with the Relative Concentration Pathway (RCP) 8.5 in red. From Burke et al. (2018).*

Since the early Eocene, about 60 million years ago, the global climate has cooled, and the amount of carbon dioxide (CO_2) in the atmosphere has declined (Burke et al., 2018). Furthermore, the last 10 000 years has been relatively stable, making it possible for humans to develop and flourish. However, both weather and climate are expected to undergo unprecedented rapid changes in the coming decades, and the scientific community is in agreement that the change is a consequence of

human-induced, or anthropogenic, climate change (IPCC, 2013). The fifth assessment report from the Intergovernmental Panel on Climate Change (IPCC) states that the current climate change is mainly because we have been, and still are, continuously emitting considerable amounts of greenhouse gases (GHGs) and aerosols into the atmosphere by burning fossil fuels. Consequently, the IPCCs further state that the future will present us with increased global atmospheric temperatures (Figure 1.2a) and altered precipitation patterns. These consequences are already apparent as we see extreme weather with increasing frequency and intensity in temperature and precipitation across the globe (Hansen et al., 2012; Mora et al., 2013).

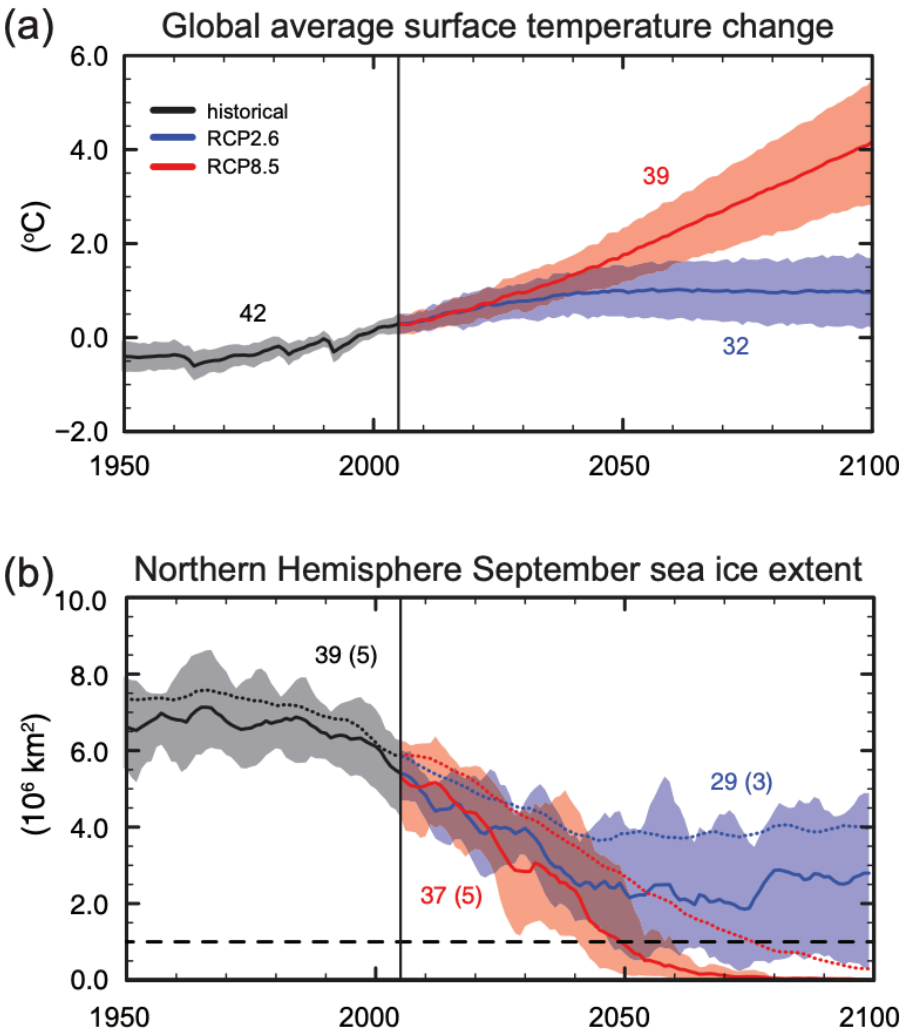

Figure 1.2 *Coupled Model Intercomparison Project, version 5 (CMIP5), multi-model simulated time series from 1950 to 2100 for (a) change in global annual mean surface temperature relative to the 1986–2005 mean, (b) Northern Hemisphere September sea ice extent (5-year running mean). For a selection of models, a time series of projections and a measure of uncertainty (shading) are shown for scenarios RCP2.6 (blue) and RCP8.5 (red). Black (grey shading) is the modelled historical evolution. For completeness, the full CMIP5 multi-model mean is also indicated with dotted lines. The dashed line represents nearly ice-free conditions. From IPCC (2013)*

Increasing temperatures will further lead to a significant reduction in sea ice extent in the northern hemisphere (Figure 1.2b). To what extent these changes will occur, highly depends upon which future path our society will follow: if we continue following a high emission pathway (RCP 8.5) or if we manage to level out our emissions (RCP 2.6). Keeping future temperatures as low as possible is crucial. Suarez-Gutierrez et al. (2018), for instance, shows that 10% of the most severe summer temperatures can be avoided by limiting future warming to 1.5 °C instead of 2 °C.

The impacts of climate change on a regional scale can be devastating, especially when a changed climate state combines with high amplitudes in the natural stochastic day-to-day variability. How much of these climate change means and extremes are causes of anthropogenic activity compared to changes in the internal variability is not clear (Wills et al., 2018). This predicament is due to local processes that might dominate global ones, giving rise to higher weather and climate variability. Also, the atmosphere is inherently chaotic, leading to a high degree of irreducible uncertainty in weather prediction and projection on local scales. Climate projections and simulations will therefore have a significant portion of uncertainty.

Hawkins & Sutton (2009) reported that, the sources of uncertainty in climate projections, on a global scale, are mainly due to emission scenarios and how the climate models are formulated. On the other hand, on a smaller scale, the internal variability contributes more (Fatichi et al., 2016; Giorgi, 2002). Hence, the local and smaller regions might show an entirely different picture and have statistical trends that differ from the global ones. It is therefore essential that we understand more of the underlying processes of internal variability and how they interact with one another.

Some areas will be more susceptible to a changing climate. This sensitivity includes regions further north like Scandinavia and the Arctic due to processes such as Arctic Amplification (AA), causing the surface air temperature to rise faster than the rest of the globe, as well as a retreating sea ice extent (Serreze & Barry, 2011; Stroeve et al.,, 2007). With areas like Scandinavia being more susceptible to future climate change, it is critical to examine how the day to day variability will be affected in order to prepare the society for future impacts and mitigation. To properly understand the Scandinavian variability, we must understand the individual processes which drive the local variability. These drivers can be processes such as the polar front jet, Arctic sea ice, volcanic eruptions North Atlantic and Arctic Oscillation (Hall et al., 2017; Vogel et al., 2018). It is essential to understand how they influence the day-to-day variability both jointly and individually.

The effects of increased temperatures on average climate quantities (Hartmann et al., 2013; Lewis & King, 2017) and, climate extremes are well studied (Betts et al., 2018; Lewis & King, 2017; Sillmann et al., 2017). Contrarily, more research is needed on changes to daily temperature and precipitation, and can be quantified using probability density functions, or PDFs. These contain information on the expected weather, which is impossible to gather from the means or extremes.

This thesis aims to expand our understanding of the day-to-day variability in Scandinavia, its stochastic nature, and how it evolves with global mean surface temperature. We will also analyse how it relates to the amount of Arctic sea ice, one of the many factors potentially influencing the Scandinavian variability. We separate Scandinavia into three regions, north, central and south, and by utilising the methods presented in Samset et al. (2019), we will examine PDFs to analyse the regional differences in daily temperature and precipitation variability. This will further be explored by using a 30-member large ensemble of climate simulations with historical and RCP 8.5 emission scenario for the period 1920-2100 conducted with the Community Earth System Model Version 1 (CESM1; Hurrell et al., 2013).

Each of the ensemble members is subjected to the same emission trajectory but begins from slightly different climatic states in 1920 so that the resulting spread of members will mimic intrinsic variability (Deser et al., 2014; Kay et al., 2015). To see this in relation to other changes, we document the evolution of the PDFs with global surface temperature. Further, we analyse the correlation between high and low Arctic sea ice extent to the day-to-day variability. To see the differences between a fully coupled model and model with fixed sea surface temperature (SST), we also made a comparison of PDFs from the two simulations. Lastly, to validate the model results, we used the latest climate reanalysis dataset from the European Centre for Medium-Range Weather Forecasts, ERA5, which covers a period from 1950 to the present.

Our results show a clear shift towards warmer climate states with increasing global surface temperatures. The winter season has the most distinct results, and we see differences between regions in Scandinavia (Figure 1.3), with the northern area standing out with a narrowing and considerable reduction in cold extremes. The southern region also stands out with an increase in temperature variability during summer. For precipitation, we find a general increase in extreme events.

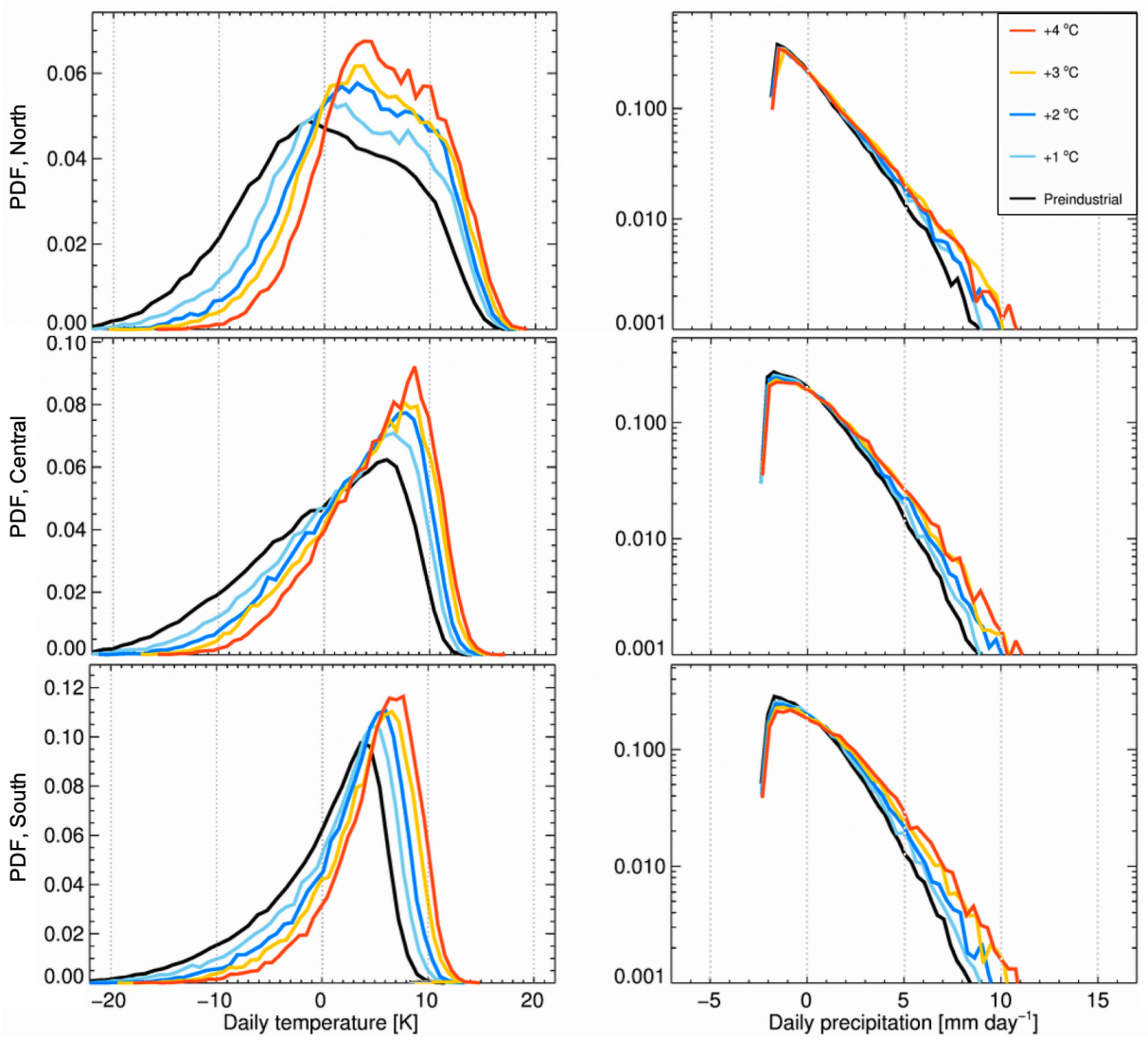

Figure 1.3 *PDFs of daily variability in temperature (left) and precipitation (right) for boreal winter (DJF). We have PDFs for the five different climate states; Preindustrial (Black) and the four global surface temperatures +1 °C, +2 °C, +3 °C and +4 °C, in light blue, blue, yellow and orange respectively. From the top, we have the regions; northern (top, central (centre), and southern Scandinavia (bottom). All numbers are relative to the winter mean at preindustrial conditions.*

In the next chapter, we will present selected theory and some general background of the climate system, the regions Arctic and Scandinavia, as well as the processes influencing it. In chapter 3, we will go through our methods and data used in the analysis. We show our results in chapter 4 and discuss our findings with relevant studies in chapter 5. Then, in chapter 6, we conclude and end with possibilities of further studies in chapter 7.

2 Background

The Scandinavian region is of particular interest to us living here. However, previous research has shown that the region has unusually high variability, which is vital to study closer in order to better understand the range of changes we could experience in the future. Scandinavia is a region in Northern Europe and consists of the countries; Norway, Sweden, Finland and Denmark. In this thesis, we want to look at day-to-day regional variability and have therefore divided Scandinavia into three sub-regions; North, South and Central, which is shown in Figure 2.1a. The Arctic is one of the leading influencers of the day-to-day variability in Scandinavia. Therefore, we also look study the Arctic and the processes affecting this region. The Arctic is commonly defined as the region within the Arctic Circle, located poleward of 66.5°N. The Arctic consists of the Arctic Ocean as well as the surrounding areas of land and seas. Everything that transpires in the Arctic has a strong impact upon the adjacent regions, such as Scandinavia, which is partly located within the Arctic circle. In this section, we will discuss different aspects of the climate system and the processes behind Scandinavian and Arctic climate.

2.1 The climate system

Within the climate system, we have five different spheres; the atmosphere, hydrosphere, geosphere, biosphere and the cryosphere (Lutgens & Tarbuck, 2016). These spheres have a complex network with constant interactions and exchanges of energy and moisture. In this section we will go through different processes in the climate system, climate change and timescales.

2.1.1 The Greenhouse effect and global circulation

Most of the energy received at the surface of the Earth, originates from the Sun. The Solar shortwave radiation is partly reflected into space or absorbed by the surface of the Earth and the atmosphere. From absorption, the atmosphere and surface heats up and emit longwave radiation back to space. However, certain gases in the atmosphere, called greenhouse gases, trap some of the outgoing longwave radiation and re-emit it back to the surface of the Earth, heating it further. This warming is called the greenhouse effect and makes our planet habitable. The balance between incoming shortwave and outgoing longwave radiation decides what kind of climate state we are in, and this state can shift continuously.

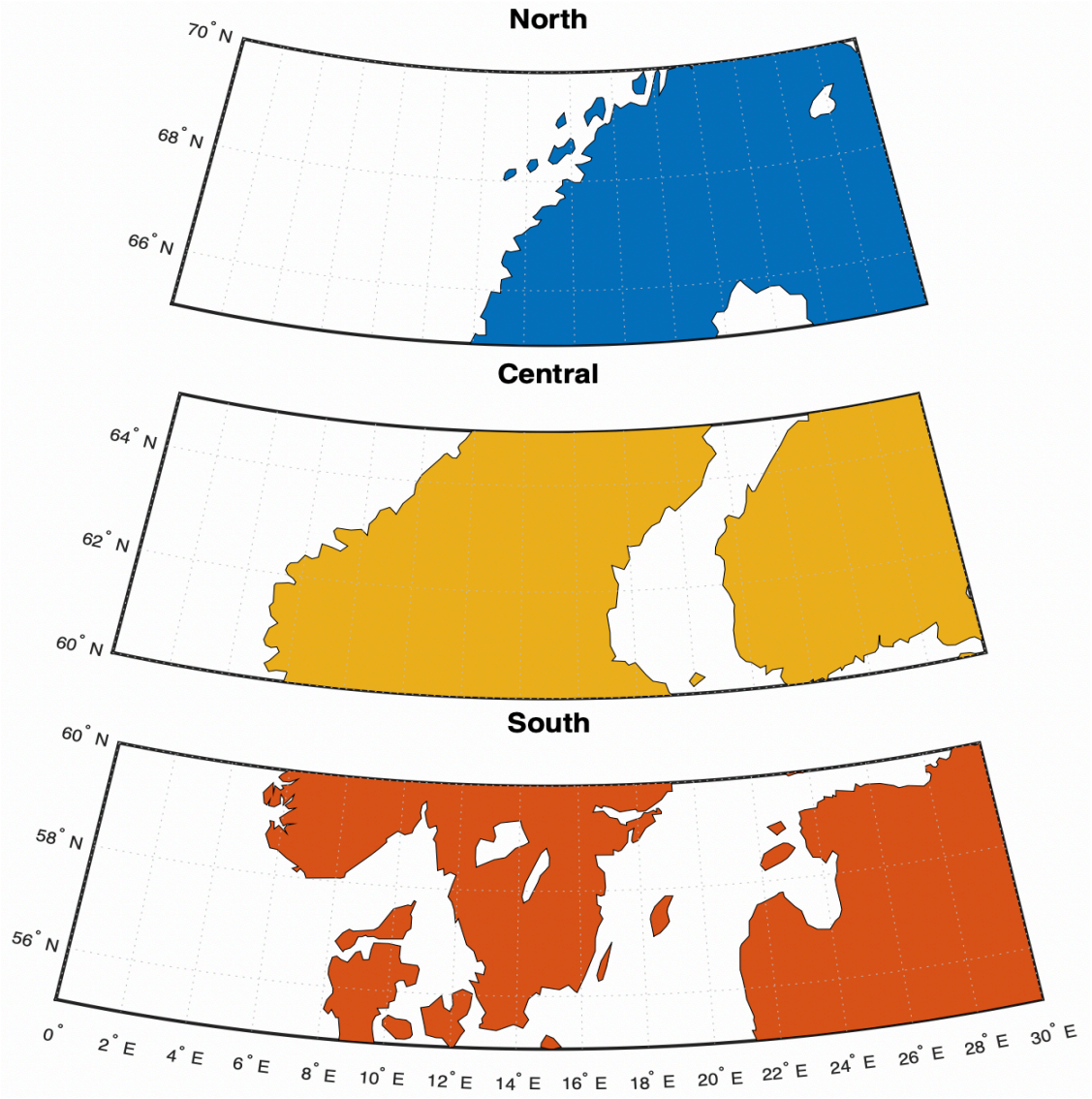

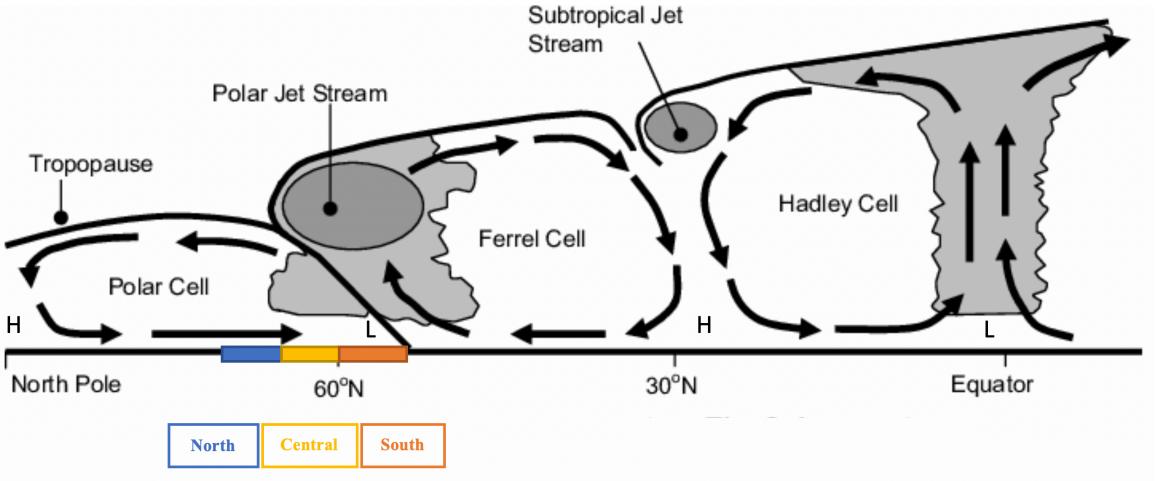

Figure 2.1 *(a) The Scandinavian region divided into three different sub-regions; North (65-70 °N), Central (60-65 °N) and South (55-60 °N). All the regions cover the same longitudes (0-30 °E). (b) The three atmospheric circulation cells; The Hadley cell, Ferrel cell and Polar cell. The Scandinavian regions are shown with colour bars.*

Because of the movements and shape of the Earth, incoming radiation is not equally distributed on the surface of the planet, which creates an energy imbalance. Firstly, Earth's rotation around its own axis causes the cycle of day and night. The tilt of the axis is what creates seasons by parts of the planet being more exposed during certain times of the years, with the highest latitudes receiving 24 hours of total darkness during winter and 24 hours with sun during summer. Lastly, since our planet is a sphere, the radiation will reach the surface at different angles, with equator receiving more concentrated and intense radiation than the poles.

All of these dynamical processes combined create a global energy imbalance, whereby the tropics experiencing an energy surplus, and the poles an energy deficit. To smooth out the temperature imbalance, energy gets transported from the tropics to the poles, in the form of winds and ocean currents. However, because of Earth's rotation, this transport of energy does not move in a straight line and is separated into three primary cells; the Hadley cell, the Ferrel cell and the Polar cell (Figure 2.1b). At the equator, warm air rise, release its moisture and cools when it moves poleward (Lutgens & Tarbuck, 2016). As the flow moves further away from the equator, it will get increasingly influenced by the Coriolis force and thus get deflected towards the right and subside back towards the surface around 20-35°N latitude. This air is relatively dry, and explaining why many of the world's deserts lie in this zone.

The subsiding air then part into one poleward branch and one equatorial branch. The poleward flow is what we call westerlies because they move from the west to the east. Lastly, we have the polar cell. Over the poles, we have a cooling of the air which subsides and moves equatorward at the surface. Eventually, the cold polar air meets the warmer air in the Ferrel cell, creating the polar front. The air then gets pushed upwards and releases moisture as it rises. The exact location of the polar front is a significant contributor to the climate in Scandinavia. When these large circulation systems combine with more regional differences in topography and surface characteristics, the result is what we can feel as the weather.

2.1.2 Climate Change

Weather is a description of current atmospheric conditions at a particular place and time, such as temperature, wind speed, cloud cover and rainfall. Climate, on the other hand, is defined as the weather over time, or the average weather (Cubasch et al., 2013). It is the statistical mean and variability of climate parameters, such as temperature and precipitation. However, these parameters do not stay constant, and several mechanisms may interact with shifting them in new directions and leading to a change in the climate. Climate change refers to changes in the mean and variability of climate parameters and when the current climate shifts from one state to another. Changes in both the internal variability and external forcing can generate such a perturbation of the climate system, and the phrase "climate change" is used both if the change has a natural or human origin (Cubasch et al., 2013). Note that climate change is not equal to global warming.

The climate has been changing throughout the Earth's history. However, anthropogenic climate change is what we experience as the present rise in temperature, change in precipitation, reduction of sea ice, rising sea level and generally more extreme weather. These changes are according to the IPCC fifth assessment report, mainly due to anthropogenic emissions of GHGs and aerosols into the atmosphere (IPCC, 2013). Emissions of GHGs have happened since the industrial revolution and is at present-day continuously increasing, resulting in increasing temperatures in the atmosphere and the oceans. Consequently, higher temperatures result in reductions in ice masses on land and the Arctic sea, confirmed by both satellite observations and in situ measurements (Cubasch et al., 2013).

2.1.3 Timescales within the climate system

The many processes in the climate system have processes which go over different temporal and spatial scales. For temporal scales of only seconds to a couple of minutes, there are processes like local turbulence, which transports momentum, heat and moisture throughout the atmosphere and oceans (Williams et al., 2017). The development of weather systems including cyclones and anticyclones (Lutgens & Tarbuck, 2016), as well as gravity waves (Williams et al., 2017), occur over timescales on the order of hours to days. Cyclones and anticyclones are high- and low-pressure systems, respectively. They are usually connected with dry weather in the case of cyclones and wet

in the case of anticyclones (Lutgens & Tarbuck, 2016). Gravity waves are big systems usually connected with dry weather conditions, and anticyclones are low-pressure systems usually associated with more precipitation. We even have processes that can last several decades like the North Atlantic and Arctic Oscillations, which we will explain in more detail later on. Representing these different timescales in global climate models is harder for a shorter time, and spatial scales since the mathematical formulations and parametrisations need to be accurate. In this thesis, we analyse how the day-to-day variability is influenced by processes, which cover a vast range of different timescales.

2.1.4 Internal variability and external forcing

The climate system has since the beginning of Earth's history varied on all timescales, under the influence of both forced and unforced processes. These two processes intertwine and drive forward the constant changes that occur over both long and short periods. Forced processes are variations caused by factors external to the climate system. They include both natural phenomena and anthropogenic influence, such as variations in the sun's output, volcanic eruptions, Earth's orbit and changes in the atmospheric composition. Internal or natural variability, on the other hand, refers to unforced variations in one or more climate parameters like temperature and precipitation, which are a result of fluctuations generated from atmospheric, oceanic, land and cryospheric processes as well as their interactions with one another.

The relationship between variability, forcing and response is dynamic. In some cases, the relationship might be straightforward and linear, but in other cases, very complicated (IPCC, 2013). Internal variability has a significant influence on climate modelling and projections of the future (Deser et al., 2014), but quantifying the nature of the internal variability is exceptionally challenging and is characterized by considerable uncertainty. Quantifying the uncertainty is especially challenging in the near-term future, as internal variability has a stronger influence on uncertainty on regional scales than it does globally (Cubasch et al., 2013; Hawkins, & Sutton, 2009; Xie et al., 2015). The internal variability is ingrained within the Earth system, and no matter the level of knowledge, we will not be able to eliminate the uncertainty (Cubasch et al., 2013).

2.1.5 Day-to-day variability

Day-to-day variability is what we experience as variations in our daily weather. Weather is influenced by both internal and external forces, local processes such as topography, and their interactions with each other. Thus, day-to-day variability is chaotic, and hence challenging to predict. The day-to-day variability, as well as the underlying processes, are therefore unique to every region and according to Coumou et al. (2018), the variability in Scandinavia is extraordinarily high, making it a difficult region to solve.

2.2 Processes Influencing Scandinavia and The Arctic

The day-to-day variability in Scandinavia is profoundly affected by both large weather systems covering the entire northern hemisphere or the globe, as well as small more local weather phenomena covering only a couple of kilometres. In this chapter, we will describe each of these processes in further detail. If not otherwise stated, most of this chapter is based on the study published by Hanssen-Bauer et al. (2009).

2.2.1 Pressure systems and global circulation

The large-scale circulation in the atmosphere is driven by a temperature difference between the Equator and the poles. The Equator receives more incoming solar radiation and has net warming, while the poles have more outgoing radiation than incoming solar leading to net cooling. This temperature gradient is offset by heat transport from the Equator to the poles in both atmosphere and ocean. This transport is not a straight line, but is influenced by topography, the rotation of the Earth and local pressure systems. The pressure systems can be divided into low and high pressure. When the air warms up it becomes lighter and rises, causing low pressure. When the air cools down, it becomes denser and sinks, producing high pressure at the surface. The movement of air from high pressure towards low pressure produces winds. Also, the strength and location of pressure systems are controlling for local weather and climate.

2.2.2 Polar Vortex

Due to Earth's tilt, the northern regions experiences both 24 hours with total darkness and 24 hours with constant light, called the "midnight sun". Total darkness occurs during the winter when the north pole is tilted away from the Sun, and as winter advances the Arctic continuously loses heat, making the area extremely cold. When the layers of air lose its heat, it compresses and sinks, making a strong low-pressure system which can eventually develop into large anticyclones over the Arctic. This system is what is called the polar vortex. The gradual subsidence within these pressure systems generates stable conditions and clear skies. The Arctic receives a minimal amount of precipitation during the year and is considered a "polar desert". This is because the air is cold and dry, making it very rare for water to condensate and gather into droplets (Lutgens & Tarbuck, 2016).

2.2.3 Westerlies

The winds in the atmosphere transfer energy, momentum and moisture. As previously mentioned, on a global scale this transfer moves from the equator to the Arctic, and then bend, due to the Coriolis force winds, creating zonal wind patterns in some areas (Lutgens & Tarbuck, 2016). In the mid-latitudes, we have a wind belt termed the westerlies, which comes from the west and moves east (Aguado & Burt, 2013).

2.2.4 Polar Jet Stream and Rossby waves

At the separation between the polar cold air and the warmer southern air, we have the polar front. The polar front is where the westerlies have a narrow band with high wind-speed called the polar jet stream, illustrated in Figure 2.2. During winter, when the temperature gradient between the two air masses is highest, the Polar jet reaches its maximum wind-speeds. Depending on the strength, the Polar jet usually follows a wavy path around the globe with long wavelengths called Rossby waves (Figure 2.3), usually consisting of four to six slow-moving waves, or meanders (Lutgens & Tarbuck, 2016). It is usually located at 9 to 12 km above sea level, and the wind speeds reaches an average of about 180 km/hr during the winter and 90 km/hr during the summer (Aguado & Burt, 2013). The jet streams latitudinal position is also dependent on the season and moves north during winter and south during summer.

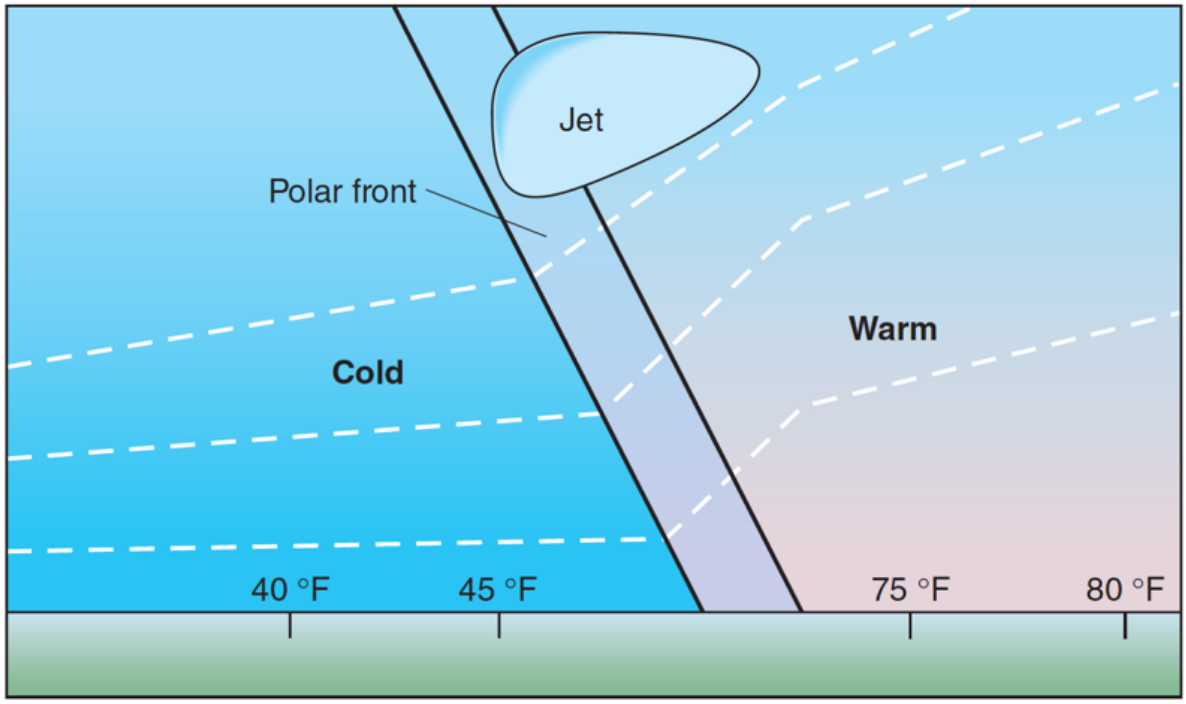

Figure 2.2 *The Polar front separates cold polar air masses from the warmer tropic air masses. The polar jet stream is situated above the polar front near the tropopause. From Aguado & Burt (2013).*

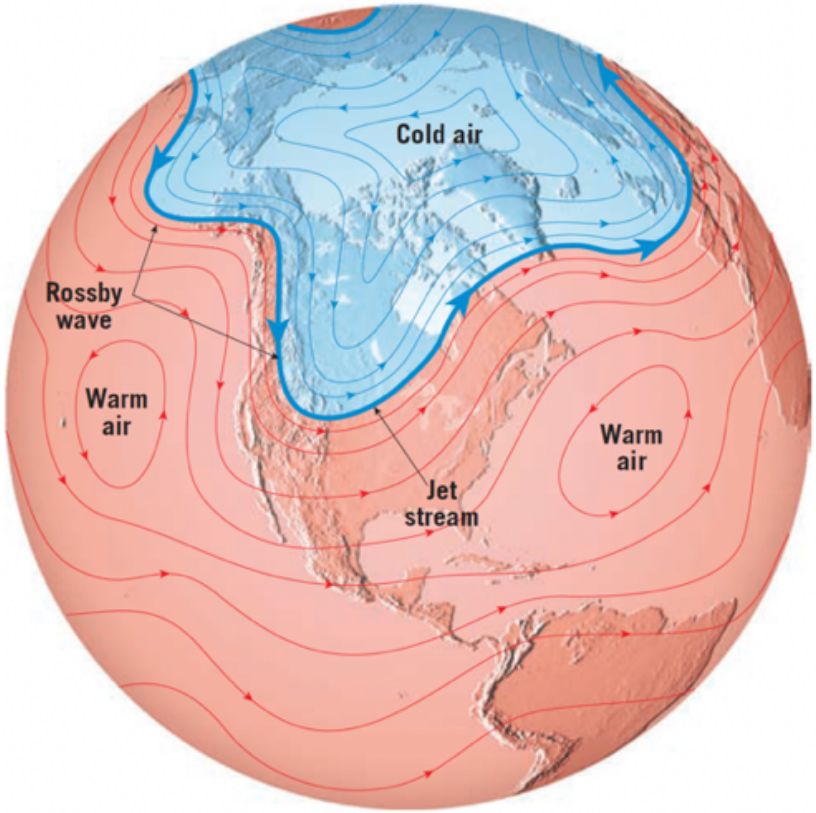

Figure 2.3 *The Polar Front jet stream in and Rossby waves (blue line), which separates the polar cold air from the warmer tropic air. From Lutgens & Tarbuck (2016).*

During winter, the jet stream moves north due to the Rossby waves tend to be fewer, have a longer wavelength and stronger winds (Aguado & Burt, 2013). Consequently, providing more humid and wet weather in the mid-latitudes. In contrast, during summer, the jet stream moves south due to more Rossby weaves, weaker winds and shorter wavelengths, which results in more dry and cold weather. Sometimes the wave can even break off and produce a burst of cold air, causing a weaker temperature gradient due to the redistribution of energy. The Rossby waves can, therefore, have a tremendous impact on the day-to-day variability in the mid-latitudes, especially when the waves have significant amplitudes.

2.2.5 Midlatitude cyclones

Midlatitude cyclones are one of the leading causes of high-frequency variability in the midlatitudes. This relationship is due to the cyclones having large interannual variability (Raible & Blender, 2004). The cyclones are storm systems that are a crucial element for the continental climate in the midlatitudes, and they are responsible for a high percentage of the annual precipitation (Lutgens & Tarbuck, 2016). Consequently, midlatitude cyclones key elements in studying the day-to-day variability in Scandinavia.

Most of the cyclones influencing northern Europe, develop in the western ocean basins and move northeast across the North Atlantic (Raible & Blender, 2004). They form in an area of low pressure where the winds flow inwards and up in a counterclockwise motion in the Northern Hemisphere. The cyclones can bring stormy weather and continuous precipitation over a large area, lasting for several days or even weeks, and the systems usually bring abrupt changes in wind, temperature and precipitation. Midlatitude cyclones are connected to the polar front and polar jet stream and follow the same seasonal paths (Aguado & Burt, 2013). Therefore, the position of the jet stream and polar front decide the location of these storm tracks, farther north during the summer months and south during the winter. The cyclones usually occur during the winter season when there is a higher temperature difference between the tropics and the North Pole, resulting in stormier weather during these periods.

2.2.6 Atlantic Ocean Circulation

The main features of the ocean climate in the North Atlantic and the Nordic seas, constitute the circulation called the Atlantic Meridional Overturning Circulation (AMOC). This circulation transports a significant amount of heat from the tropics to the North Atlantic with its adjacent regions. The NAC has a poleward extension, the Norwegian Atlantic Current (NwAC), which transports heat up to Scandinavia. AMOC is the Atlantic part of a much bigger circulation system called the thermohaline circulation, which is a global-scale circulation. Density differences drive the circulation due to changes in temperature and salt concentration, generating an overturning in the water (IPCC, 2001). Warm and salty water masses are transported northwards near the surface; it is then cooled and sinks as it is transported back south (Hanssen-Bauer et al., 2009). This circulation will have fluctuations and is sensitive to changes in parameters such as precipitation, evaporation, continental run-off and sea ice concentration.

2.3 Modes of variability

Modes of Variability are specific patterns in the climate system with identifiable characteristics, typically with oscillatory behaviour. The patterns usually switch between phases, giving different regional and sometimes global effects on climate parameters, such as wind speed, precipitation, temperature and surface pressure. Modes of variability are increasingly identified as fundamental influencers on interannual and longer-term variability (IPCC, 2001). However, they also affect the day-to-day variability, especially if oscillations within modes overlap in a way that amplifies certain weather phenomena. In this thesis, we will focus our attention on the modes which exist and influences the day-to-day variability in northern hemispheric high latitudes. Some essential modes of variability in the northern hemisphere are the North Atlantic Oscillation (NAO) and the Arctic Oscillation (AO).

2.3.1 The North Atlantic Oscillation

The NAO is the dominant mode of atmospheric circulation variability in the region around the North Atlantic Ocean (Deser et al., 2017). The NAO is usually used as a way of predicting future long-term weather patterns. As illustrated in figure 2.4, the NAO affects the pressure strengths of the surface Icelandic low pressure and the Azores high pressure. The pressure gradient between these two regions will influence the strength of the westerlies coming in from the Atlantic Ocean

(Årthun et al., 2017). The NAO has, therefore, a particularly significant influence on the variability in the wind, precipitation and temperature patterns, especially during winter in Europe (Casanueva et al., 2014).

The fluctuations in the NAO index have a range of timescales ranging from intra-seasonal to multi-decadal but are usually measured in days. The measurements are made by taking the difference in pressure between the Icelandic low and Azores high. When the pressure gradient is large, we have a positive phase, and when the gradient is low, we have a negative phase (Williams et al., 2017). As seen in Figure 2.4, the positive phase is associated with stronger westerlies and more wet, mild and stormy weather in northern Europe. For the negative phase, the westerlies will be reduced in strength and northern Europe will experience drier and colder conditions. Under anthropogenic forcing, the NAO might have a shift towards the positive phase, and a displacement in the different centres-of action towards the end of 2100 (Deser et al., 2017).

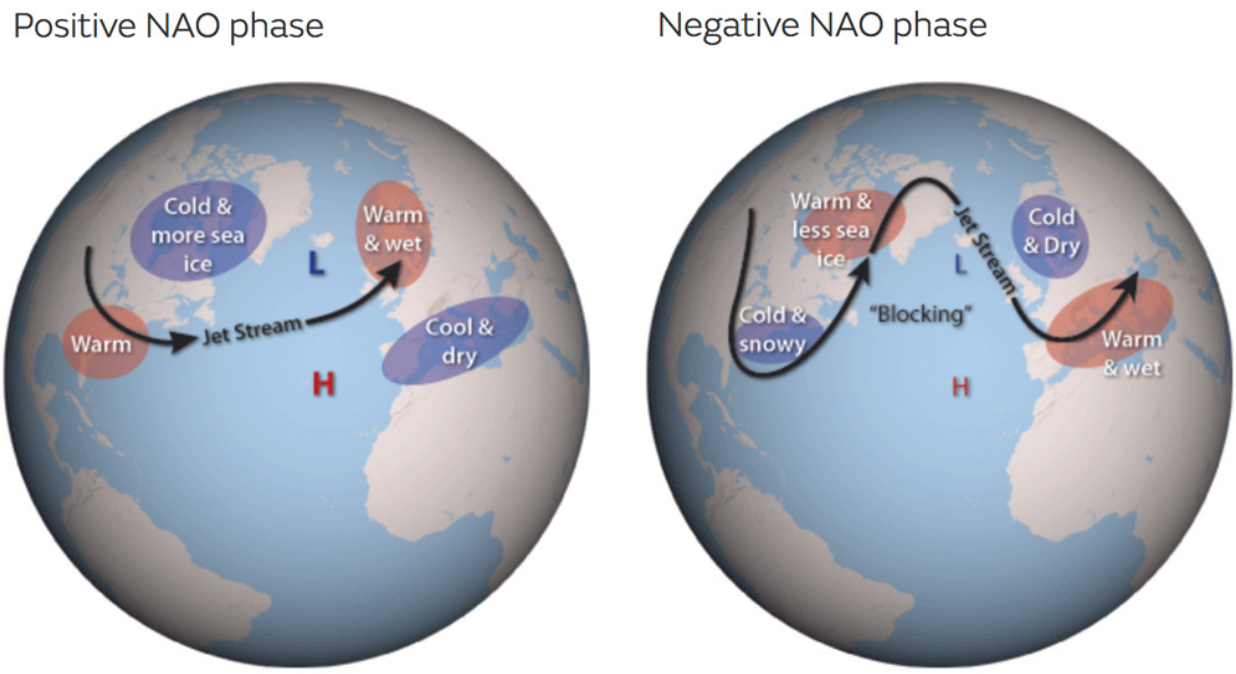

Figure 2.4 *Overview over the North Atlantic Oscillation for both the positive (left) and negative (right) phase. The positive phase is characterised by stronger pressure systems, stronger westerly winds, less Rossby waves and warm and wet weather in Northern Europe. The negative phase has weaker pressure systems, weaker westerlies, more Rossby waves and cold and dry conditions in Northern Europe. From NOAA*

2.3.2 The Arctic Oscillation

The AO, also called the Northern Annular Mode, is a large-scale pattern of climate variability which exchanges atmospheric mass between the Arctic region and the mid-latitudes in the Northern Hemisphere. The AO, like the NAO, consists of two phases (Figure 2.5), whereby it can stay within one of them for days or even months. In the positive phase (left), the polar vortex over the Arctic is stronger, creating stronger westerly winds in the subpolar latitudes (Rigor et al., 2002). The strong polar vortex holds the cold air in the Arctic and brings warm and wet weather to the mid-latitudes and Europe. When we have a negative phase, the pressure system is weaker than usual in the Arctic. This phase generates a weaker polar vortex and weaker westerlies. As a result, cold, Arctic air pushes its way farther south, creating cold weather and winter storms in Europe.

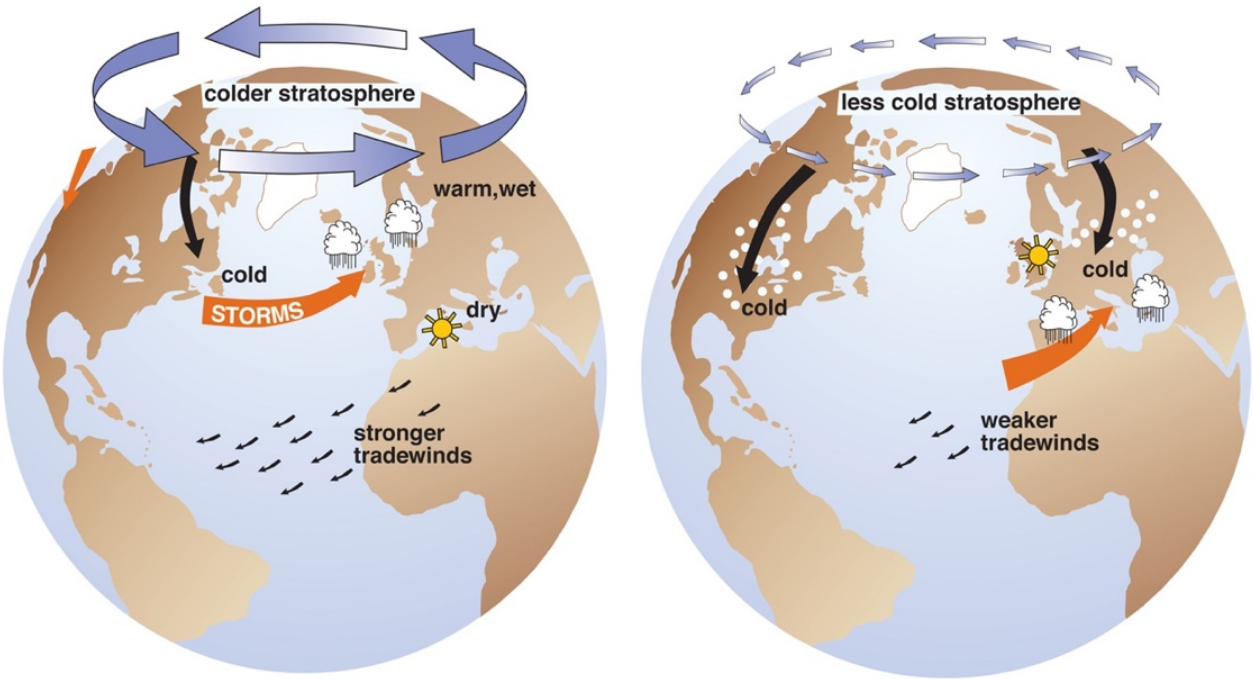

Figure 2.5 *Effects of the positive (left) and the negative (right) phase of the Arctic Oscillation. The positive phase gives stronger polar vortex, stronger westerlies and more warm and wet weather in Scandinavia. The negative phase gives weaker polar vortex, weaker westerlies and cold and dry weather in Scandinavia. From* NSIDC

2.3.3 Teleconnections

Teleconnections are a fundamental part of the climate system and consist of links across the globe, between non-bordering geographical regions. They are atmospheric variability patterns over large spatial scales and timescales of months to years (Hulley & Ghent, 2019). These patterns can be connected to Rossby waves and nonlinear zonal interactions, and the teleconnections are especially strong during the boreal winter season. One such Teleconnection is the Arctic response to changes in Asian emissions of aerosols during the boreal winter (Wilcox et al., 2019). Aerosol emission increases lead to abnormal northeasterly flow over Scandinavia and anticyclonic circulation over North Atlantic, which drives cold air into the region and drying over western Europe. If anthropogenic aerosol emissions were to be strongly reduced, this might lead to a further half of degree increase in temperatures in addition to that caused by greenhouse gas emissions. Wilcox et al. (2019) also argue that Europe and the Arctic might be particularly sensitive to such an aerosol reduction.

2.4 Climate in Scandinavia

Since Scandinavia is located at a high latitude, the region experiences a net loss of radiation to space. However, due to large scale circulations, both in the atmosphere and ocean, the area receives energy from other parts of the globe. Furthermore, there are significant annual differences in the amount of received solar energy throughout the year. The differences are most substantial in northern Norway and the Arctic, with midnight sun during summer and complete darkness during winter.

The Scandinavian climate is strongly influenced by atmospheric and ocean circulations, as well as modes of variability like the NAO and AMO. The region lies in a zone where the westerlies are dominating the wind conditions (Figure 2.6b). The sea level pressure fields (SLP), and the processes they affect, regulates the westerlies and thus a large portion of the temperature and precipitation in Scandinavia on monthly to decadal timescales (Hanssen-Bauer et al., 2005). These pressure fields guide and decide the strength and direction of the winds, which passes over the region. For example, during situations with high NAO index, when there is a significant pressure difference between the Icelandic low and the Azores high, Scandinavia can experience stronger westerlies, mild and humid air and more intense and frequent storms.

Moreover, the Scandinavian climate is also influenced by surrounding masses of water such as the Atlantic Ocean, and the Norwegian Sea. As can be seen in Figure 2.6a, the North Atlantic Current (NAC) with its poleward extension, the Norwegian Atlantic Current (NwAC), brings heat from the equator up to higher latitudes. This heat source and the nutrients that the current brings are necessary for the marine ecosystems in the Norwegian Sea and the Barents Sea. The heat from the current is a critical element in making the Scandinavian region milder than other areas at the same latitude, and it makes the entire coast ice-free (Aguado & Burt, 2013). The winter temperatures can be up to 10 to 20 degrees higher than the average temperature at other areas in the same latitude.

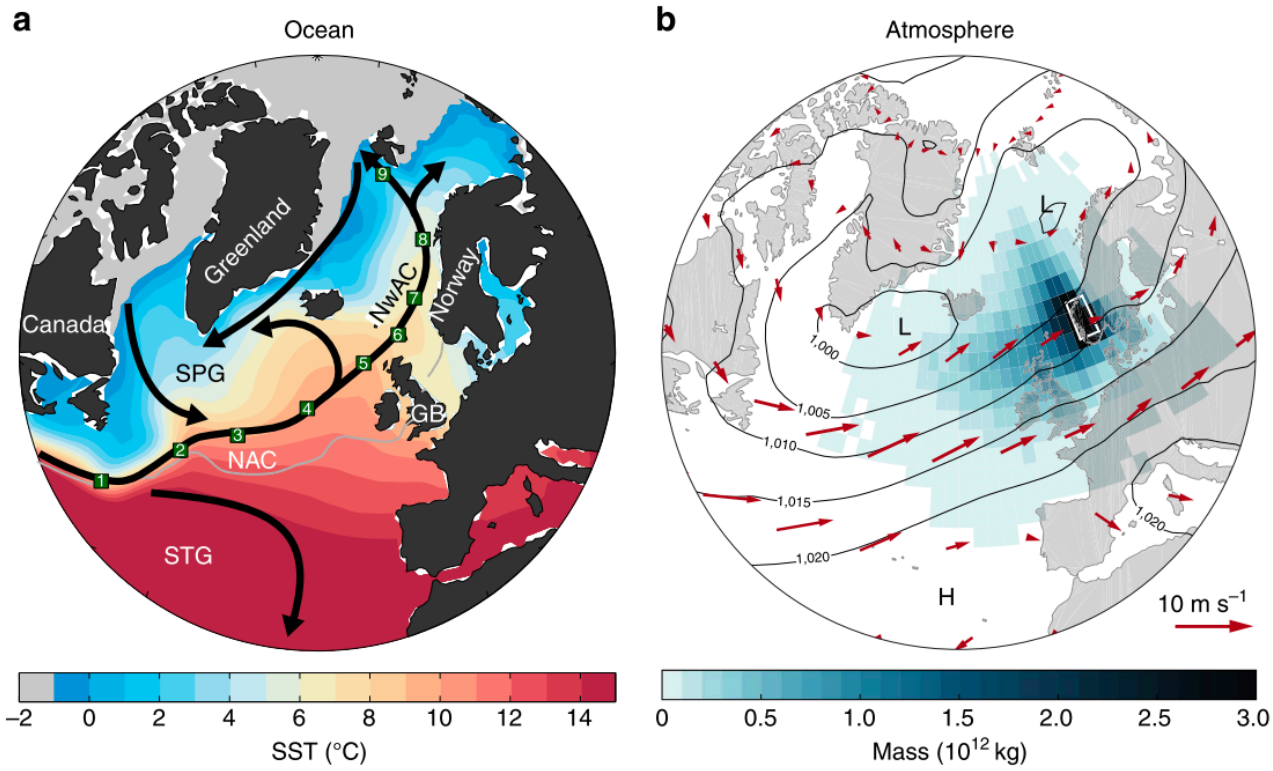

Figure 2.6 *Ocean and atmosphere circulation in the North Atlantic region. (a) Sea surface temperatures (SST) in colours and the major ocean currents in black arrows, such as the North Atlantic Current (NAC) and the poleward extention, Norwegian Atlantic Current (NwAC). (b) Mean winds at 925 hPa (arrows) and sea level pressure (black contours) between 1998–2008 from the model Era-Interim70. H/L indicates the centers of the high and low pressure systems. In blue shading we have the distribution of air in the planetary boundary layer. From Årthun et al. (2017).*

Because of the proximity to the Atlantic Ocean, the atmospheric temperatures in coastal regions will be more constant throughout the year. This consistency is due to water having a high heat capacity. Ocean and land areas respond differently to incoming solar radiation because of differences in heat capacity. Land areas have a lower heat capacity and heat up and cool down faster than the ocean, and have thus a more significant difference between highest and lower temperatures. Areas further from the ocean, therefore, has more variability in temperature, with colder winters and warmer summers, than coastal regions. Coastal areas will also receive the major part of the Gulf stream's heat and moisture, making them high on precipitation and low on snow cover during winter.

Even though fluctuations in the ocean are slower than in the atmosphere, rapid variation is observed in the Nordic seas. This variation is due to the location between warm and saline water in the south and colder freshwater in the north. Therefore, the circulation can be influenced by both sides, and such changes can have a big impact on both Scandinavia, and the overall global dynamics since the entire climate system is interconnected.

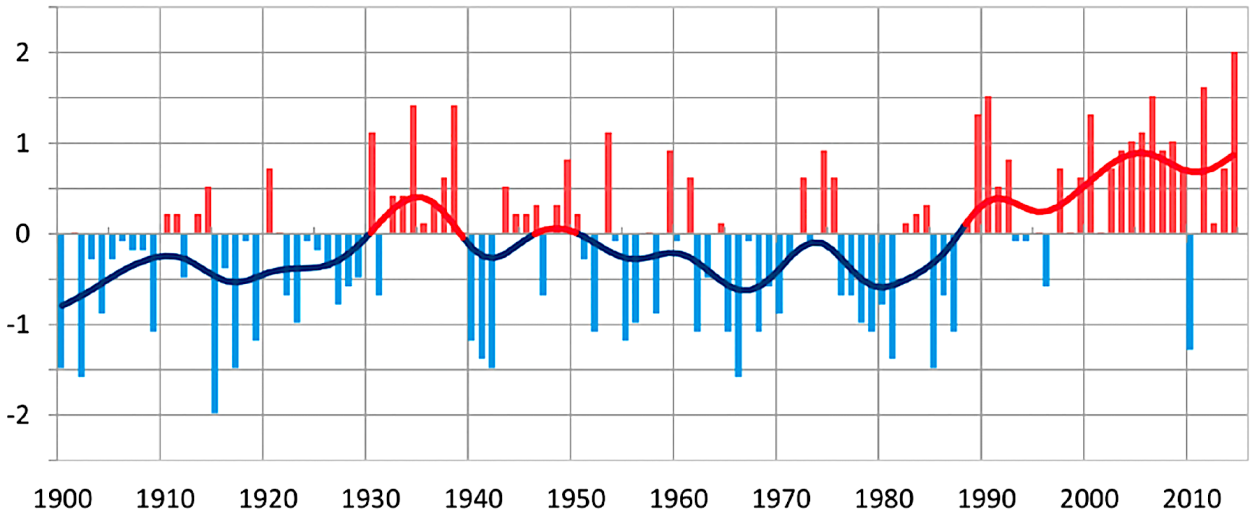

Figure 2.7 *Annual temperatures for the Norwegian mainland during 1900–2014. The figure shows deviations (°C) from the mean during the period 1971–2000, and we can see an increase in temperatures with approximately 1 degree during the last 40 years. From Hanssen-Bauer et al. (2009)*

When we look at the region at a local scale, there are several different types of climates: i) The western coastal zones have a maritime climate, ii) the northern and central areas are mostly subarctic or arctic, and iii) the eastern parts have a subarctic and temperate climate. Changes within the large-scale circulation patterns, such as cyclone intensity and heat content in the Norwegian Atlantic Current, can lead to variations in these local climates. Since Norway covers almost all of Scandinavia's latitudes, it can serve as a good representative. However, even though Norway covers almost all latitudes, the climatic characteristics can be quite different in other Scandinavian areas that are not as influenced by the westerlies and coastal climate.

The annual mean temperature in Norway, during the reference period 1971-2000, was +1.3 °C (Hanssen-Bauer et al., 2009), but the differences between regions are substantial. The coastal and southern regions experience the highest overall annual temperatures. As we can see in Figure 2.7, there has been an increase in this temperature during the last 40 years of approximately 1 °C, which is consistent with the global levels (IPCC, 2013). The temperature increase has been largest for the northern regions, especially during spring and autumn. The increase in temperature is the smallest during the winter.

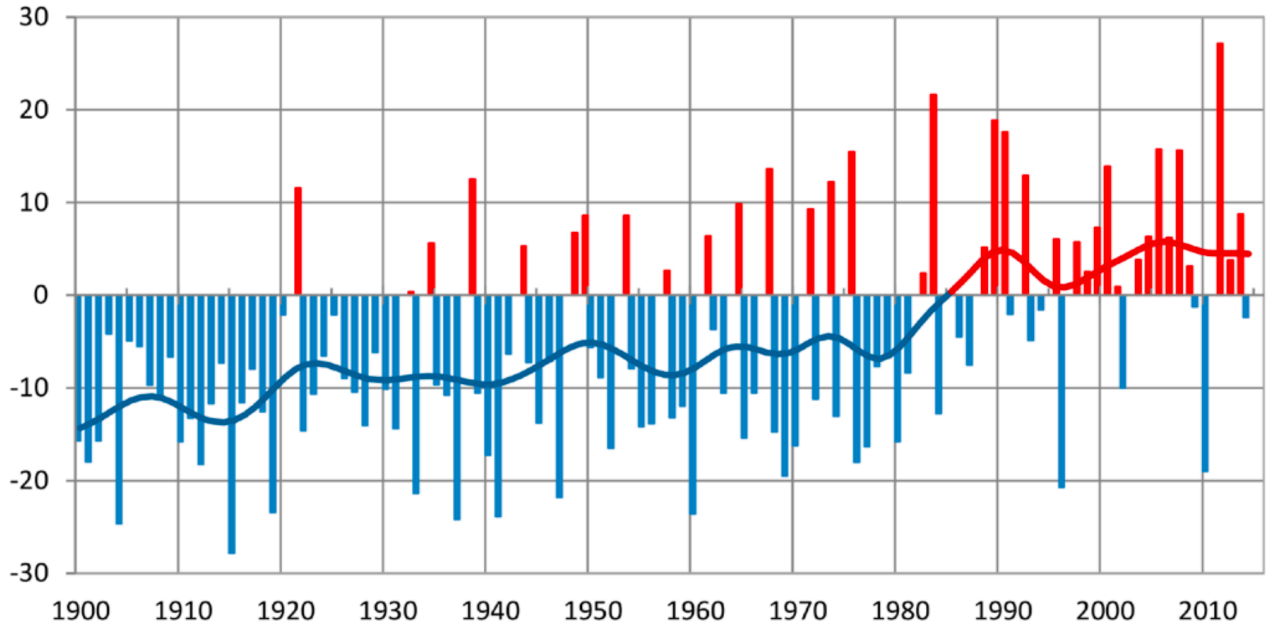

Figure 2.8 *Annual precipitation for the Norwegian mainland during 1900–2014. The figure shows deviations (%) from the mean during the period 1971–2000, and we can see an increase in precipitation during the last 40 years. From Hanssen-Bauer et al. (2009).*

For precipitation, during the reference period (1971-2000), the Norwegian annual mean precipitation is approximately 1600 mm. The western and central regions receive the most annual mean precipitation (~3500 mm). This is because of the close location to the heat and moisture of the ocean and the westerlies, which brings it into the country. Further inland, the air has lost most of its moisture, and thus we find the lowest annual mean precipitation in these regions (~300 mm). In the north, the annual precipitation decreases somewhat as well, which is mostly due to decreasing temperatures. In Figure 2.8, we see that during the last 40 years, there has been an increase in the amount of annual precipitation in Norway of approximately 18%.

2.5 Sea Ice

Sea ice is frozen seawater which is floating because ice is less dense than liquid water (Lutgens & Tarbuck, 2016). The sea ice does not have a continuous surface but consists of blocks of ice (ice floes) with areas of open water between (leads), creating a dynamic pattern that always moves with the winds above or currents underneath. In this section we will go into how the sea ice forms and how it interacts with ocean and atmosphere. We will also explain the ice-albedo-feedback, the polar amplification and how the sea ice is influenced by climate change.

2.5.1 Formation

The Arctic sea ice is diverse in structure and thickness, varying from region to region. Depending on season and temperature in the atmosphere and surrounding water, the ice grows and shrinks in extent and thickness. Throughout the year, the sea ice extent is at its peak in March and at its lowest in September (Figure 2.9). In figure 2.10, we can see the location of the sea ice border for September in 2006 and 2017. The ice grows by water freezing and shrinks by melting. However, the ice can also be compressed or expanded due to external forces. In this case, the ice can get much thicker than if it grew thermodynamically. Mechanical separation of the ice does not necessarily lead to decreasing ice but can enhance wintertime growth by exposing more liquid water to the colder air above. When new ice is made, it spends over a month to grow thicker than 1 meter. During the year, the Arctic has areas which are entirely covered by ice, called multi-year ice, which is thicker and more robust. The amount of the different types of ice effects how the ice influences surrounding processes in the atmosphere and ocean.

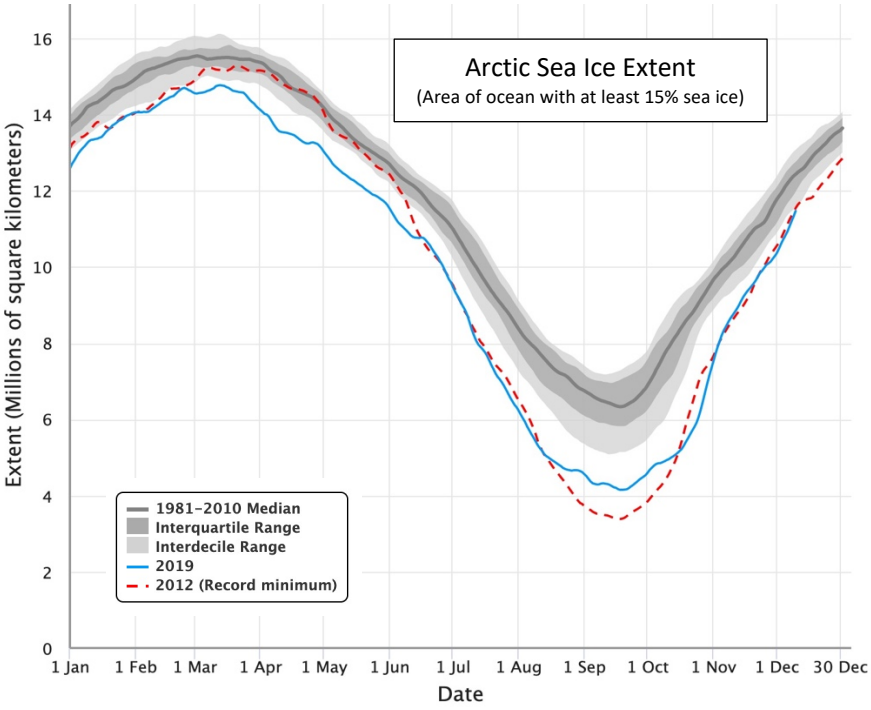

Figure 2.9 *Evolution of the Arctic sea ice extent, in millions of square kilometres, throughout the year. Illustrated for the 1981-2010 median in grey, 2019 in blue and for the record minimum, 2012, in red. From the National Snow and Ice Data Center (NSIDC).*

Figure 2.10 *Map over The Arctic with the Arctic Ocean, multiple seas and land areas, as well as September sea ice extent for 2006 and 2017. From Arctic Centre, University of Lapland.*

2.5.2 Air-Sea-Ice interactions

When the sea ice converges and diverges, it influences the interactions between the water, ice and atmosphere. Thicker ice made from convergence and freezing, works as an insulator between the water and atmosphere, making it harder for the heat in the ocean to be released into the atmosphere. Most of the heat is thus transferred from the Arctic Ocean to the atmosphere by the leads and thin ice (Rigor et al., 2002). Thinner ice, or no ice, makes it possible for heat to escape into the atmosphere, prolonging the melting season. Ice has also a higher albedo than water, meaning it reflects more of the incoming solar radiation. This reduction in reflection results in the water absorbing more solar radiation, leading to even further heating.

Processes that increase the amount of open water and thin ice have a significant impact on the flux of heat from the Arctic Ocean to the atmosphere, and consequently have a substantial effect on surface atmospheric temperatures (Rigor et al., 2002). Fluctuations in the AO phase from negative to positive phase during the winter can more than double the amount of new thin ice, making the Arctic lose 50% more heat. More open water will also impact the moisture flux to the atmosphere by the increase of evaporation from the ocean surface.

2.5.3 Ice-Albedo-Feedback and the Arctic Amplification

Another essential property of the sea ice is its ability to reflect a big part of the insolation due to its bright surface. The percentage of the incoming solar radiation, which is reflected by the surface, is called its albedo (Aguado & Burt, 2013). Sea ice has a higher albedo than almost any natural surface, thus leading to a cooling of the Earth system by reflecting a large portion of the insolation to space. When we have a temperature increase, more of the sea ice will melt away and we will have a retreat of the ice margins. Less sea ice will lead to exposure of more of the much darker ocean surface and because of the darker colour the ocean surface has a lower albedo than the sea ice. The ocean will absorb much more of the incoming radiation, heating the ocean further and leading to enhanced melting of the sea ice. Thus, this is a positive feedback mechanism called the ice-albedo-feedback, where the original change is enhanced. The ice-albedo-feedback is one of the reasons why the higher latitudes have a much higher warming rate than the rest of the globe. This effect is called the AA and is why the poles are the most exposed regions to anthropogenic climate change and increasing temperatures.

2.5.4 Changing Arctic climate

According to the latest report by IPCC, the extent and thickness of the Arctic sea ice have decreased continuously, with September in 2012 being the record low (Aguado & Burt, 2013, Cubasch et al., 2013). According to Hanssen-Bauer et al. (2009), the sea ice will decrease for all months of the year; the ice thickness will be further reduced, there will be less old ice and more first-year ice, higher sea ice drift speed and an increased length of the melting season. All of these future changes point to less sea ice in the Arctic. This reduction means that larger surfaces, once covered by ice with a high albedo, will be replaced by darker ocean surfaces that absorb more of the incoming solar radiation. Furthermore, a thinning of the remaining sea ice will make it more susceptible to further melting. More energy absorbed by the Arctic oceans will lead to an increase in the atmospheric temperature of the region, promoting even more melting. Finally, due to AA, global warming will have particularly strong consequences in the Arctic regions, leading to a further decrease in sea ice extent and thickness (Hanssen-Bauer et al., 2009). This result is in line with the general agreement of climate models (Aguado & Burt, 2013), which projects that Arctic waters might be ice-free in the 2030s.

3 Data and Methods

In this thesis, we use PDFs to analyse how daily temperature and precipitation from the CESM LENS changes with different levels of global warming. We also study how the PDFs change in correlation with a high or low amount of sea ice extent in the Arctic. For each of the issues mentioned above, we have made PDFs for all seasons and regions in Scandinavia.

3.1 Climate Modelling

Climate modelling is an attempt to understand and imitate processes in the climate system, through numerical calculations of varying complexity. The purpose is to understand how climate system processes interact with each other, what kind of feedback they produce, and how they will evolve in the future. The climate system's physical, biological and chemical principles are very intricate and must be simplified with a series of mathematical equations and approximations. Approximations are used when we lack the appropriate knowledge or information, or when the modelling becomes too slow or costly to use (McGuffie & Henderson-Sellers, 2005).

Processes in the climate system run on different temporal and spatial scales; therefore, the resolution of the model is critical. The choice depends on which part of the climate system that is of interest, and whether we want to investigate local and short timescales or global and longer timescales. In the spatial resolution, the atmosphere, oceans and land are divided into grid cells, with each cell covering specific latitudes and longitudes. The resolution decides the size of the grid cells and can be specified as km or degrees of latitude/longitude. Grids in the vertical direction is usually represented as layers and more layers mean higher resolution. The temporal resolution specifies the timestep size within the model.

Since both the climate principles and resolutions can be approached in different ways, we have a large number of distinctive climate models. The simplest model is the Energy balance models which are zero or one-dimensional. The most advanced today are the large-scaled fully coupled global Earth System models, which are developed to take into account the entire climate system and the carbon cycle, and can be run for hundreds of years with a relatively high resolution (McGuffie & Henderson-Sellers, 2005; Xie et al., 2015).

3.1.1 Large Ensembles and Initial Condition Ensembles

Climate modelling is under constant development, and one of the fundamental advances is the opportunity to run a large number of simulations using less computational power and time. The Large Ensembles (LENS) consists of a substantial quantity of climatic realizations using the same model and covers the same period in time. Initial Condition Ensembles is model runs where each simulation differs from each other with a slightly changed or perturbed initial condition (Deser et al., 2017). Small changes in initial conditions will amplify over time (McGuffie & Henderson-Sellers, 2005), making the climate simulations very different from each other. The external forcing is kept precisely the same for all the runs, and the resulting ensemble spread will mimic internal variability (Kay et al., 2015). To be able to estimate the total ensemble spread of the model accurately, a high number of simulations is required (Olonscheck & Notz, 2017). Consequently, the LENS with perturbation of initial conditions provides an excellent resource and makes it possible to disentangle the internally generated variability from the external contributions and thus study climate change in the presence of natural variability.

3.1.2 Representative Concentration Pathways

How much the climate will change over the coming decades is dependent on the development of our future society. How will climate policies be implemented? How will economic and population growth look? The choices we make will govern our emissions in the coming years and since our future path is not set in stone, we need to prepare for every scenario as well as the potential impacts. Thus, Representsative Concentration Pathway (RCP) scenarios, with different emission levels of GHGs, aerosols and land use have been created (Xie et al., 2015). These scenarios are used as input into global climate models which analyse future climate development.

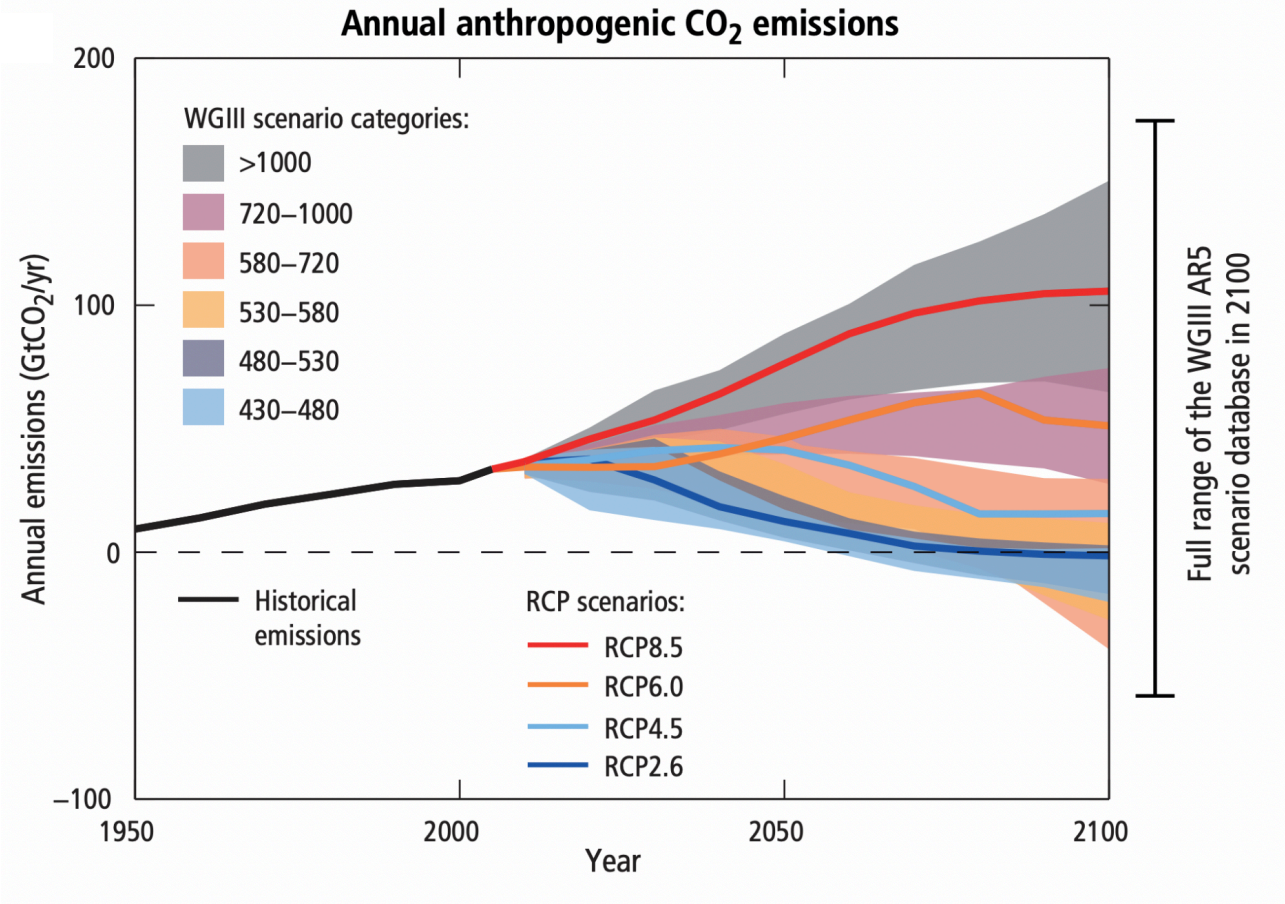

Figure 3.1 *Four different global greenhouse gas emission pathways from the year of 2000 to 2100. All scenarios come from the latest Assessment Report from IPCC (AR5). Illustration from IPCC (2013).*

In the fifth assessment report, the IPCC presented four emission scenarios which can be seen in Figure 3.1, RCP 2.6, RCP 4.5, RCP 6.0 and RCP 8.5 (IPCC, 2013). The numbers at the end represent radiative forcing in the year 2100, relative to the preindustrial conditions (Kay et al., 2015). Radiative forcing is a measure of the additional energy taken up by the Earth system due to enhanced greenhouse effect and is expressed in W/m^2. The GHGs is usually a positive forcing, leading to a global temperature rise, while the extra aerosols give a negative radiative forcing and cool the planet. RCP 2.6 is the lowest emission scenario, followed by RCP 4.5 and RCP 6.0 and ending up with RCP 8.5.

RCP 8.5 is the emission scenario that we concentrate on in this study and represents the most extreme future pathway. The scenario includes assumptions of high population growth, slow income growth, modest technological change, weak climate change policies and high energy demand (Riahi et al., 2011), leading to a high radiative forcing at the end of the century. The RCP 8.5 is used in the CESM LENS because it gives the biggest range of climate states and makes it possible to look at the entire range of possible future warming levels. In this thesis, we sort years from the RCP 8.5 run, as well as the other runs, into warming levels, thereby making the analysis independent of what kind of scenario that has been used.

3.1.3 CESM1 Large Ensemble

We have taken advantage of the availability of a Large Initial Condition Ensemble and used the output from the Community Earth System Model Large Ensemble (CESM LENS) to investigate the intrinsic variability of daily temperature and precipitation in the region of Scandinavia. The LENS dataset has a horizontal resolution of 1°x1° and is a fully coupled global climate model (Kay et al., 2015). The model has been forced with historical emissions from 1850 to 2005, and with RCP8.5 from 2006 until 2100. Therefore, the ensemble provides computer simulations of the past, present and possible future climate.

Since the CESM1 LENS is a global coupled climate model, it consists of several components. The CESM includes five models, one for the atmosphere, sea-ice, land, ocean and land-ice. It also has a coupler which passes information between the different models. For the atmosphere, it uses a global atmospheric general circulation model called the Community Atmosphere Model, version 5 (CAM5) with 1°x1° horizontal resolution and 30 layers in the vertical direction. The ocean component is the Parallel Ocean Program version 2 (POP2) with 60 vertical layers. For land, we have the Community Land Model (CLM). For land-ice, we have the Community Ice-Sheet Model (CISM), which represents the ice dynamics and predicts ice sheet retreat and sea-level rise. Lastly, for sea-ice, we have the Community Ice CodE, version 4 (CICE4). The CESM also includes land carbon cycle calculations, diagnostic biogeochemistry calculations for the ocean ecosystem and the atmospheric carbon dioxide cycle (Kay et al., 2015).

3.2 Datasets and variables

From the output of the CESM LENS we are interested in three key variables; the mean daily precipitation (PRECT), the mean surface air temperature (TREFHT) and the sea ice fraction in the Arctic (ICEFRAC). As seen in Table 3.1, we have used several ensembles in this thesis. Each ensemble consists of a different amount of ensemble members, and each ensemble member consists of a different amount of total years.

Table 3.1 *Overview of the different ensembles used in this thesis. All has been run by the CESM1 LENS. Each ensemble contains of a different amount of ensemble members which again consists of a certain amount of years.*

Ensemble	Abbreviation	Ensemble members	Years
Preindustrial control	piControl	18	1350
Historical	hist	33	2827
RCP 8.5	RCP8.5	33	3135

Firstly, the preindustrial control (piControl) is a coupled atmosphere and ocean control run where climate condition of the preindustrial era has been kept constant for all the years (Taylor et al., 2009). This means that emissions of gases and the aerosol content of the atmosphere have not changed during the simulation. The control run makes it possible to study internal variability in the absence of climate change. The historical run, on the other hand, is dynamic, meaning that conditions like insolation, emissions and land-use change continuously, in agreement with observations. Lastly, we have the RCP 8.5 run, which represents future climatic conditions up to the year 2100. RCP 8.5 is also a dynamic run, with constantly changing conditions which are following the RCP 8.5 scenario. When the year of 1920 is reached, each of the ensemble members starts from an identical initial state, except for a small perturbation to the atmospheric temperature (Kay et al., 2015). As can be seen in Figure 3.2, the initial state in 1920 is obtained from the first ensemble member, which in 1850 branched out from the control run.

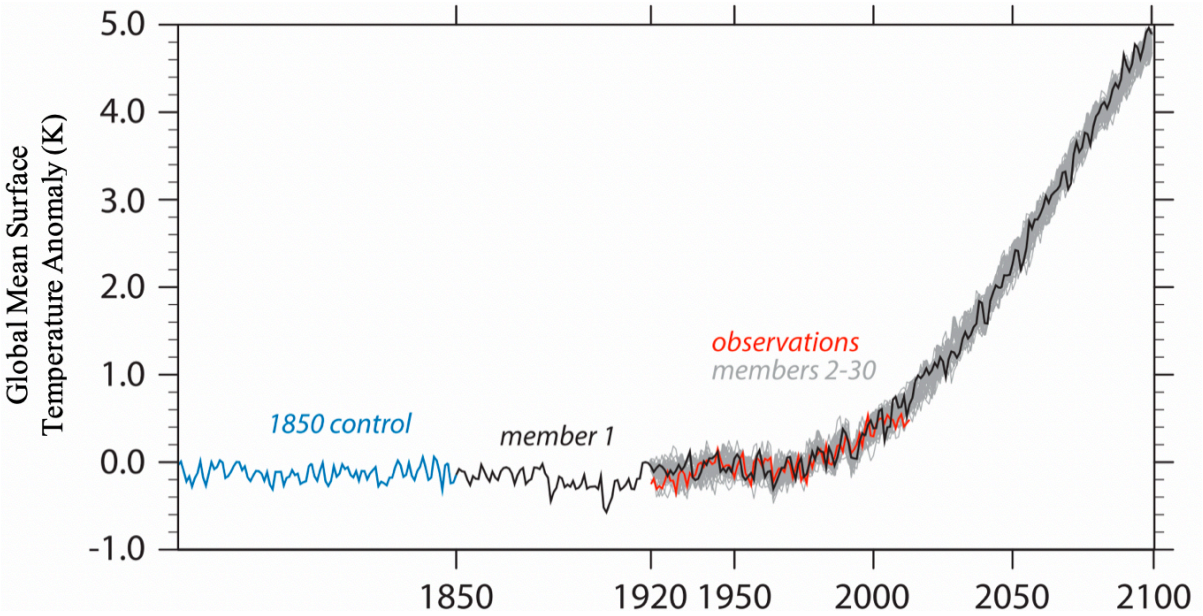

Figure 3.2 *Global surface temperature anomaly from the 1961–90 base period for the 1850 preindustrial control run, individual ensemble members (1-30), and observations. From Kay et al. (2015).*

For temperature and precipitation, we have used the output from all the ensembles, the piControl, hist and RCP 8.5. For sea ice extent, we have only used the piControl because we were interested in studying the correlation between the sea ice extent and the day-to-day variability in Scandinavia without the influence of anthropogenic climate change. For all the ensembles, except for the sea ice fraction, we have a continuous daily output which will be useful for studying the extremes in the near-term future. For the sea ice fraction, we have monthly output.

3.2.1 Masking of land areas

In this thesis, we have chosen to focus on areas containing land. Therefore, a land mask has been made in order to separate the areas with and without land. All grid cells within our region are weighted by having a number between zero and one. This number tells us the amount of land the cell contains, or the land fraction. If the fraction is less than 50 per cent, meaning that the grid contains a small island, it will be set to zero and thereby contain only water. The resulting land area mask has higher numbers representing a higher land fraction and thus a more significant weighting. Each variable in a grid cell is multiplied with this land area mask.

3.2.2 Regional means

When we simulate the climate, we separate the Earth's surface into regions or grid cells. Higher resolution gives more grid cells within a region. In order to construct PDFs, we make regional means over all grid cells within each of our regions and every timestep. In this thesis, we have used a Gaussian grid, which is a coordinate system used for spheres (Figure 3.3). Each grid cell is formed as a rectangle and each latitude band has an equal amount of these cells. This means that the region averages are weighted by latitude because of grid cells closer to the poles continuously get smaller because the radius of the Earth is reduced. For surface temperature and precipitation, the averages have been made for a daily time step over the longitudes 0-30°E and each subregion; North (65-70°N), Central (60-65°N) and South (55-60°N). For the ice fraction, averages are made for every month over the entire area north of the 60°N latitude band.

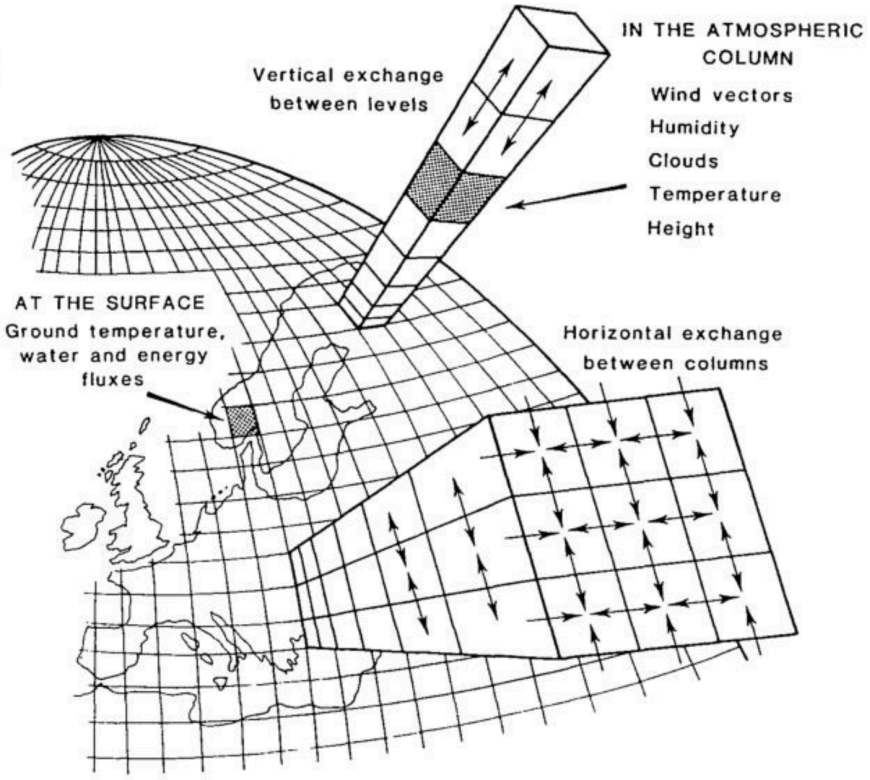

Figure 3.3 *Illustration of the Gaussian grid with grid cells in the horizontal and vertical levels. Note that this figure has a 3°x 3° resolution, while we use1°x 1°. From Henderson-Sellers & McGuffie (1987).*

3.3 Reanalysis

To be able to validate the modelling output from CESM1 LENS, its performance needs to be tested by comparing the results with present and past weather and climate. This validation can be done by using reanalysis data, which combines model output with collected observations and creates a numerical description of the recent climate. The European Centre for Medium-Range Weather Forecasts (ECMWF) produces climate reanalysis, with ECMWF ReAnalysis (ERA5) being the fifth and latest version (Hennermann & Berrisford, 2019). The ERA5 provides hourly data of climate parameters such as surface air temperature, pressure, wind, rainfall and soil moisture. The datasets go from 1979 to 2018 and have a resolution of 30 km or approximately 0.25^{o} x 0.25^{o} with 137 vertical levels in the atmosphere. The data is openly available from the Climate Data Store (CDS) infrastructure. The variables considered in this thesis is daily temperature and precipitation. We use all the years included in the dataset to reproduce the PDFs for the same regions and see if these PDFs match those already produced with CESM1.

3.4 PDFs as a tool to investigate day-to-day variability

PDFs can quantify the properties of day-to-day variability for climate parameters and their sensitivity to changes in climate. Changes in climate can lead to changes such as frequency and intensity of temperature and precipitation extremes (Field et al., 2012). Even though the extremes are the weather events farthest away from the mean, and “less likely” to occur, they are also the outcome with most significant societal impacts and are therefore particularly important when trying to predict future changes (IPCC, 2001).

Changes in weather extremes can be seen as changes in the overall mean, variance or shape of a PDF. In general, PDFs are used to indicate the probability of different outcomes for a variable and are usually in the shape of a Gaussian curve. They can give a much more complete picture of the day-to-day variability than if we were to focus on means and extremes because we can analyse how the overall shape of the PDFs changes (Cubasch et al., 2013). A relatively small shift in the shape of a climate variable can result in an immense rise in the frequency of extreme events and thus have large possible impacts on societies.

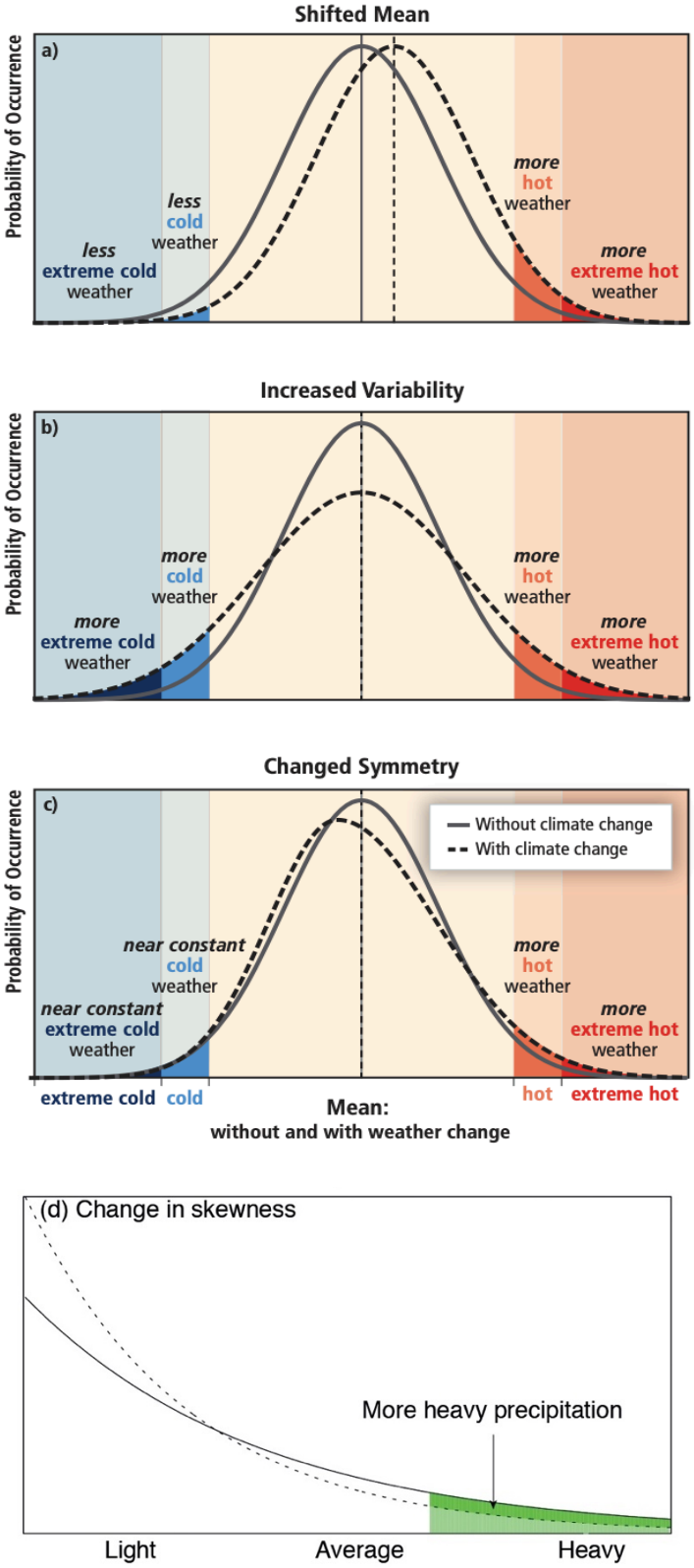

Figure 3.4 *Schematic showing the effects of a changing climate on the daily temperature PDFs. (a) shift in the overall mean giving les cold extremes and more hot extremes. (b) Increase in the variability of the distribution giving more extremes in both cold and hot extremes. (c) Change in the overall shape of the PDF giving more hot extremes but with the cold extremes staying constant. (d) Change in the skewness of the precipitation PDF can give changes towards more heavy precipitation. From Field et al. (2012).*

Looking at Figure 3.4a, we can see that an increase in the mean temperature will lead to an increased probability of days with hot and extremely hot weather, and a decrease in the number of days with cold weather. When we have an increase in variance, as seen in panel b, the extreme weather will be more frequent in the day-to-day variability. It is also possible to have an overall shift in the shape of the distribution, as seen in panel c in Figure 3.4, which can combine the effects of both the mean and variability changes. For precipitation, we can have a change in the skewness of the distribution, which can lead to more or less extreme precipitation (Figure 3.4d).

3.5 Analysis Techniques

In this section, we will present the methods used for each part of our analysis, both for the Scandinavian daily variability with warming levels and the Scandinavian daily variability with changing sea ice extent.

3.5.1 Day-to-day variability with warming levels

The first step in our analysis is to see how the Scandinavian day-to-day variability is affected by different levels of global warming. This analysis follows the same method used by (Samset et al., 2019). First, we sorted all years by which warming level they belong in. Each warming level is calculated by taking the global mean surface temperature (GMST) anomaly from the preindustrial baseline mean. It is important to notice that by grouping years together based on warming levels, we no longer have a dataset which follows a timeline. Thus, we lose the ability to analyse variability, which covers interannual and longer timespans. On the other hand, this categorisation makes it possible to separate the different warming levels and their individual properties.

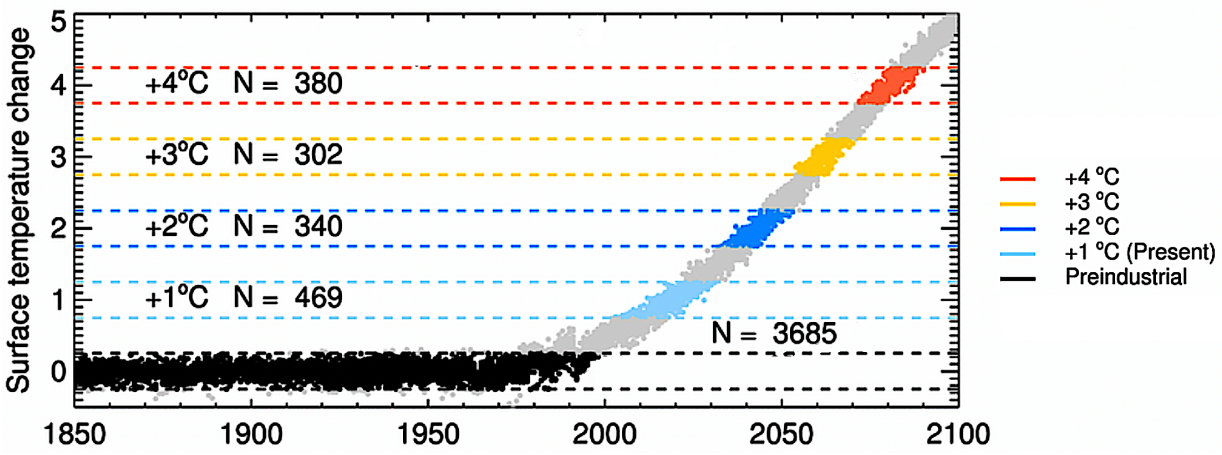

Figure 3.5 *Selection of years from the CESM1 Large Ensemble. Each dot represents a global annual mean surface temperature anomaly relative to the baseline average. Each category represented with individual colour and number of years, N.*

In Figure 3.5, each dot represents a year in the LENS, which spans from 1850 to 2100 for all the 30 ensemble members. Black dots are years considered to represent the preindustrial period, with anomalies within ±0.25 of the preindustrial baseline. Further, the surface warming has been separated into several levels covering a certain temperature interval, each with a width of 0.5 °C and represented by an individual colour. Each level is surface temperature anomalies relative to the preindustrial mean. Light blue is for warming level 1.0 ± 0.25 °C, blue for 2.0 ± 0.25 °C, yellow for 3.0 ± 0.25 °C and orange for 4.0 ± 0.25 °C. These colours have been used throughout the rest of the analysis to make it easier to separate the changes of the different warming levels.

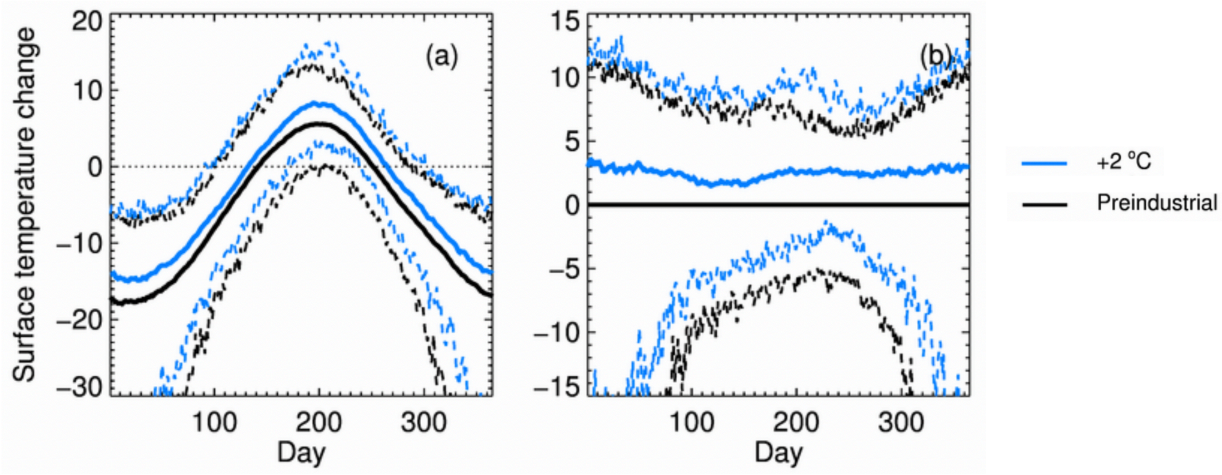

Figure 3.6 *The annual cycle of regional mean daily surface temperature in southern Scandinavia. (a) The mean (solid) and spread (dotted) of the annual cycle of the preindustrial baseline (black) and the +2 °C warming level (blue). (b) As a, but with the seasonality removed and only the anomalies from the preindustrial baseline mean showing.*

For our three regions, northern, central and southern Scandinavia, we have calculated the regional daily mean of surface air temperature and precipitation for each of the warming levels. The regional daily means are calculated over all the years within each warming category. (see section 3.1.5 for more details of calculation of the regional mean). By using the regional means, we can visualise the annual cycle for each of the warming categories and see how the mean and variation changes for each warming level.

In Figure 3.6a, we have the annual cycle of daily surface temperature, with southern Scandinavia as an example in this case, with the mean in solid line and the variation in the dotted lines. The preindustrial simulation in black and the +2 °C warming level in blue. In order to isolate the daily variability from the seasonal cycle, we remove the annual cycle by subtracting the preindustrial baseline mean from the daily means. The result is shown in Figure 3.6b, where we can see the anomalies in means and variations of the warming level from the preindustrial baseline mean. Already here, we can clearly see the changes between the baseline and a 2 °C warmer world, we can also see the difference in variability amid seasons.

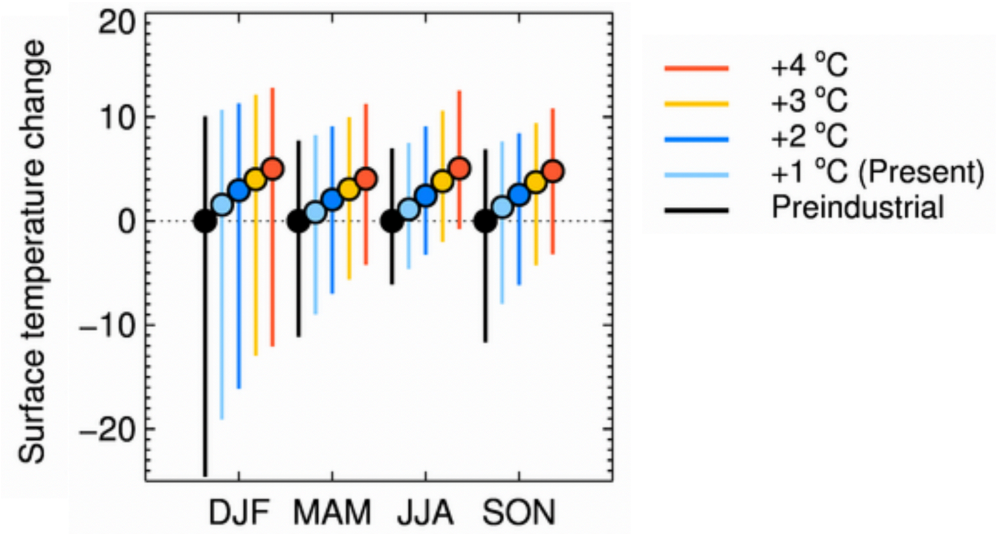

Figure 3.7 *Seasonal mean and range for the daily variability in southern Scandinavia. For the preindustrial baseline and all of the four warming levels. The dots represent the means and the vertical lines is the temperature distribution width of the regional mean daily surface temperature.*

To be able to see how the daily variability changes between seasons, we divide the annual cycle in Figure 3.6b into the four boreal seasons, which can be seen in Figure 3.7. December, January and February (DJF) represents winter. March, April and May represent spring. June, July and August (JJA) represent summer and September, October and November (SON) represents fall. Each season and each warming level are represented with a line showing the width of the distribution of the daily regional surface mean temperature. By averaging over seasons, we lose some variability within each month and smooth out some of the chaotic behaviour of the daily variability in temperature and precipitation. On the other hand, this will give us a better estimation and skill in predicting the seasonal changes. We see that the overall daily surface temperature increases with higher global warming levels and that the highest daily temperature variability is during winter.

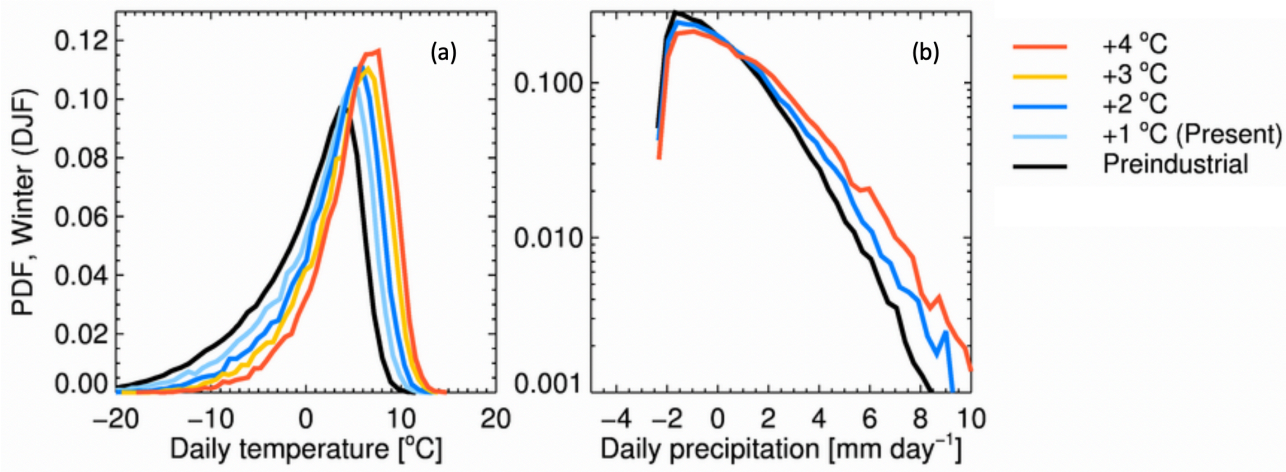

Figure 3.8 *PDFs for southern Scandinavia during winter (DJF) (a) PDFs of regional daily temperature, for baseline and warming levels. (b) PDFs of regional daily mean precipitation, for baseline and the two warming levels +2 °C and +4 °C.*

Further, we make PDFs of the day-to-day variability of temperature and precipitation (See section 3.4 for more details on PDFs). These PDFs can be viewed as cross-sections of the distributions in Figure 3.6b, along the temperature axis, but for an average of the winter season. The width of the PDFs is reflected in the vertical lines of Figure 3.7. Figure 3.8 shows the shape and spread of the PDFs of regional daily temperature and precipitation, from the preindustrial baseline mean. The full distributions are shown for the baseline and all warming levels during wintertime (DJF) for southern Scandinavia. The PDFs give a good overview of both the mean and variability with increasing temperature anomaly. They can be plotted for all the different seasons, which will give a good prediction on the development within each season with increasing global warming. Indicators like change in mean and spread of the distribution are good indicators to analyse what kind of impacts the different warming levels will generate, and for which seasons these impacts will be most severe.

Lastly, to see how the extreme weather is influenced under increasing amounts of global warming, we have analysed the upper tails of the PDFs. For both temperature and precipitation PDFs, the top preindustrial 99th percentile threshold has been quantified (Figure 3.9). Then, for each of the warming levels, we have calculated the percentage of each dataset which is located above this 99th percentile preindustrial limit, indicating possible future increases in the warmest and wettest days.

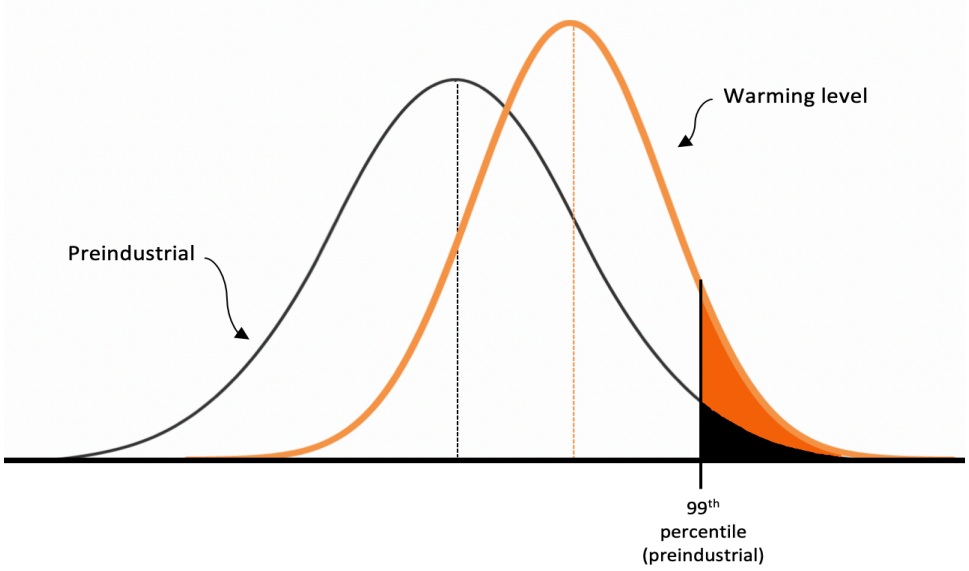

Figure 3.9 *The upper 99th percentile preindustrial threshold where 1% of the dataset is above this limit (black). In orange is the amount of the warming level dataset which I located above the 99thpercentile preindustrial threshold.*

3.5.2 Day-to-day variability with changing sea ice extent

Next, we analyse the daily variability in temperature and precipitation for the different regions in Scandinavia with changing sea ice extent. This analysis follows much of the same methodology as for warming levels, but with some exceptions. The most significant difference is that in this case, we are not looking into how the relationship between sea ice and daily weather variability evolves with future scenarios and anthropogenic influences. We are, on the other hand, interested in how the underlying natural variations in Arctic sea ice extent and the daily variability in temperature and precipitation in Scandinavia influence each other.

Due to natural sea ice variability being our focus, we only use the simulated years from the preindustrial control run from the 18 ensemble members. Instead of separating the years into categories of warming levels, in this case, we group years based on if they have high or low sea ice extent. We have also chosen to focus on the sea ice extent in the two months of March and September, due to them having the overall highest and the lowest amount of sea ice during the year. Therefore, we will analyse how the daily variability in temperature and precipitation are correlated to March and September sea ice.

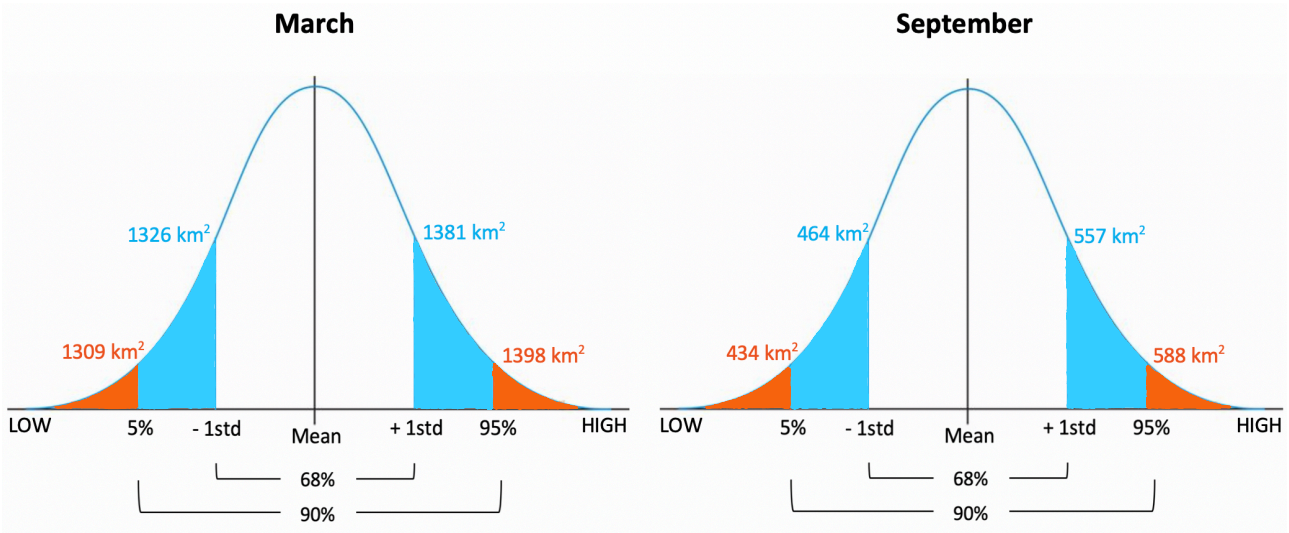

Figure 3.10 *Illustration of the high and low threshold for the Arctic sea ice extent during March and September. Blue lines represent the higher and lower thresholds for ± 1 standard deviation, with 68% of the dataset included in the "normal" sea ice extent. Orange lines represent the higher and lower thresholds for 5-95%, with 90% of the dataset included in the "normal" sea ice extent.*

As illustrated in Figure 3.10, for each of the months we have chosen a low and high level of sea ice extent based upon thresholds at 5 – 95% and ± one standard deviation (std). For March, the low thresholds are 1326 × 10^4 km^2 (-1std) and 1309 × 10^4 km^2 (5%), and the high are 1381 × 10^4 km^2 (+1std) and 1398 × 10^4 km^2 (95%). For September, the low thresholds are 464 × 10^4 km^2 (-1std) and 434 × 10^4 km^2 (5%), and the high thresholds are 557 × 10^4 km^2 (+1std) and 588 × 10^4 km^2 (95%). After the years have been sorted into high, low and normal sea ice extent levels, the same method as previously has been used. Contrarily from before, we produce PDFs of daily temperature and precipitation for each month and each region and not for seasons. In particular, we analyse, for March and September, the co-variation between sea ice extent and daily temperature or precipitation during the same month. An example can be seen in Figure 3.11 for March in Northern Scandinavia, with the upper and lower limit of sea ice is calculated as one standard deviation from the mean sea ice extent.

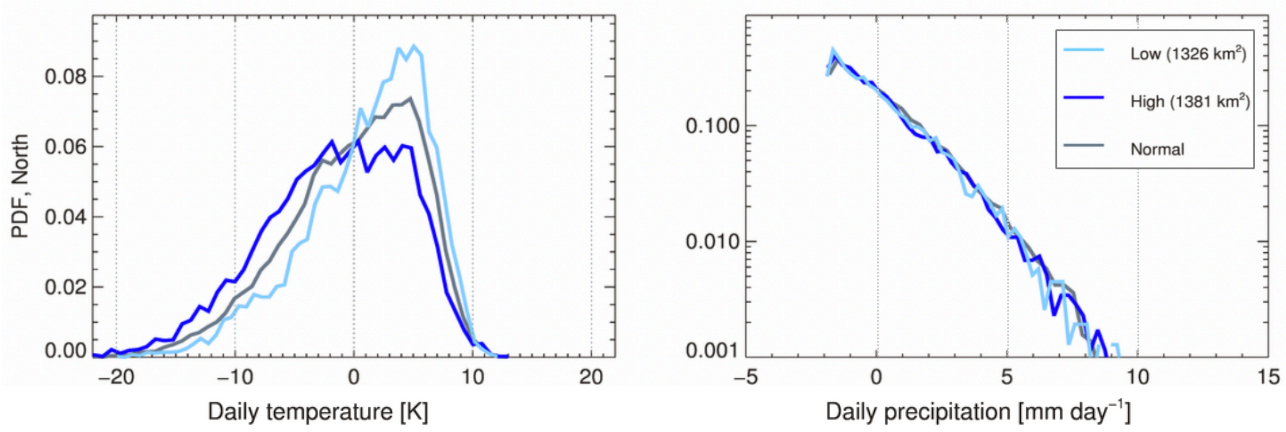

Figure 3.11 *PDFs of Northern Scandinavian daily temperature (left) and precipitation (right) variability for the month of March, with normal (grey), high (dark colour) and low amounts (light colour) of sea ice extent in × 10^4 km^2. The upper and lower limit is calculated as one standard deviation away from the mean sea ice extent. Temperature and precipitation values are relative to the mean at preindustrial conditions.*

4 Results

In this chapter, we first present the annual cycles of temperature and precipitation. Then we show a comparison of two model runs; fixed SST and fully coupled model. Further, we present core features of the daily temperature and precipitation, as well as the evolution of its variability with warming levels and Arctic sea ice extent. PDFs are used to give a more in-depth insight into the future possibilities in the day-to-day variability in Scandinavia, in addition to the mechanisms influencing it. We illustrate the changes in daily climate variability within each season, for all of our regions; north, central and southern Scandinavia. Lastly, we show a comparison of the CESM LENS data with ERA5 reanalysis.

4.1 Annual cycles of temperature and precipitation

To be able to understand how changes might be embodied in our future climate, we need to understand the present. Therefore, in Figure 4.1, we show the present annual cycles of surface temperature and precipitation within each of our subregions, northern Scandinavia, central Scandinavia and southern Scandinavia. As stated by the latest report of IPCC, we have, at present, global warming of one degree Celsius compared to preindustrial times (Hartmann et al., 2013). Therefore, each of the annual cycles in Figure 4.1 has been plotted with the years within the category of warming level 1 and represents our present daily mean and variability in temperature and precipitation within Scandinavia.

For temperature, in Figure 4.1, from the daily mean in solid lines, we see that the average temperature gets colder further north. The daily maximum and minimum temperatures are shown in dashed lines for every region, and we can see that the difference is smallest during summer and largest during wintertime, especially for the northern region winter. Moreover, the most significant difference between summer and winter temperatures takes place in the north. For precipitation, the variability is higher further north, there is also a somewhat more significant difference in the amount of precipitation between the seasons. We also see a slight temporal shift in maximum, with the southern regions experiencing more precipitation later in the year than in the north.

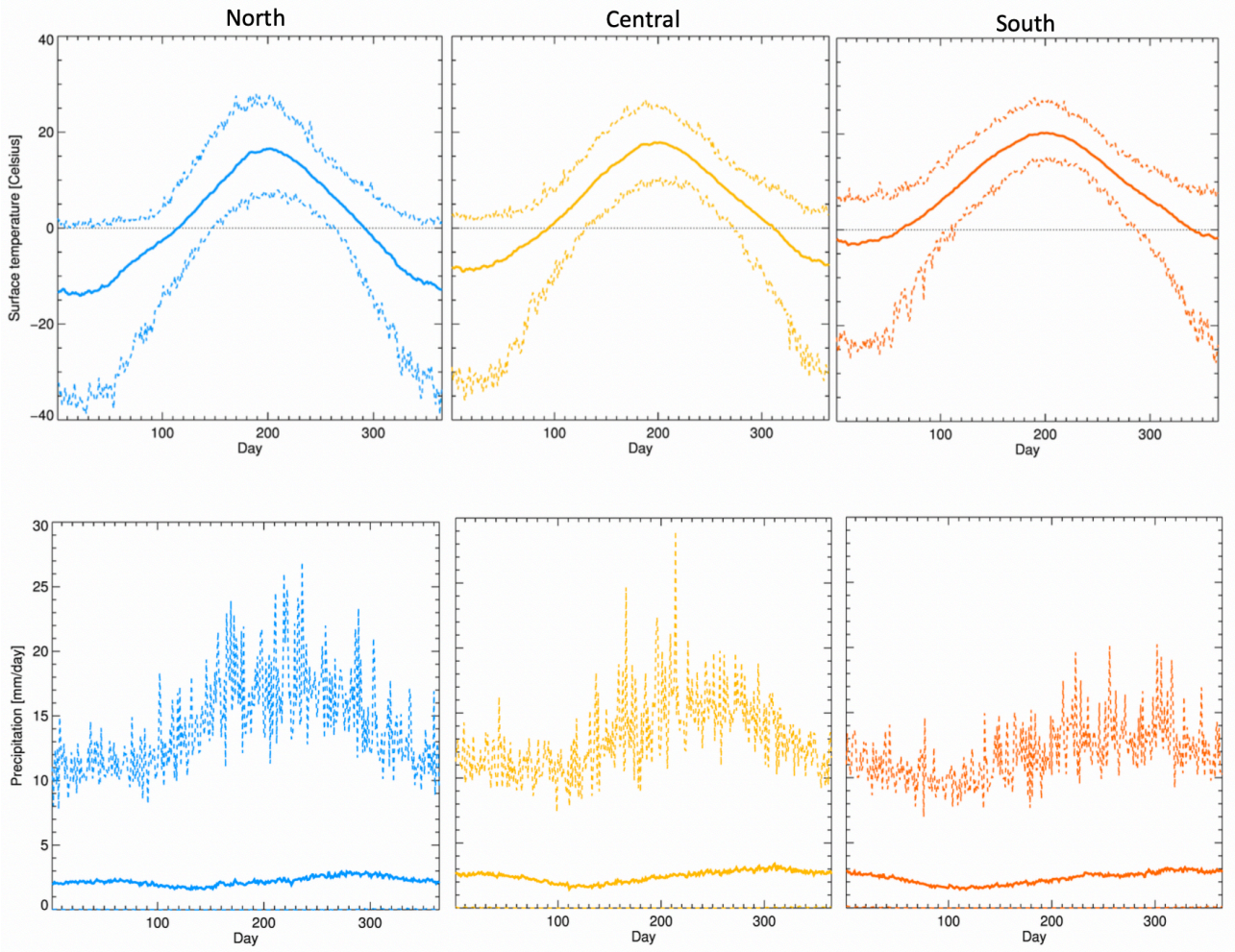

Figure 4.1 *The annual cycles of surface temperature and precipitation in the different regions of Scandinavia for +1 °C global warming. Daily mean in solid line and the daily variability in dotted line. From the left; Northern Scandinavia in blue, Central Scandinavia in yellow and Southern Scandinavia in orange.*

4.2 Fixed SST vs coupled modelling

We have performed a comparison between the PDFs of the preindustrial run from a fully coupled model and a model with fixed SST. A fully coupled model requires much more computer capacity and takes longer to run than the simpler counterpart. This capacity difference is because the model with fixed SST excludes ocean dynamics and predetermines the SST, which is given to the model as a boundary condition. Therefore, we can expect fixed SST simulations to sample a different component of internal variability than fully coupled ones, and it is essential to study if, and how, this model simplification would compromise results of analyses, such as the one we perform here.

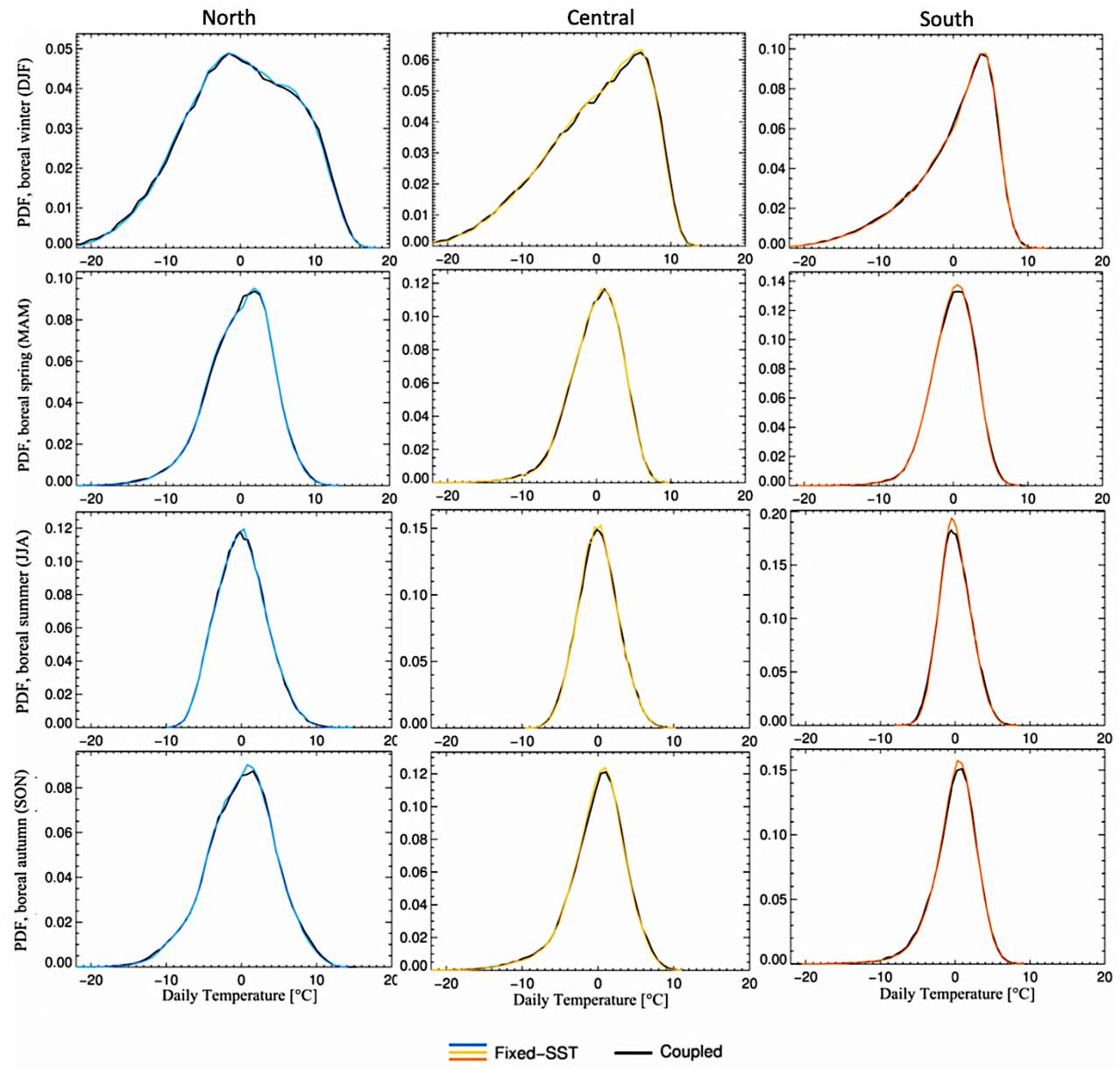

Figure 4.2 *Comparison of temperature PDFs from a model run with fixed-SST and fully coupled model, both for the preindustrial run. From the left, we have the regions; North, Central and Southern Scandinavia. From the top we have the seasons boreal winter (DJF), boreal spring (MAM), boreal summer (JJA) and boreal autumn (SON).*

Figure 4.2 shows that the fixed and coupled model runs are very similar to each other, almost identical. This is counterintuitive to our initial thoughts which were that some differences between the two should be observed due to the added oceanic processes influencing the daily variability in Scandinavia. This will be further questioned in the discussion. If we were to follow these results, simulations should be sufficiently accurate using the fixed SST instead of the fully coupled model. However, since the simulations had already been executed in advance, we chose to use the fully coupled model simulation in the present analysis.

4.3 Day-to-Day Variability in Scandinavia

In this section, we present PDFs of the regional daily surface temperature and precipitation variability, for the preindustrial climate state and each of the global surface temperature anomalies (+1 ºC, +2 ºC, +3 ºC and +4 ºC). Both the surface temperature and precipitation have been averaged over our three regions; northern, central and southern Scandinavia (See Methods for additional details). Further, the PDFs are seasonally resolved for all the boreal seasons; winter (DJF), spring (MAM), summer (JJA) and autumn (SON), which are all presented in more detail. Lastly, for temperature and precipitation, we look at the amount of the dataset which is located above the preindustrial 99th percentile (see section 3.5.1).

Each Scandinavian region has different daily variability in weather parameters, due to factors such as topography, varying climate zones and atmospheric dynamics. Therefore, the PDFs will vary in shape and width depending on which region they are calculated for. As we will see, in most cases for central and southern regions, they are approximately Gaussian. However, for the winter season, the lower cold tails are much larger, especially for northern Scandinavia. In general, the precipitation distributions differ in shape from the temperature PDFs since they have a wider tail towards higher precipitation intensities. There is also a notably smaller difference between the global surface temperature levels, making a greater distribution overlap.

In general, the precipitation distributions differ in shape from the temperature PDFs since they have a wider tail towards higher precipitation intensities and a clear zero point (no precipitation). There is also a notably smaller difference between the global surface temperature levels, making the distribution overlap much more, showing that precipitation is generally much more variable than temperature.

4.3.1 Boreal Winter

In Figure 4.3, we show the evolution of daily temperature and precipitation probability distributions with increasing global warming during the boreal winter, across our three regions. The shape of the temperature PDFs is slightly different compared to the other seasons, with a generally broader shape and wider tails towards the colder temperatures. Overall for the boreal winter, we can see that on the left side of the PDFs, the broad cold tail becomes gradually smaller with increasing global surface temperatures. The changes in cold extremes are more pronounced than in the warm extremes on the right side, resulting in a warmer climate state with less daily variability.

For the northern region in Figure 4.3, we have the most significant overall PDF changes out of the three regions, with a shift towards higher temperatures, overall narrowing and, a major loss of extreme cold temperatures. This marked loss of extreme cold days can translate into a warmer winter climate with less temperature variability compared to preindustrial times. This reduces the amount of extremely cold temperatures in the Arctic regions and we can also see that it looks increasingly similar to more southern climates.

For the central and southern regions, with increasing global surface temperatures, we also have shifts towards higher temperatures and narrowing distributions. There is also a similar, yet less pronounced loss of cold days. However, in the warmer upper tails of the distributions, we can see from table 4.1 that the southern region displays the largest change from preindustrial climate. Compared to the 1% of the preindustrial dataset (per definition), the +4 ºC dataset has approximately 22% above the preindustrial 99 percentile temperature threshold. In other words, there is a 22 times higher likelihood of extreme warm temperatures (defined as the top 1% of preindustrial conditions) in the future southern Scandinavian winter temperatures.

In the case of precipitation, we see a markedly increase in daily variability in all of our regions, due to an increase in extreme precipitation with higher global surface temperatures. The most significant change can be identified in southern Scandinavia with an increase to 3.3% from the preindustrial 1% in the +4 ºC dataset (Table 4.2).

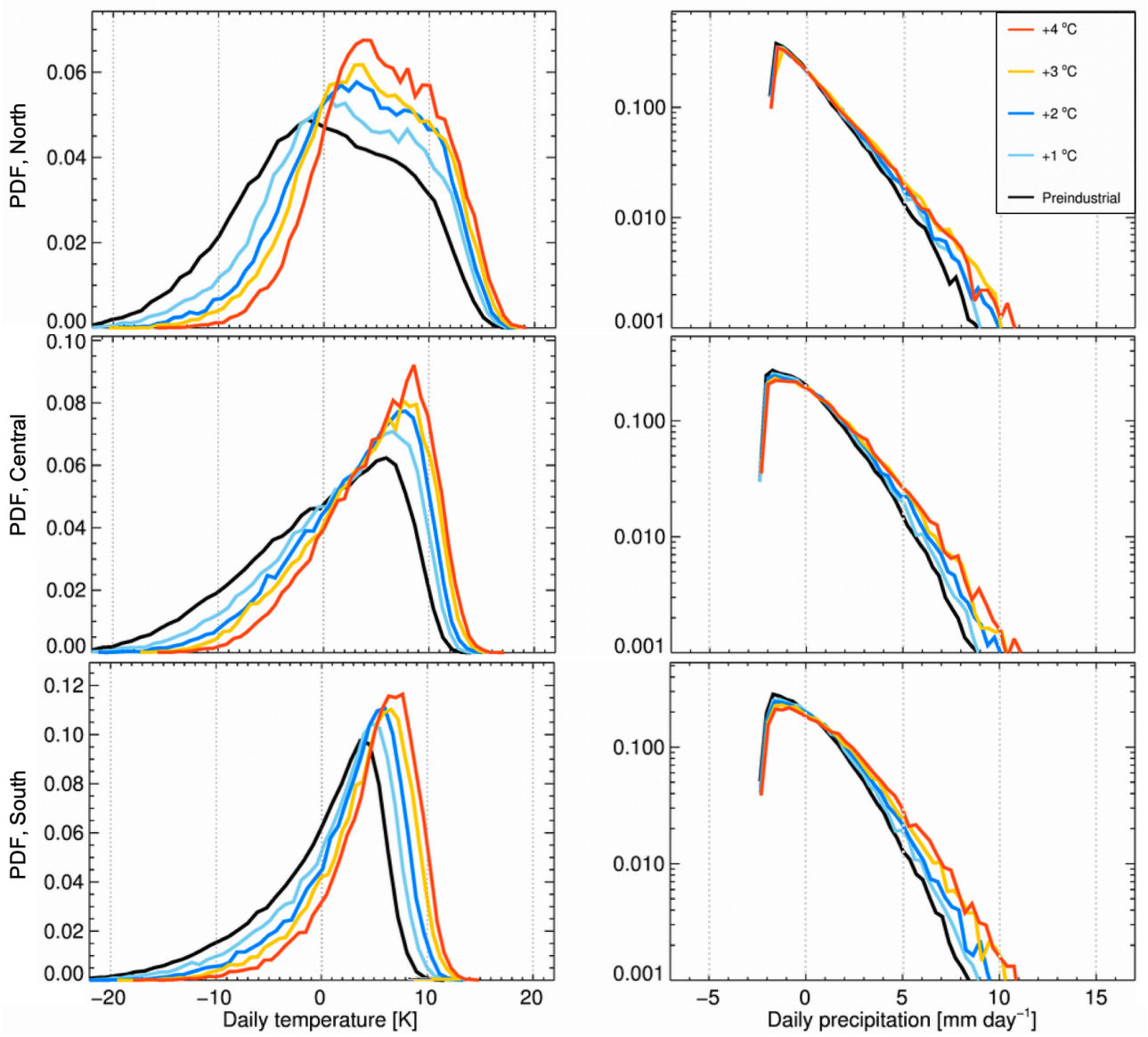

Figure 4.3 *PDFs of daily variability in temperature (left) and precipitation (right) for boreal winter (DJF). We have PDFs for the five different climate states; Preindustrial (Black) and the four global surface temperatures +1 °C, +2 °C, +3 °C and +4 °C, in light blue, blue, yellow and orange respectively. From the top, we have the regions; northern (top, central (centre), and southern Scandinavia (bottom). All numbers are relative to the winter mean at preindustrial conditions.*

Table 4.1 *The preindustrial 99th percentile threshold for boreal winter temperatures. Per definition, 1% of the preindustrial dataset lies above the 99th percentile. For each global warming level, the 99th percentile is used in calculating the percentages of each dataset located above this threshold. Calculated for each region.*

	Preindustrial 99% [K]	**+1 ºC** [%]	**+2 ºC** [%]	**+3 ºC** [%]	**+4 ºC** [%]
North	14.0	2.0	2.8	4.1	5.6
Central	10.9	2.6	4.5	7.7	10.3
South	8.3	3.7	8.1	15.2	22.3

Table 4.2 *The preindustrial 99th percentile threshold for boreal winter precipitation. Per definition, 1% of the preindustrial dataset lies above the 99th percentile. For each global warming level, the 99th percentile is used in calculating the percentages of each dataset located above this threshold. Calculated for each region.*

	Preindustrial 99% [mm/day]	**+1 ºC** [%]	**+2 ºC** [%]	**+3 ºC** [%]	**+4 ºC** [%]
North	6.2	1.39	1.63	2.22	2.38
Central	6.1	1.30	1.79	2.32	2.64
South	5.8	1.37	1.86	2.75	3.33

4.3.2 Boreal Spring

In Figure 4.4, we can see that the boreal spring has a more classic Gaussian shape in the temperature distributions compared to the winter season (Figure 4.3). We notice that in the PDFs the northern region has a shorter and broader distribution, indicating a climate with larger daily variability compared to the southern region. Also notice that the precipitation PDFs for northern Scandinavia show a wider tail towards higher precipitation levels, thus having a higher amount of precipitation during the spring season. Concerning temperature PDFs, the warming levels have a clear shift away from the preindustrial distribution and towards higher temperatures (Figure 4.4), indicating warmer climate states and a higher probability for extreme warm temperatures (Table 4.3). It is also possible to identify a stronger narrowing of the distributions by increasing latitude, with the northern regions experiencing the most dramatic narrowing and thus less daily temperature variability.

Table 4.3 *The preindustrial 99th percentile threshold for boreal spring temperatures. Per definition, 1% of the preindustrial dataset lies above the 99th percentile. For each global warming level, the 99th percentile is used in calculating the percentages of each dataset located above this threshold. Calculated for each region.*

	Preindustrial 99% [K]	**+1 ºC** [%]	**+2 ºC** [%]	**+3 ºC** [%]	**+4 ºC** [%]
North	8.8	2.4	4.1	7.5	13.0
Central	6.8	3.2	8.5	16.4	24.3
South	6.0	3.1	8.3	15.8	23.7

Table 4.4 *The preindustrial 99th percentile threshold for boreal spring precipitation. Per definition, 1% of the preindustrial dataset lies above the 99th percentile. For each global warming level, the 99th percentile is used in calculating the percentages of each dataset located above this threshold. Calculated for each region.*

	Preindustrial 99% [mm/day]	**+1 ºC** [%]	**+2 ºC** [%]	**+3 ºC** [%]	**+4 ºC** [%]
North	6.6	1.32	1.71	2.07	2.25
Central	5.9	1.29	1.69	2.02	2.52
South	5.2	1.39	1.96	2.38	2.87

In approaching a +4 ºC global warming level, the temperature PDFs of central and northern Scandinavia looks continuously more similar to the distribution of southern Scandinavia, indicating a levelling of the regional variability differences and a northern climate more comparable to the southern region, similar to the winter season. From Figure 4.4 and Table 4.4, we find a clear widening of the high tails of the precipitation PDFs, with similar results across all three regions, indicating an increase in extreme precipitation with anthropogenic global warming.

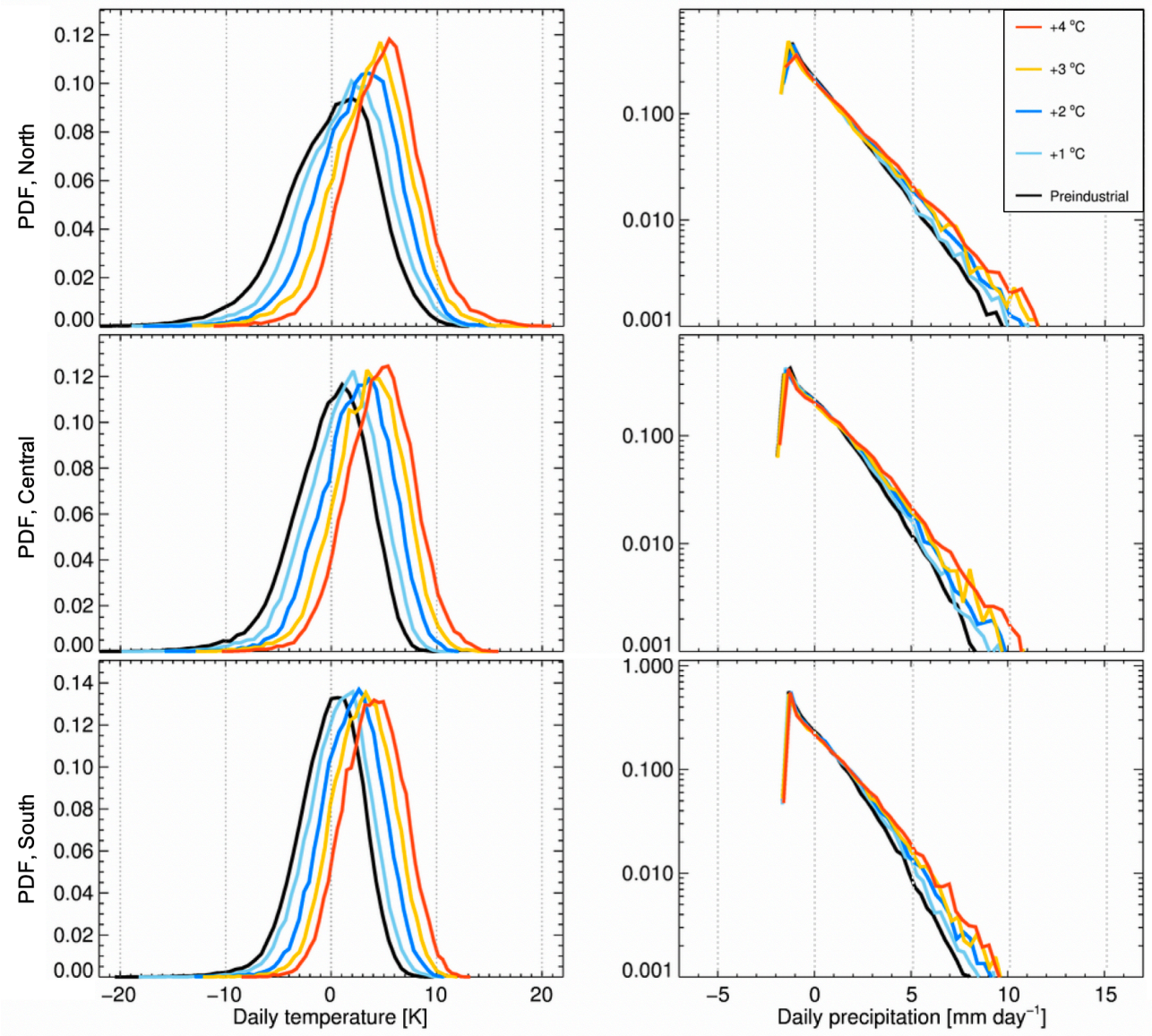

Figure 4.4 *PDFs of daily temperature (left) and precipitation (right) variability for boreal spring (MAM). We have PDFs for the five different climate states; Preindustrial (Black) and the four global surface temperatures +1 °C, +2 °C, +3 °C and +4 °C, in light blue, blue, yellow and orange respectively. From the top, we have the regions; northern (top, central (centre), and southern Scandinavia (bottom). All numbers are relative to the spring mean at preindustrial conditions.*

4.3.3 Boreal Summer

The boreal summer also has a gaussian shape of the temperature PDFs, with higher variability in the northern region (Figure 4.5). However, with increasing global surface temperature, the summer season displays a widening of the temperature PDFs for each of our regions, meaning an increase in daily variability with increasing global surface temperatures. In Figure 4.5 and Table 4.5, we see a widening of the high tails, particularly for the southern region. For 4 °C warming, 44% of the dataset is above the preindustrial 99% threshold, making the probability of extreme heat increase in a warmer future climate state. Precipitation in the northern region has a much wider high tail for the summer season than for any of the other seasons, almost reaching an anomaly of 15 mm/day away from the preindustrial mean for a 4 ºC global warming (Figure 4.5). For the other two regions, particularly southern Scandinavia does not experience a large change in the precipitation distributions. This can be seen in Table 4.6, where the values for southern Scandinavia are very close to 1% and even lower than 1% for +4 ºC, thus having a small decrease in the upper tail.

Table 4.5 *The preindustrial 99th percentile threshold for boreal summer temperatures. Per definition, 1% of the preindustrial dataset lies above the 99th percentile. For each global warming level, the 99th percentile is used in calculating the percentages of each dataset located above this threshold. Calculated for each region.*

	Preindustrial 99% [K]	**+1 ºC** [%]	**+2 ºC** [%]	**+3 ºC** [%]	**+4 ºC** [%]
North	8.2	3.7	7.9	15.4	23.5
Central	6.4	3.9	10.0	20.8	32.4
South	5.2	3.9	12.3	28.7	44.5

Table 4.6 *The preindustrial 99th percentile threshold for boreal summer precipitation. Per definition, 1% of the preindustrial dataset lies above the 99th percentile. For each global warming level, the 99th percentile is used in calculating the percentages of each dataset located above this threshold. Calculated for each region.*

	Preindustrial 99% [mm/day]	**+1 ºC** [%]	**+2 ºC** [%]	**+3 ºC** [%]	**+4 ºC** [%]
North	9.0	1.31	1.57	1.75	1.74
Central	7.3	1.24	1.44	1.56	1.76
South	6.4	1.14	1.14	1.04	0.99

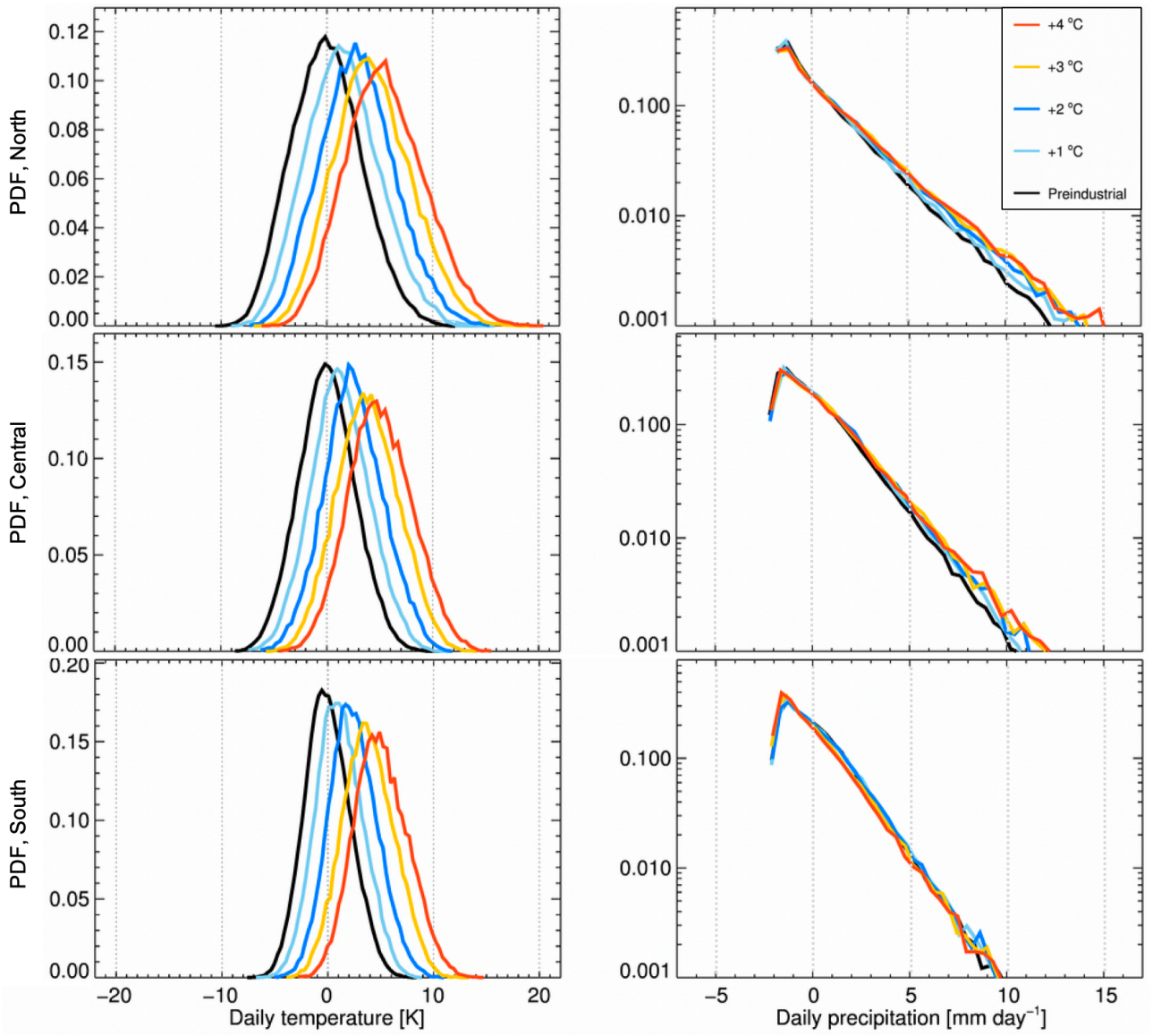

Figure 4.5 *PDFs of daily temperature (left) and precipitation (right) variability for boreal summer (JJA). We have PDFs for the five different climate states; Preindustrial (Black) and the four global surface temperatures +1 °C, +2 °C, +3 °C and +4 °C, in light blue, blue, yellow and orange respectively. From the top, we have the regions; northern (top), central (centre), and southern Scandinavia (bottom). All numbers are relative to the spring mean at preindustrial conditions.*

4.3.4 Boreal Autumn

The boreal autumn also has a Gaussian shape in the temperature PDFs and higher variability in the northern regions (Figure 4.6). With increasing global temperatures, we see similar behaviour as spring in both temperature and precipitation, except for narrower temperature distributions in central and southern Scandinavia. All regions are projected to have a narrowing of the distributions and a shift of the daily temperature mean towards higher temperatures, resulting in warmer climate states with less variability. Like previous seasons, we observe a loss of cold autumn extremes, especially in the northern region. Southern Scandinavia has the biggest shift in the high tail for the autumn season, with approximately 35% of the +4 ºC warming dataset above the preindustrial 99-percentile threshold (Table 4.7). For precipitation in Table 4.8, all regions are predicted to have a widening of the high tails during the autumn season. This means an extreme precipitation increase as we have higher global surface temperatures, with the most noticeable change being in the northern region with approximately 2.5 times larger probability of extreme precipitation events.

Table 4.7 *The preindustrial 99th percentile threshold for boreal autumn temperatures. Per definition, 1% of the preindustrial dataset lies above the 99th percentile. For each global warming level, the 99th percentile is used in calculating the percentages of each dataset located above this threshold. Calculated for each region.*

	Preindustrial 99% [K]	**+1 ºC** [%]	**+2 ºC** [%]	**+3 ºC** [%]	**+4 ºC** [%]
North	10.2	2.2	3.3	6.1	10.4
Central	7.6	3.2	6.2	11.2	19.4
South	5.8	4.1	9.7	20.4	34.7

Table 4.8 *The preindustrial 99th percentile threshold for boreal autumn precipitation. Per definition, 1% of the preindustrial dataset lies above the 99th percentile. For each global warming level, the 99th percentile is used in calculating the percentages of each dataset located above this threshold. Calculated for each region.*

	Preindustrial 99% [mm/day]	**+1 ºC** [%]	**+2 ºC** [%]	**+3 ºC** [%]	**+4 ºC** [%]
North	8.0	1.45	1.80	2.33	2.47
Central	7.6	1.27	1.72	2.00	2.25
South	6.8	1.22	1.48	1.88	2.20

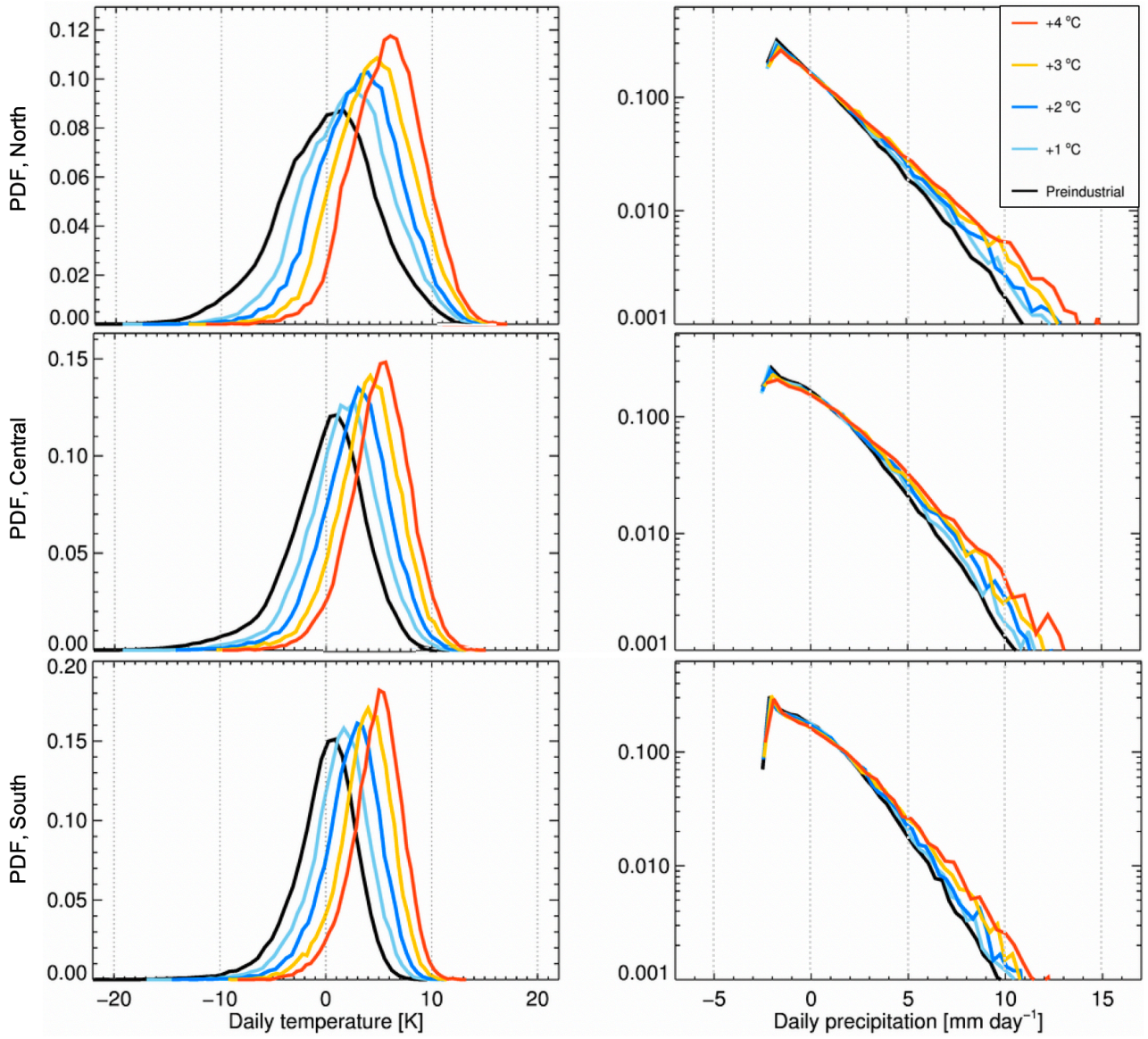

Figure 4.6 *PDFs of daily temperature (left) and precipitation (right) variability for boreal autumn (JJA). We have PDFs for the five different climate states; Preindustrial (Black) and the four global surface temperatures +1 °C, +2 °C, +3 °C and +4 °C, in light blue, blue, yellow and orange respectively. From the top, we have the regions; northern (top, central (centre), and southern Scandinavia (bottom). All numbers are relative to the spring mean at preindustrial conditions.*

In all seasons, there is a clear shift in daily temperature PDFs towards the high tails with global warming, translating into an alteration of the preindustrial climate state towards warmer temperatures for all regions and seasons. Narrower temperature distributions are also found in almost all cases, indicating that there will be a smaller range of temperatures in a warmer future, apart from the boreal summer where we see a broadening and an increase in daily variability. For increasing global surface temperatures, the change in precipitation is in most parts positive and increasing in line with a warmer climate. We find a substantial increase in extreme precipitation for all categories, except in southern Scandinavia which, shows a small decrease in extreme precipitation during summer.

4.4 Day-to-Day variability with Arctic sea ice extent

In this section, we present PDFs of the daily surface temperature and precipitation variability, with respect to levels of Arctic sea ice extent; high, low and normal. We compare monthly results for the regions of Scandinavia. It is important to note that we only analyse data from the preindustrial period to isolate the effects of natural day-to-day variability from the variability created from anthropogenic influences. As we also have sorted years into three different Arctic sea ice levels, the temporal evolution is lost, and we cannot analyse the correlations across the years. This means that we can only analyse interactions within each year and not interactions between one year and the next. Therefore, we have chosen to analyse how Arctic sea ice extent in March and September correlates to the variability in each month during the year. March and September are chosen since they are the months which has the highest and lowest quantities of Arctic sea ice concentrations.

The upper and lower limits of sea ice extent were initially set with the 5-95% interval which, would be characterised as the normal sea ice extent. All above the 95^{th} percentile is classified as high sea ice extent, and all below the 5^{th} percentile is classified as the low sea ice extent. These results can be seen in appendix A.1 and A.2. We found that, with these strict limits, results ended up being very chaotic, probably due to the small number of years landing on the outside of the 5-95% interval. Therefore, we lowered the limits so that the normal sea ice extent would lie within one standard deviation of the mean, or approximately 68%. For March the one standard deviation interval goes from the lower limit of 1326×10^4 km^2 to the upper limit at 1381×10^4 km^2, for September, on the other hand, the lower limit is located at 464×10^4 km^2 and the upper limit at 557×10^4 km^2.

4.4.1 Day-to-Day variability in the months of March and September

For March and September, the most prominent relationship between temperature and sea ice extent can be found in the northern regions, especially for the sea ice extent in March (Figure 4.7). We can see that the light blue line is narrower and shifted more towards the right, meaning that with higher March temperatures we will have a reduction in the March sea ice. Higher temperatures in Scandinavia influence the Arctic by lowering the sea ice extent. The dark blue line, on the other hand, is shifted towards the left and colder temperatures. This shift means that for colder daily temperatures during March, we will also have an increase in Arctic sea ice. There are similar shifts for the central (yellow) and southern regions (red) as well, but not to the same extent as northern Scandinavia. We do not see a similar connection in September (Figure 4.8), where the lines are on top of each other and hard to separate. This means that the September day-to-day temperature variability does not influence the Arctic sea ice extent during September.

We see the strongest correlation in the northern Scandinavia, where there is a significant difference between the PDFs for high and low Arctic sea ice. This can be caused by the regions more Arctic climatic zone and more in direct contact with the same atmospheric and oceanic systems. The signal can also be seen in central and southern Scandinavia, just slightly weaker. For September (Figure 4.8), which is the month with the lowest Arctic sea ice extent, we cannot detect any prominent signal in the daily variability in temperature or precipitation. During this period, there are most likely other processes playing a more significant role in influencing the daily variability. It is also difficult to separate the cause and effect, in this case, to assess whether the sea ice influences the daily temperature, or if the temperature influences the sea ice extent.

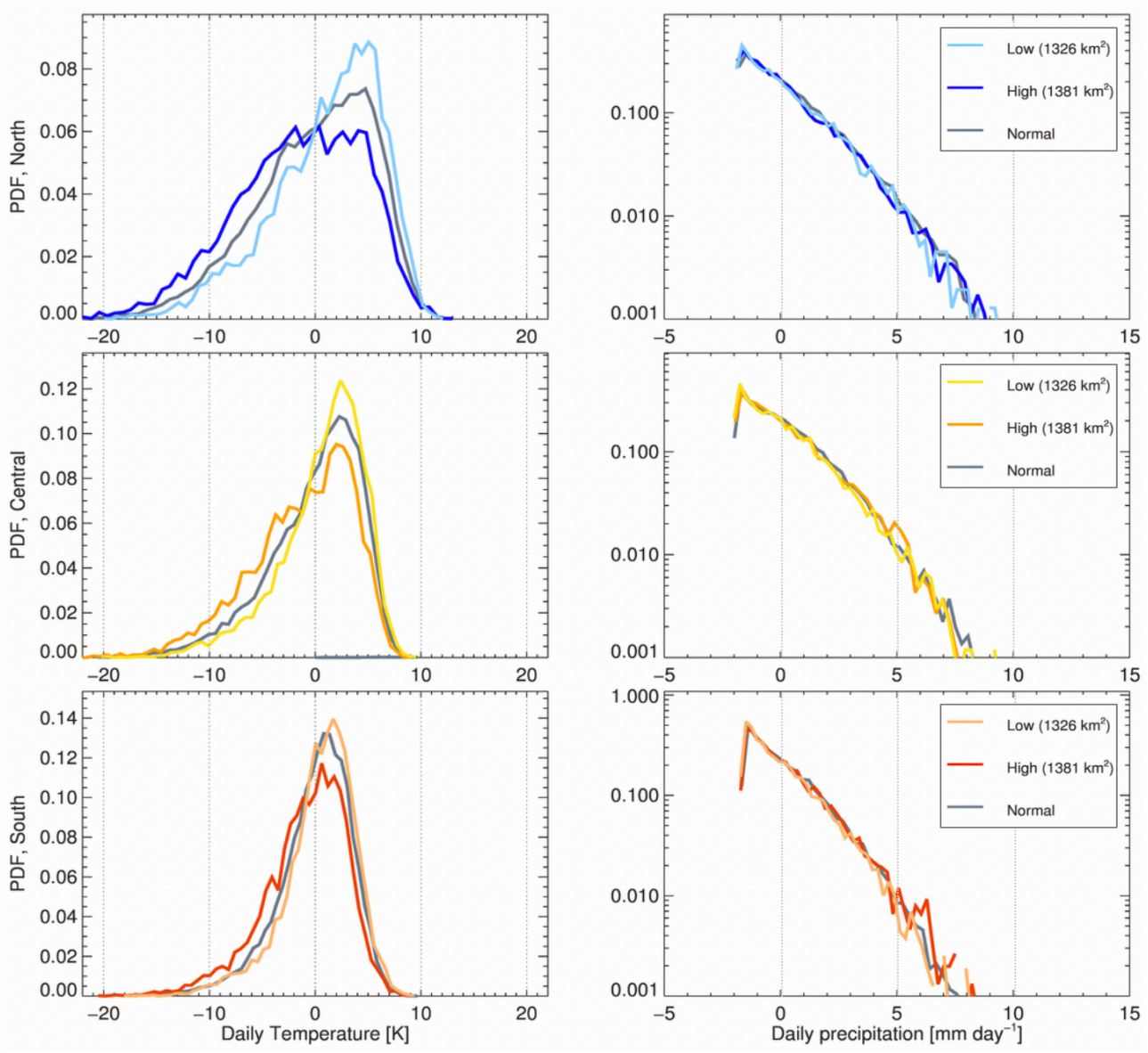

Figure 4.7 *PDFs of daily temperature (left) and precipitation (right) variability for the month of March, with normal (grey), high (dark colour) and low amounts (light colour) of sea ice extent in $\times 10^4$ km^2. The upper and lower limit is calculated as one standard deviation away from the mean sea ice extent. From the top, we have the regions; northern (top, central (centre), and southern Scandinavia (bottom). All temperature and precipitation values are relative to the mean at preindustrial conditions.*

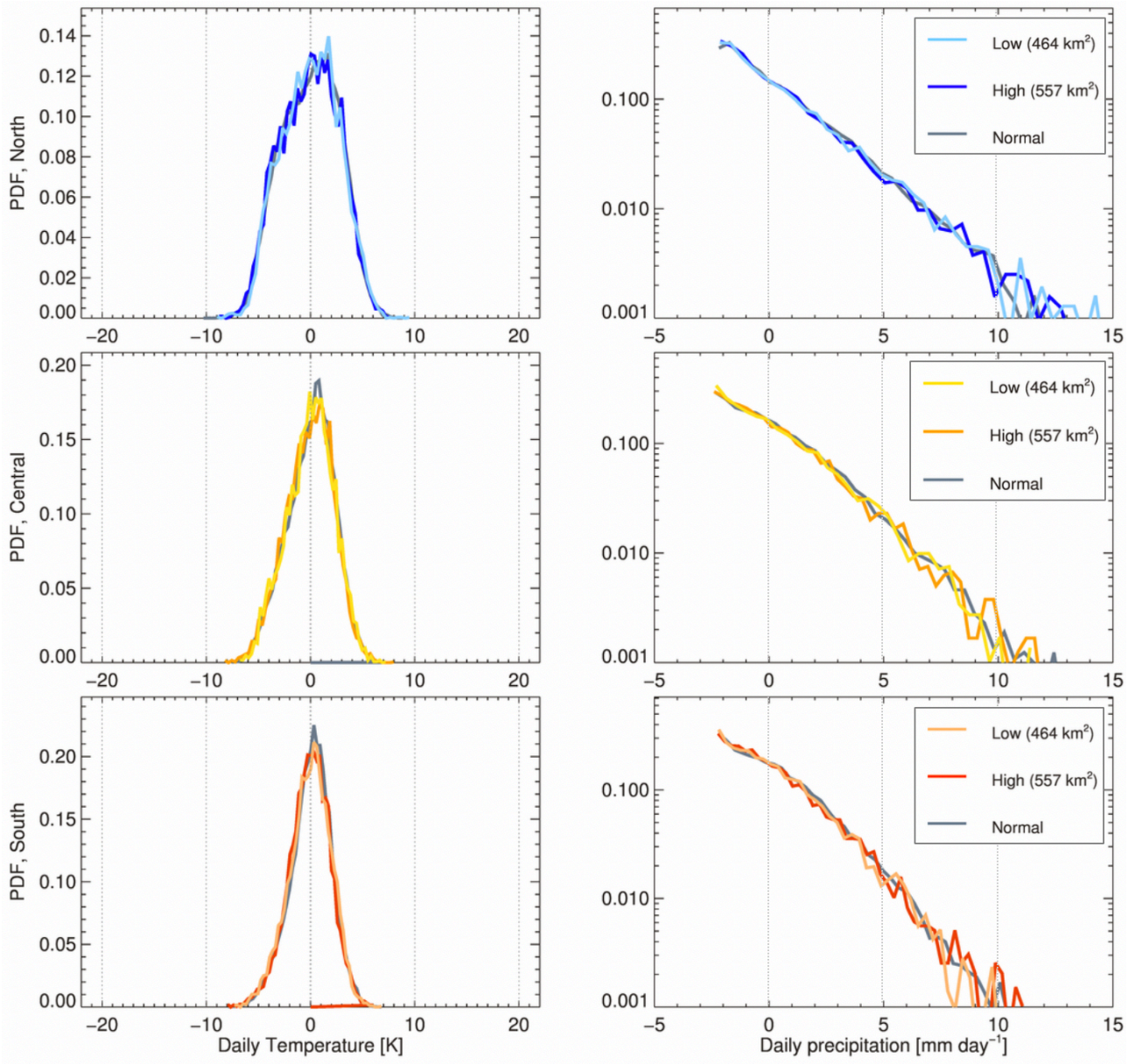

Figure 4.8 *PDFs of daily temperature (left) and precipitation (right) variability for the month of September, with normal (grey), high (dark colour) and low amounts (light colour) of sea ice extent .The upper and lower limit is calculated as one standard deviation away from the mean sea ice extent in $\times 10^4$ km^2. From the top, we have the regions; northern (top), central (centre), and southern Scandinavia (bottom). All temperature and precipitation values are relative to the mean at preindustrial conditions.*

4.4.2 Day-to-Day variability during the winter months

When analysing the evolution of daily variability throughout the year, the most apparent connection and a correlation between Arctic sea ice extent and daily weather variability in Scandinavia can be seen during the winter seasons for all regions (Figure 4.9). We can see that a shift towards higher temperatures (to the right) during the three months; January, February and March leads to less sea ice extent in March (light coloured lines). For colder day-to-day temperatures (shifted to the left) we also get more sea ice extent in the Arctic (dark coloured lines). This points to the daily temperatures influencing the sea ice extent, and not the other way around. We have also analysed the rest of the months, which can be seen in greater detail in the appendix (A.3-A.8). Due to the precipitation having a high intrinsic variability, we have chosen to focus our attention on the temperature, which shows the most noticeable changes in relation to the Arctic sea ice extent.

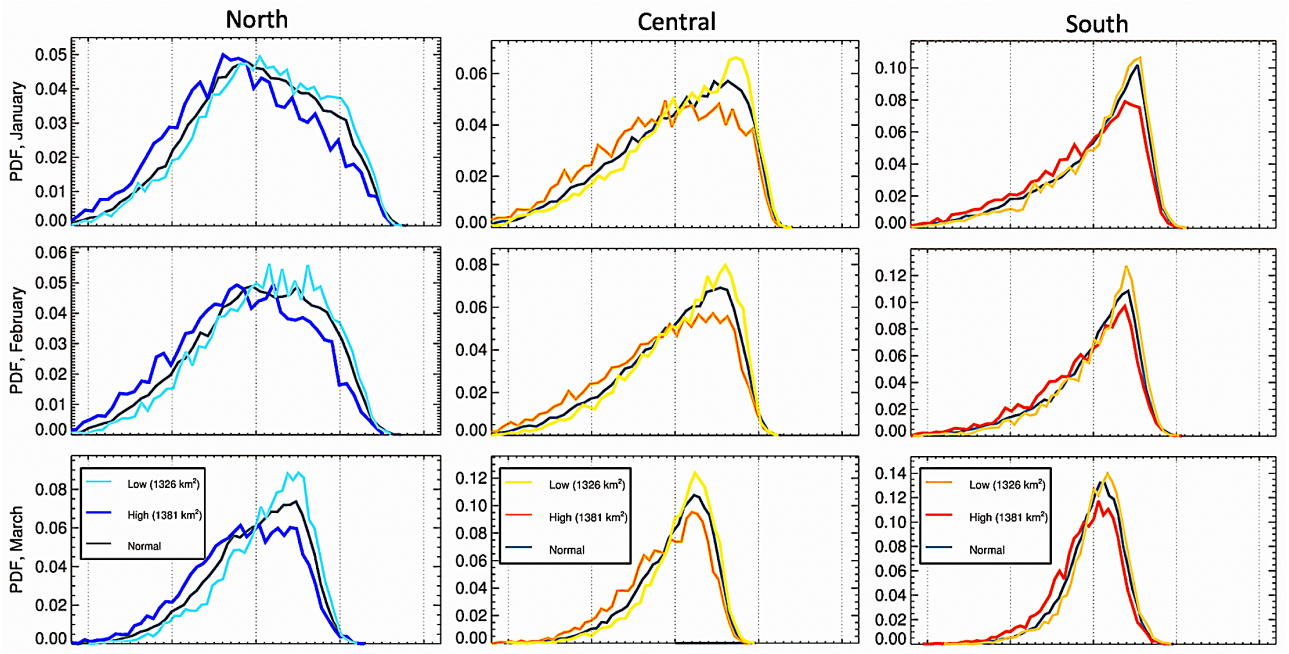

Figure 4.9 *PDFs of daily temperature (left) variability for the months of January, February and March, and the March sea ice extent, with normal (grey), high (dark colour) and low amounts (light colour) of sea ice extent. The upper and lower limit is calculated as one standard deviation away from the mean sea ice extent* $in \times 10^4\ km^2$. *From the left, we have the regions; northern, central and southern Scandinavia. All temperature values are relative to the mean at preindustrial conditions.*

We have also studied how the Scandinavian temperatures affect the sea ice extent in September, which is the period of the year with the least amount of sea ice. From Figures A.9 to A.14 in the Appendix, we can see that in the months leading up to September, there is no indication for a similar correlation between the summer temperature and September sea ice extent as for the winter temperatures and sea ice extent in March. However, it is possible to see a similar correlation between winter temperature and September sea ice, indicating that winter temperatures have an overall stronger signal for both September and March sea ice.

In general, it is difficult to say how the daily variability correlates to the Arctic sea ice extent in March and September. However, the most prominent relationship can be found during the winter season. Higher temperatures in Scandinavia influences the Arctic by lowering the amount of sea ice extent in March. For lower temperatures, there is also the opposite effect of increasing sea ice extent the following March.

4.5 Reanalysis

In order to validate the model output from the CESM LENS, we have compared the preindustrial and +1 ºC warming level with the ERA5 dataset, which at the time of writing runs from 1979 to 2018. In Figure 4.10, we combine the daily temperature from the three datasets and compare the shapes of the PDFs. The +1 ºC will be slightly shifted to the right due to its use of the preindustrial run as its baseline. Therefore, we will only look at the overall shape of the distributions and not changes due to this shift.

From Figure 4.10, we see that there are prominent differences in the boreal winter for all regions. The model output has a more significant shift towards higher temperatures and has larger temperature variability, especially in the northern Scandinavia. For the rest of the seasons in central and southern Scandinavia, the model is in good agreement with ERA5 and gives a good prediction. The predictions for the winter season do not seem to have the same good agreement, with ERA5 having a narrower distribution for all seasons. This result gives an indication that the CESM LENS model does not correctly reproduce winter season climates and climate processes, especially for northern Scandinavia.

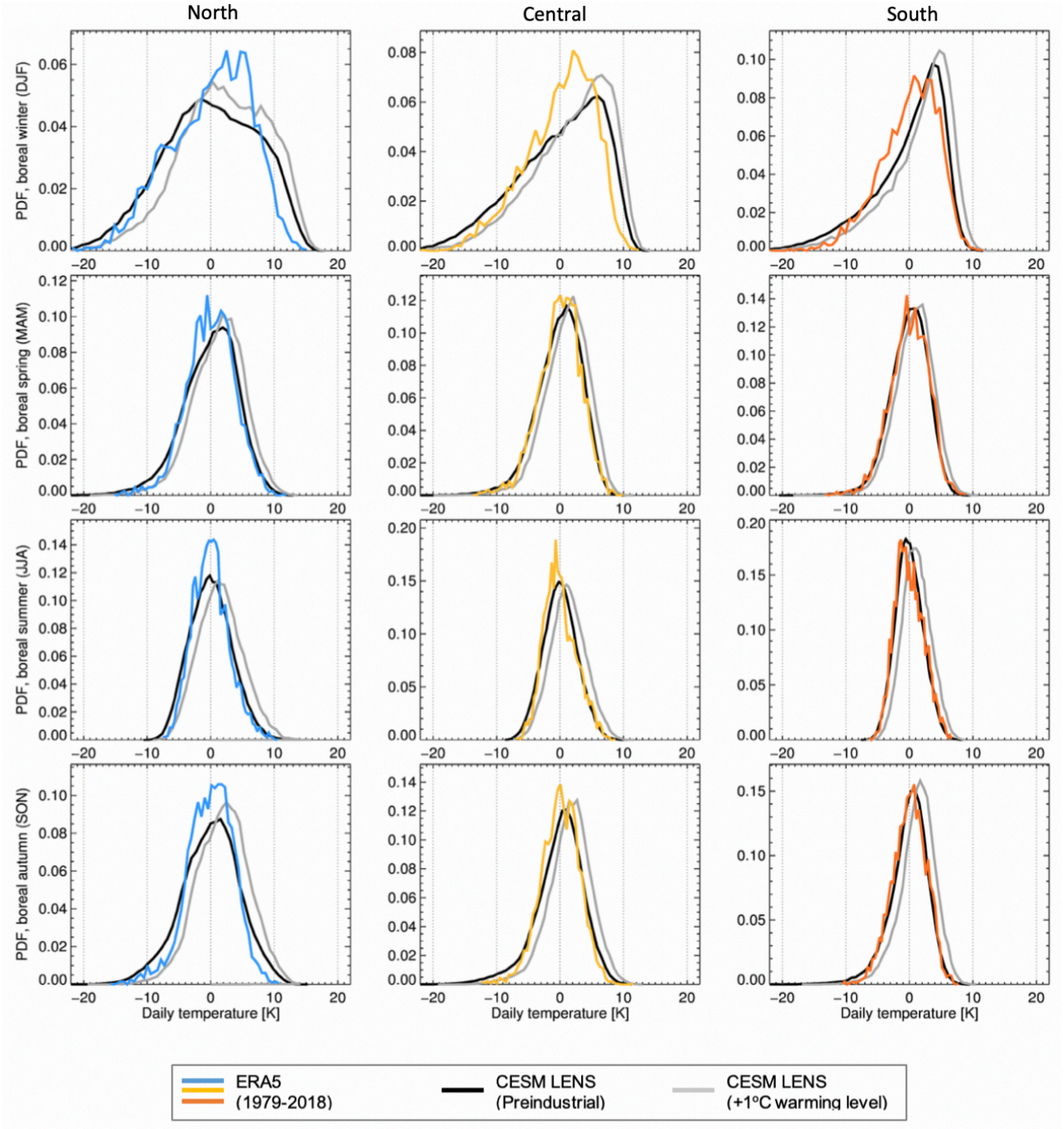

Figure 4.10 *Reanalysis with CESM LENS (preindustrial) in black, CESM LENS +1 °C in grey, and ERA5 in colour. From the left, we have the regions; northern, central and southern Scandinavia. From the top we have the boreal seasons, winter, spring, summer and autumn.*

5 Discussion

In this section, we will discuss the results of the previous section and compare them with previously executed studies. We begin with the results from the fixed versus coupled model comparison, then the daily variability with global warming, followed by daily variability with sea ice extent and reanalysis. We round up the section with a discussion around possible uncertainties.

5.1 Fixed SST vs coupled modelling

The Scandinavian climate is substantially influenced by both atmospheric and oceanic variability, through modes of variability such as NAO (primarily atmospheric) and the AMO (predominantly oceanic). Hence, we would expect that a correct representation of Scandinavian day-to-day weather would depend on dynamical modelling of both the atmosphere and the ocean. However, in section 4.2, we found that there is little difference between the modelling output with the two setups for this particular model. Independent analysis shows that this is the case also for other regions than Scandinavia (not shown here). Since Scandinavia also has such close proximity to adjacent water masses like the North Atlantic and the Nordic Seas, the daily variability would intuitively be influenced by removing the oceans dynamical properties.

As a further example, when a natural or anthropogenic forcing influences the Earth system, we can have both fast responses, covering time scales of days to weeks, or slow responses, covering longer timescales (Myhre et al., 2016). The atmospheric component can have fast changes in variability and reacts quickly to atmospheric forcing. The ocean, on the other hand, has a large thermal capacity, making it react slower to changes. By running a comparison between fixed SST and coupled simulations, we hopefully separate these two responses, by fixed SST having more of the fast responses and the coupled simulations having both fast and slow responses. This may serve as a reason for why we would expect differing distributions from the two simulations. With fixed SST, we should lose the larger variations caused by the link between ocean and atmosphere, which in turn would change the resulting PDFs. Instead, we find nearly identical distributions over the preindustrial period.

Performing a similar comparison, Liu & Wu (2004) analysed how the atmosphere responds to North Pacific December SST anomalies by comparing a fully coupled ocean-atmosphere general circulation model run with a fixed SST run. They showed that atmospheric variability depends on the coupling between ocean and atmosphere, creating a significant temperature difference between the coupled and fixed SST run, which is in contrast to what we have found here. Rodwell et al. (2004) showed that the North Atlantic atmosphere drive much of the SST variability during intraseasonal and interannual timescales. However, at longer timescales, this relationship could be flipped around, with SST anomalies influencing the atmospheric climate variability. A similar result could be found for the Norwegian sea, with the SST having possibilities for climate predictions on a decadal scale for surface air temperature and precipitation over Norway (Årthun et al., 2017). According to (Barsugli & Battisti, 1997), when considering decadal timescales, most of the effects of coupling between the midlatitude atmosphere and ocean gives the result of reduced temperature damping. For intraseasonal and interannual timescales, on the other hand, the atmosphere is the primary source of variability in the climate system.

As previously mentioned, in a coupled run, the ocean consists of large masses of water with very slow dynamics. For changes to occur in the SST, the forcing would need to be very strong, or last for more extended periods. Over shorter periods, however, such as on monthly time scales, the ocean can mimic an infinite heat sink due to its vast heat capacity, especially during winter when the mixed layer is deep (Barsugli & Battisti, 1997). This property of being an infinite heat sink is similar to the effect of having fixed SST during a model run (Sutton & Mathieu, 2002). In the situation of fixed SST, the atmospheric variability will be significantly dampened because the water absorbs a vast amount of energy without increasing its temperature. Consequently, there will not be heat fluxes going back into the atmosphere and no positive feedback – producing less variability in the atmosphere.

Considering that both of our simulations are with the preindustrial climate, there will perhaps not be substantial changes to produce large enough ocean variability to influence the atmosphere. Thus, the fixed SST can give the same distribution as a fully coupled model. For future anthropogenic changes, however, the ocean may not work as an infinite heat sink and play a larger role in how the daily weather variability evolves. The exact reason why the PDFs have practically identical characteristics has not been identified, and this result is worth exploring further.

5.2 Day-to-Day Variability in Scandinavia

In section 4.3, we found that for the day-to-day variability there is a shift towards warmer climate states for all boreal seasons, reduced temperature variability during the winter, spring and autumn, and an increase in summer variability. In the case of precipitation variability, we found an increase in extreme events across all seasons, except for southern Scandinavia during summer.

Increases in both regional temperature and precipitation with warming levels are in line with the fifth assessment report from IPCC (Kovats et al., 2014). Northern Scandinavia, with a significant narrowing and loss of cold extremes, stands out with the most substantial changes in the shape of both the daily PDFs for temperature and precipitation, especially for the winter season. Several other studies reached similar results for the boreal winter. By analysing an Atmosphere-Ocean General Circulation Model, Førland et al. (2009) found that, at the end of the 21st century, warming of the Arctic and northern regions is strongest during winter and autumn. Holmes et al. (2016) established that during winter, the temperature variability will decrease with future anthropogenic changes. Fischer et al. (2012) utilised global and regional models from the ENSEMBLES project. They also found that at the end of the 21st century, northern Europe will experience a decrease in winter variability, and more specifically, they showed that the cold extremes would warm faster than the mean. These findings are consistent with our results of a narrowing winter distribution and the faster loss of extreme cold temperatures compared to the increase in warm extremes, with the northern Scandinavia being the most prominent.

According to (Masato et al. (2014) this reduction in cold extremes in northern Europe might be due to weaker temperature gradient between equator and the Arctic and a negative phase of the NAO. Deser et al. (2017) also conclude with NAO having a dominant role in European winter temperature variability with increasing global warming. Dai et al. (2019), on the other hand, suggest that the decrease in Arctic sea ice has a more pronounced influence and will lead to increasing A during the cold season. This will consequently lead to reductions in the amount of extremely cold temperatures in the Arctic region and make it increasingly similar to more southern climates. Since the Northern Scandinavia is located at higher latitudes and is within the Arctic regions, the AA might influence this area more than the central and southern regions.

In contrast to the other seasons, in addition to a shift towards warmer daily temperatures, the summer season displays a widening of the temperature PDFs for each of our regions, meaning an increase in daily variability with increasing global surface temperatures. Fischer et al. (2012), Kovets et al. (2014) and Suarez-Gutierrez et al. (2018) showed that the summer variability in southern and central Europe will increase as the hot extremes warm faster than the mean. This suggests that in our analysis, southern Scandinavia might have similar future weather characteristics as the more southern parts of Europe. When analysing changes in monthly surface temperature variability with increasing GHG emissions, Holmes et al. (2016) also found that during summer, the variability over land areas in the midlatitudes will increase. They point to thermal advection as an essential mechanism to explain these patterns in monthly variability. Coumou et al. (2018), however, point to AA as a primary contributor to European summer temperature variability. They show that due to increasing AA we will have a weakening in the westerlies and storm tracks, resulting in more persistent hot and dry extremes.

Both Hall et al. (2017) and Trouet et al. (2018) show that the location of the North Atlantic Polar front jet is crucial for prediction of summer weather. Utilising two tree-ring records to analyse the Polar jet variability, Trouet et al. (2018) show that during recent years we have a northward shift of the summer jet stream and an increase in interannual meridional movement, or more Rossby waves. More Rossby waves lead to more frequent blocking pattern, resulting in increasing heatwaves and droughts in northern Europe.

In the case of precipitation, we see a marked increase in daily variability in almost all of our regions, which is consistent with IPCC (Kovats et al., 2014). The only exception is in southern Scandinavia, which shows a small decrease in extreme precipitation during summer. Førland et al. (2009) also show an increase in northern region precipitation for all seasons, specifically in winter and spring. Nevertheless, it is important to note that precipitation in this region is already low, and a substantial increase can thus lead to only a small increase in daily precipitation. Even though precipitation gives a weaker signal to future global warming than temperature, Mahony & Cannon, (2018) found that dependencies between precipitation and different climate parameters create more substantial departures from natural variability than if the same parameters are viewed separately. This suggests that mechanisms of precipitation change are intricate and.

5.3 Day-to-Day variability correlations with Arctic sea ice extent

We have presented distributions for regional daily temperature and precipitation for high, low and normal Arctic sea ice extent. To be able to isolate the effects of natural daily variability from anthropogenic influences, we only used data from the preindustrial period. Due to the high degree of intrinsic variability in daily precipitation, leading to difficulties in extracting a signal for weak internal forcing such as sea ice changes, we chose to focus our analysis on the temperature variability. For March and September, the most prominent relationship between Arctic sea ice extent and temperature variability can be found in the northern regions, which is within the Arctic. We find a more pronounced relationship between the March sea ice extent and daily temperature variability during the winter months; January, February and March. Higher (lower) temperatures in Scandinavia reduces (increases) the amount of Arctic sea ice. The remaining months did not give a clear signal between the two, suggesting that the temperature variability influences the amount of sea ice in March and that the reversed situation of sea ice influencing temperature variability is not as crucial for intra-annual time scales.

Koenigk et al. (2019) studied how variations in the Arctic sea ice influenced interannual winter temperatures in northern Europe land areas. They found that the main reason for extremely cold winters is not sea ice variability but variability in atmospheric dynamics, which is broadly consistent with our results. They also show that reduced sea ice in late summer has a link to a negative phase in NAO the following winter. Hall et al. (2017) also investigated a connection between reduced sea ice in late summer/autumn, which they found to result in decreased North Atlantic polar jet latitude and speed the following summer. Hence, a link between autumn sea ice extent, when the sea ice is at its lowest, and the following year might be possible, but due to our way of sorting years into categories of sea ice makes such analysis difficult within the present analysis.

Even though this thesis does not look at how this correlation might change with future anthropogenic changes, several studies have analysed the connection between future global warming and reduced Arctic sea ice extent and its effect on Scandinavian weather and climate. According to the newest special report on the ocean and cryosphere from the IPCC, the evolution with reduced sea ice extent is highly uncertain and dependent on our emission and mitigation path

in the coming years (Meredith et al., 2019). They also show that from the year 2050, different paths of sea ice reduction appear. However, in general, due to AA there will be a higher future increase in Arctic surface temperatures than for the rest of the globe, which will leading to a considerable reduction in Arctic sea ice and changes in large circulation systems.

Due to the ice-albedo-feedback, we will have enhanced melting and increased ocean upper mixed layer temperature during summer. Even though we have the most reduction in sea ice extent and increase in SSTs during summer and early fall, the response in air temperature and precipitation over adjacent continents is strongest during winter (Deser et al., 2010; Overland & Wang, 2010). This response is due to air surface temperatures dropping below SST temperature, and the excessive heat from the ocean is released as longwave radiation, heating the lower troposphere. Higher temperatures lead to a decreased equator-pole temperature gradient, which affects the circulation patterns. Coumou et al. (2018), points to a weakening in the westerlies and storm tracks, resulting in more persistent hot and dry extremes during summer. By analyzing two tree-ring records, Trouet et al. (2018) also found that the combination of future sea ice decline and increasing AA lead to; a northward jet stream shift, increased meridional jet stream, increase in atmospheric blockings, and higher frequency of heatwaves and droughts.

Moreover, Petoukhov & Semenov (2010) and Nakamura et al. (2015) show that reduced Arctic sea ice during the winter season can promote a negative phase of the NAO and AO, and abnormal easterly winds. Consequently, we will have a more meridional jet stream and cold air advected from the Arctic, causing a higher probability of cold winter extremes over Northern Europe. Another factor is the effect from the melting freshwater from the sea ice on ocean circulation. Increasing SST and a reduction in salinity due to more freshwater, can induce more stability in the ocean and a weaker AMOC (IPCC, 2013). This weakening may contribute to less heat transported to Scandinavia, and according to Hanssen-Bauer et al. (2009), the annual average temperatures in Norway can have a reduction of 5-10 ° C. However, they establish that this is highly unlikely.

Our findings show no significant correlation of the sea ice extent on Scandinavian variability at intra-annual timescales. However, as discussed here, this relationship can change with increasing anthropogenic global warming and a more substantial reduction in Arctic sea ice. In Scandinavia, this can lead to more persistent hot and dry extremes during summer and cold extremes during winter, and, even though highly unlikely, a weakening of the AMOC.

5.4 Reanalysis

Comparing the daily temperature distributions of the preindustrial and +1 ºC warming level from CESM LENS (preindustrial and +1ºC) with the reanalysis from ERA5 gave some interesting results. We found the most prominent differences during boreal winter for all regions, especially in northern Scandinavia. For almost all seasons in central and southern Scandinavia, the model is in good agreement with ERA5 and gives a good representation of current daily variability in surface air temperature. This result is consistent with other studies such as Rondeau-Genesse & Braun (2019), wh found that while biases do exist in CESM LENS, the ensemble adequately reproduces the spatial patterns of observed surface air temperature as well as the interannual variability.

The representation for the winter season does not seem to have the same good agreement, with ERA5 having a narrower distribution for all seasons. This result indicates that the CESM LENS model does not correctly reproduce winter season climates and climate processes, especially for northern Scandinavia. When analysing the NAO with the CESM LENS, Deser et al. (2017), found that both the spatial patterns and amplitudes of surface air temperatures are consistent with the observations at almost all locations. Exceptions are some regions, like central Europe, which have higher temperature anomalies in the simulations compared to observations. This is in line with our results, mainly during the winter season, where we have higher frequencies in warmer temperatures (Figure 4.10). McKinnon et al. (2017) comes to similar conclusions for North America during winter focuses and suggests that the CESM LENS internal variability in surface air temperature is largely overestimated over the period 1966 to 2015.

Dai & Bloecker (2019) analyse two fully coupled climate models to quantify how internal climate variability influences surface air temperature and precipitation. They found that the CESM1 LENS global mean was statistically comparable with observations in temperature and precipitation during 1979-2014, but this is not the case for local precipitation. Also studying precipitation, Pendergrass and Deser (2017), compared distributions from CESM1 to satellite observations, finding that the model has a higher frequency of light rain, especially over subtropical oceans. Further, they suggest that this could be due to inadequate representation of stratocumulus clouds in the model. Nonetheless, they conclude that there are gaps in CESM1 representation of rain frequency distributions.

In this thesis, we analyse and compare quite small spatial regions, which can explain the differences between the model and ERA5 reanalysis. The resolution of the CESM1 might be too coarse to resolve important regional processes in Scandinavia correctly. Since northern Scandinavia have the most significant difference, maybe these local processes have a bigger influence here. Another factor might be that specific processes influencing the northern climate are poorly represented in the model, giving the simulation an underqualified interpretation of the actual weather and climate. This poor representation of the daily variability may be a problem for CESM1 alone. It is also important to note that ERA5 is also a model and built with a combination of observations and estimations, meaning that it is not necessarily a perfect representation of real-life.

5.5 Uncertainty

The results displayed in this thesis are based upon a single large model ensemble and not intercomparison projects like CMIP5, which contains several models. Uncertainty in results may arise from distinctions and deficiencies in setup and representation of real physical processes, which may differ from one model to another or between the real world and models. Rondeau-Genesse and Braun (2019) found that the equilibrium climate sensitivity (models increase in temperature in response to a doubling of CO_2 concentration) for CESM1 is above the CMIP5 average, which is likely to affect the rate of mean global warming. However, Kay et al. (2015) noted that for winter surface air temperature, the CESM1 has a similar spread in North America as the CMIP5.

As previously mentioned in section 2.3.1, the North Atlantic Oscillation is the dominant mode of atmospheric variability in the Scandinavian region. It greatly influences local weather parameters like temperature, precipitation and wind due to changes in intensity and location of the North Atlantic Polar jet stream and the associated pressure systems. If the NAO is not adequately represented in the CESM1 LENS, this can lead to dissimilarities between the model output and the ERA5. Therefore, the representation of the NAO in the CESM1 is crucial for our results. However, we have not validated the NAO representation in the CESM1. However, Deser et al. (2017) compared the NAO variability over Europe from the historical portion of the CESM1 LENS with observations. They found, given the observational record length of that is available, the model produces a credible interannual NAO. However, due to the observational record being short, it will not be possible to validate for longer NAO trends which might induce uncertainty.

Since Scandinavia consists of both continental regions in the east and coastal areas in the west, there can be major differences in weather and climate at local spatial scales, resulting in large temperature gradients. Førland et al. (2009), also showed that the continental areas would experience higher amounts of warming than the coastal counterparts. Impacts like heatwaves and droughts can thus be much more severe in the eastern parts of Scandinavia. These kinds of conditions can have a very high societal impact risk and understanding and prediction at a local scale are therefore essential. CESM LENS might not have a good enough resolution to correctly resolve important and local processes. Therefore, a regional climate model might be more appropriate.

As a part of this analysis, we chose to sort the years into warming levels and sea ice levels. Thus, the temporal signal between years is lost, and we cannot analyse the correlations across years or longer timescales. We cannot find correlations between processes that have variability over several years, but it makes it possible to identify patterns for years with similar characteristics. By making this design choice of sorting the years into levels, some results are challenging to extract. However, it is important to note that by changing this design, the CESM LENS dataset can easily be analysed in other ways.

6 Conclusion

Unpredictable internal variability can both amplify or decrease future changes in the climate when added with anthropogenic climate change. In some cases, the internal variability can also surpass and hide the anthropogenic signal. This is especially observed for higher latitudes as well as on local scales, such as Scandinavia, which can have weather and climate patterns significantly differing from the global means. Future changes in average climate quantities have already been investigated thoroughly, but changes to daily weather parameters have not been studied as much. Thus, the purpose of this thesis was to investigate Scandinavian day-to-day variability of temperature and precipitation, in correlation to future global warming and sea ice extent. The distributions are resolved for all seasons and the three regions; northern, central and southern Scandinavia. We utilized the 30-member CESM1 Large Ensemble with historical and RCP 8.5 emissions for the period 1920-2100. The ensemble members are subjected to the same radiative forcing but begin from slightly different climatic states in 1920, resulting in a spread that mimics stochastic variability. By utilising PDFs, we have presented the evolution of daily variability in temperature and precipitation.

Key findings for day-to-day variability with warming levels:

- For all regions and future boreal seasons, we find a shift of the daily temperature mean towards a warmer climate state, increasing with higher global warming levels.
- Temperature distributions become narrower for all seasons, except for boreal summer which has a broadening and thus an increase in day-to-day variability.
- Northern Scandinavia has the most substantial changes in PDFs, with decreased variability in the future due to a pronounced reduction in cold extremes.
- For almost all regions and future boreal seasons, we find an increase in the likelihood of extreme precipitation, except for southern Scandinavia during summer, which experiences a slight decrease.

Key findings for daily variability with Arctic sea ice levels:

- Prominent correlations are found between boreal winter temperatures and the March sea ice. Higher and lower (lower) temperatures in Scandinavia will respectively reduce or increase the Arctic sea ice extent.
- Arctic sea ice is most likely not the primary driver of daily variability in Scandinavia.

Further, we have compared fixed sea ice temperature (SST) model simulations with fully coupled runs and find that they are virtually identical, pointing to the need for further investigation. To validate the model, we have used the ERA5 climate reanalysis dataset, which shows good agreement for central and southern Scandinavia, but discrepancies in the northern regions.

We need to properly understand how internal intrinsic variability interacts with anthropogenic climate change on a local scale, in order for us to prepare for future risks and impacts. Moreover, we need to understand what drives this variability, which will be different depending on the location of the region and the processes influencing it. Such analysis is vital if we want to project and predict future changes in weather and climate adequately. Through studying literature, a number of the links identified in this thesis were expected. Nevertheless, we underline the importance of studying not only average properties but the full distributions, as well as incorporate internal variability. Further investigation of possible causal mechanisms and links are also needed, which is explained in better detail in the next section.

7 Further study

For future work, several issues and topics should be explored further. The most natural expansion of this study may be to investigate the correlation across years and see if the sea ice correlation acquires a different result. This expansion would be particularly interesting for the late summer/early autumn sea ice and the following year.

Another possible direction is comparing and changing the type of model and resolution to get more reliable results. The CESM1 LENS has a 1° x 1° horizontal resolution, which makes each grid box approximately 100 km x 100 km. Such coarse resolution is sufficient for modelling large-scale features but makes it necessary to parameterise many sub-grid scale processes. Thus, results should be interpreted with caution. A possible expansion would be using models or regional climate models with higher resolution, which would achieve better approximation when compared to observations. This change would correctly resolve for atmospheric and ocean processes, which cover smaller and more local spatial scales, such as convection and land-surface processes (Fischer et al., 2012; Hentgen et al., 2019).

As mentioned, different models have various setups and representations of real processes and using only one model can lead to biased results. A possible extension could consequently be a validation of the representation of the NAO variability and magnitude from the CEMS1 LENS to ERA5. This is because Scandinavian weather variability is highly influenced by the location and intensity of the North Atlantic Polar jet stream, and thus the strength of the NAO. Another possibility would be to look into Large Ensembles from other models to see if they have similar distributions compared to the CESM1. Analysis of the winter months in the northernmost regions should be particularly illuminating since this is where we find the most marked changes in CESM1 – but also the strongest deviations from ERA5. Model intercomparison projects can also be an option, but in this case, there will be uncertainties related to differences between models. In all cases, there will be a need to validate the overall results against reanalysis and observations.

In this thesis, we have only explored the correlation between day-to-day variability and Arctic sea ice. Exploration of alternative drivers of variability in Scandinavia would be needed in order to project the future weather and climate accurately. Since this study indicate that atmospheric variability in most parts drives the day-to-day variability, interesting correlations could be found for

processes such as the AMO, NAO, the polar front jet and volcanic eruptions. The ocean has undergone much less study, but should also be of interest. An interesting topic would be to determine how the atmosphere responds to Atlantic and Nordic sea-surface temperature variability.

Due to potentially high risk for extreme weather and impact on local scales, we show the importance and significance of further quantifying expected changes to internal variability. Even though our results are subject to uncertainties surrounding a single model like the CESM1 and the relatively low resolution, our method can be expanded for future studies with a focus on other regions. Each region will have distinctive distributions of day-to-day variability due to differences in location, topography, and which models of variability and teleconnections that influence the area.

Another interesting area for further research would be to build possible future storylines for Scandinavia and other regions. When all the different factors influencing a region has been analysed and understood in the best possible way, they can be combined to create possible futures, or storylines. Different storylines can project physically plausible future scenarios which have high societal impacts. They are not necessarily the most likely outcome, but they can give an indication of what can transpire, once specific patterns are combined.

8 References

Aguado, E., & Burt, J. E. (2013). *Understanding Weather and Climate* (6th ed.). https://doi.org/10.1017/CBO9781107415324.004

Barsugli, J. J., & Battisti, D. S. (1997). The Basic Effects of Atmosphere-Ocean Thermal Coupling on Midlatitude Variability. *Journal of the Atmospheric Sciences*, *55*(4). https://doi.org/10.1175/1520-0469(1998)055<0477:TBEOAO>2.0.CO;2

Betts, R. A., Alfieri, L., Bradshaw, C., Caesar, J., Feyen, L., Friedlingstein, P., … Wyser, K. (2018). Changes in climate extremes, fresh water availability and vulnerability to food insecurity projected at 1.5°C and 2°C global warming with a higher-resolution global climate model. *Philosophical Transactions of the Royal Society A: Mathematical, Physical and Engineering Sciences*, *376*(2119). https://doi.org/10.1098/rsta.2016.0452

Burke, K. D., Williams, J. W., Chandler, M. A., Haywood, A. M., Lunt, D. J., & Otto-Bliesner, B. L. (2018). Pliocene and Eocene provide best analogs for near-future climates. *Proceedings of the National Academy of Sciences of the United States of America*, *115*(52), 13288–13293. https://doi.org/10.1073/pnas.1809600115

Casanueva, A., Rodríguez-Puebla, C., & González-Reviriego, N. (2014). Variability of extreme precipitation over Europe and its relationships with teleconnection patterns. *Hydrol. Earth Syst. Sci*, *18*, 709–725. https://doi.org/10.5194/hess-18-709-2014

Coumou, D., Di Capua, G., Vavrus, S., Wang, L., & Wang, S. (2018). The influence of Arctic amplification on mid-latitude summer circulation. *Nature Communications*, *9*(1), 2959. https://doi.org/10.1038/s41467-018-05256-8

Cubasch, U., D. Wuebbles, D. Chen, M.C. Facchini, D. Frame, N. Mahowald, and J.-G. Winther, 2013: Introduction. In: Climate Change 2013: The Physical Science Basis. Contribution of Working Group I to the Fifth Assessment Report of the Intergovernmental Panel on Climate Change [Stocker, T.F., D. Qin, G.-K. Plattner, M. Tignor, S.K. Allen, J. Boschung, A. Nauels, Y. Xia, V. Bex and P.M. Midgley (eds.)]. Cambridge University Press, Cambridge, United Kingdom and New York, NY, USA.

Dai, A., & Bloecker, C. E. (2019). Impacts of internal variability on temperature and precipitation trends in large ensemble simulations by two climate models. *Climate Dynamics*, *52*(1–2), 289–306. https://doi.org/10.1007/s00382-018-4132-4

Dai, A., Luo, D., Song, M., & Liu, J. (2019). Arctic amplification is caused by sea-ice loss under increasing CO2. *Nature Communications*, *10*(1), 121. https://doi.org/10.1038/s41467-018-07954-9

Deser, C., Hurrell, J. W., & Phillips, A. S. (2017). The role of the North Atlantic Oscillation in European climate projections. *Climate Dynamics*, *49*(9–10), 3141–3157. https://doi.org/10.1007/s00382-016-3502-z

Deser, C., Phillips, A. S., Alexander, M. A., Smoliak, B. V., Deser, C., Phillips, A. S., … Smoliak, B. V. (2014). Projecting North American Climate over the Next 50 Years: Uncertainty due to Internal Variability*. *Journal of Climate*, *27*(6), 2271–2296. https://doi.org/10.1175/JCLI-D-13-00451.1

Deser, C., Tomas, R., Alexander, M., & Lawrence, D. (2010). The seasonal atmospheric response to projected Arctic sea ice loss in the late twenty-first century. *Journal of Climate*, *23*(2), 333–351. https://doi.org/10.1175/2009JCLI3053.1

Fatichi, S., Ivanov, V. Y., Paschalis, A., Peleg, N., Molnar, P., Rimkus, S., … Caporali, E. (2016). Uncertainty partition challenges the predictability of vital details of climate change. *Earth's Future*, *4*(5), 240–251. https://doi.org/10.1002/2015EF000336

Field, C. B., Barros, V., Stocker, T. F., Qin, D., Dokken, D. J., Ebi, K. L., … Midgley, P. M. (2012). *Managing the Risks of Extreme Events and Disasters to Advance Climate Change Adaptation. A Special Report of Working Groups I and II of the Intergovernmental Panel on Climate Change*.

Fischer, E. M., Rajczak, J., & Schär, C. (2012). Changes in European summer temperature variability revisited. *Geophysical Research Letters*, *39*(19). https://doi.org/10.1029/2012GL052730

Førland, E. J., Benestad, R. E., Flatøy, F., Hanssen-Bauer, I., Haugen, J. E., Isaksen, K., … Ådlandsvik, B. (2009). *Climate development in North Norway and the Svalbard region during 1900-2100*. https://doi.org/10.3354/cr029255

Giorgi, F. (2002). Dependence of the surface climate interannual variability on spatial scale. *Geophysical Research Letters*, *29*(23), 16-1-16–4. https://doi.org/10.1029/2002GL016175

Hall, R. J., Jones, J. M., Hanna, E., Scaife, A. A., & Erdélyi, R. (2017). Drivers and potential predictability of summer time North Atlantic polar front jet variability. *Climate Dynamics*, *48*(11–12), 3869–3887. https://doi.org/10.1007/s00382-016-3307-0

Hansen, J., Sato, M., & Ruedy, R. (2012). Perception of climate change. *Proceedings of the National Academy of Sciences of the United States of America*, *109*(37). https://doi.org/10.1073/pnas.1205276109

Hanssen-Bauer, I., Achberger, C., Benestad. R.E., Chen, D., & Førland, E. J. (2005). Statistical downscaling of climate scenarios over Scandinavia. *Climate Research*, *29*(3), 255–268. https://doi.org/10.3354/cr029255

Hanssen-Bauer, I., Drange, H., Førland, E. J., Roald, L. A., Børsheim, K. Y., Hisdal, H., … Ådlandsvik, B. (2009). *Klima i Norge 2100*.

Hartmann, D. L., Tank, A. M. G. K., Rusticucci, M., Alexander, L. V., Brönnimann, S., Charabi, Y. A. R., … Zhai, P. (2013). Observations: Atmosphere and Surface. In Intergovernmental Panel on Climate Change (Ed.), *Climate Change 2013 - The Physical Science Basis* (pp. 159–254). https://doi.org/10.1017/CBO9781107415324.008

Hawkins, E., & Sutton, R. (2009). The Potential to Narrow Uncertainty in Regional Climate Predictions. *Bulletin of the American Meteorological Society*, *90*(8), 1095–1108. https://doi.org/10.1175/2009BAMS2607.1

Henderson-Sellers, A., & McGuffie, K. (1987). *A climate modelling primer* (1st ed.). Wiley.

Hennermann, K., & Berrisford, P. (2019). ERA5 data documentation - Copernicus Knowledge Base. Retrieved September 5, 2019, from https://confluence.ecmwf.int/display/CKB/ERA5+data+documentation

Hentgen, L., Ban, N., Kröner, N., Leutwyler, D., & Schär, C. (2019). Clouds in Convection-

Resolving Climate Simulations Over Europe. *Journal of Geophysical Research: Atmospheres*, *124*(7), 3849–3870. https://doi.org/10.1029/2018JD030150

Holmes, C. R., Woollings, T., Hawkins, E., de Vries, H., Holmes, C. R., Woollings, T., … Vries, H. de. (2016). Robust Future Changes in Temperature Variability under Greenhouse Gas Forcing and the Relationship with Thermal Advection. *Journal of Climate*, *29*(6), 2221–2236. https://doi.org/10.1175/JCLI-D-14-00735.1

Hulley, G. C., & Ghent, D. (2019). *Taking the temperature of the Earth : steps towards integrated understanding of variability and change* (1st ed.). Elsevier.

Hurrell, J. W., Holland, M. M., Gent, P. R., Ghan, S., Kay, J. E., Kushner, P. J., … Marshall, S. (2013). The Community Earth System Model: A Framework for Collaborative Research. *Bulletin of the American Meteorological Society*, *94*(9), 1339–1360. https://doi.org/10.1175/BAMS-D-12-00121.1

IPCC, (2001) Climate Change 2001: The Scientific Basis. Contribution of Working Group I to the Third Assessment Report of the Intergovernmental Panel on Climate Change [Houghton, J.T., Y. Ding, D.J. Griggs, M. Noguer, P.J. van der Linden, X. Dai, K. Maskell, and C.A. Johnson (eds.)]. Cambridge University Press, Cambridge, United Kingdom and New York, NY, USA, 881pp

IPCC, (2013). Climate Change 2013: The Physical Science Basis. Contribution of Working Group I to the Fifth Assessment Report of the Intergovernmental Panel on Climate Change [Stocker, T.F., D. Qin, G.-K. Plattner, M. Tignor, S.K. Allen, J. Boschung, A. Nauels, Y. Xia, V. Bex and P.M. Midgley (eds.)]. Cambridge University Press, Cambridge, United Kingdom and New York, NY, USA, 1535 pp, doi:10.1017/CBO9781107415324.

Kay, J. E., Deser, C., Phillips, A., Mai, A., Hannay, C., Strand, G., … Vertenstein, M. (2015). The community earth system model (CESM) large ensemble project : A community resource for studying climate change in the presence of internal climate variability. *Bulletin of the American Meteorological Society*, *96*(8). https://doi.org/10.1175/BAMS-D-13-00255.1

Koenigk, T., Gao, Y., Gastineau, G., Keenlyside, N., Nakamura, T., Ogawa, F., … Yang, S. (2019). Impact of Arctic sea ice variations on winter temperature anomalies in northern hemispheric land areas. *Climate Dynamics*, *52*(5–6), 3111–3137. https://doi.org/10.1007/s00382-018-4305-

Kovats, R.S., R. Valentini, L.M. Bouwer, E. Georgopoulou, D. Jacob, E. Martin, M. Rounsevell, and J.-F. Soussana, (2014) Europe. In: Climate Change 2014: Impacts, Adaptation, and Vulnerability. Part B: Regional Aspects. Contribution of Working Group II to the Fifth Assessment Report of the Intergovernmental Panel on Climate Change [Barros, V.R., C.B. Field, D.J. Dokken, M.D. Mastrandrea, K.J. Mach, T.E. Bilir, M. Chatterjee, K.L. Ebi, Y.O. Estrada, R.C. Genova, B. Girma, E.S. Kissel, A.N. Levy, S. MacCracken, P.R. Mastrandrea, and L.L. White (eds.)]. Cambridge University Press, Cambridge, United Kingdom and New York, NY, USA, pp. 1267-1326

Lewis, S. C., & King, A. D. (2017). Evolution of mean, variance and extremes in 21st century temperatures. *Weather and Climate Extremes*, *15*. https://doi.org/10.1016/j.wace.2016.11.002

Liu, Z., & Wu, L. (2004). Atmospheric Response to North Pacific SST: The Role of Ocean-Atmosphere Coupling. *Journal of Climate*, *17*(9), 1859–1882. https://doi.org/10.1175/1520-0442(2004)017<1859:ARTNPS>2.0.CO;2

Lutgens, F. K., & Tarbuck, E. J. (2016). *The Atmosphere: An Introduction to Meteorology* (13th ed.). Pearson.

Mahony, C. R., & Cannon, A. J. (2018). Wetter summers can intensify departures from natural variability in a warming climate. *Nature Communications*, *9*(1), 783. https://doi.org/10.1038/s41467-018-03132-z

Masato, G., Woollings, T., & Hoskins, B. J. (2014). Structure and impact of atmospheric blocking over the Euro-Atlantic region in present-day and future simulations. *Geophysical Research Letters*, *41*(3), 1051–1058. https://doi.org/10.1002/2013GL058570

McGuffie, K., & Henderson-Sellers, A. (2005). *A Climate Modelling primer* (3rd ed.). https://doi.org/10.1017/CBO9781107415324.004

McKinnon, K. A., Poppick, A., Dunn-Sigouin, E., & Deser, C. (2017). An "Observational Large Ensemble" to Compare Observed and Modeled Temperature Trend Uncertainty due to Internal Variability. *Journal of Climate*, *30*(19), 7585–7598. https://doi.org/10.1175/JCLI-D-16-0905.1

Meredith, M., M. Sommerkorn, S. Cassotta, C. Derksen, A. Ekaykin, A. Hollowed, G. Kofinas, A. Mackintosh, J. Melbourne-Thomas, M.M.C. Muelbert, G. Ottersen, H. Pritchard, and E.A.G. Schuur, (2019). Polar Regions. In: IPCC Special Report on the Ocean and Cryosphere in a Changing Climate [H.-O. Pörtner, D.C. Roberts, V. Masson-Delmotte, P. Zhai, M. Tignor, E. Poloczanska, K. Mintenbeck, A. Alegría, M. Nicolai, A. Okem, J. Petzold, B. Rama, N.M. Weyer (eds.)]. In press.Mora, C., Frazier, A. G., Longman, R. J., Dacks, R. S., Walton, M. M., Tong, E. J., … Giambelluca, T. W. (2013). The projected timing of climate departure from recent variability. *Nature*, *502*(7470), 183–187. https://doi.org/10.1038/nature12540

Myhre, G., ForSter, P. M., Samset, B. H., Hodnebrog, Ø., Sillmann, J., Aalbergsjø, S. G., … ZwierS, F. (2016). *PDRMIP: A Precipitation Driver and Response Model Intercomparison Project—Protocol and Preliminary Results*. https://doi.org/10.1175/BAMS-D-16-0019.1

Nakamura, T., Yamazaki, K., Iwamoto, K., Honda, M., Miyoshi, Y., Ogawa, Y., & Ukita, J. (2015). A negative phase shift of the winter AO/NAO due to the recent Arctic sea-ice reduction in late autumn. *Journal of Geophysical Research*, *120*(8). https://doi.org/10.1002/2014JD022848

NSIDC: The Arctic Oscillation. (n.d.). Retrieved August 30, 2019, from https://nsidc.org/sites/nsidc.org/files/images//AO-schematic-wallace-1500px.jpg

Olonscheck, D., & Notz, D. (2017). Consistently Estimating Internal Climate Variability from Climate Model Simulations. *Journal of Climate*, *30*(23), 9555–9573. https://doi.org/10.1175/JCLI-D-16-0428.1

Overland, J. E., & Wang, M. (2010). Large-scale atmospheric circulation changes are associated with the recent loss of Arctic sea ice. *Tellus, Series A: Dynamic Meteorology and Oceanography*, *62*(1), 1–9. https://doi.org/10.1111/j.1600-0870.2009.00421.x

Petoukhov, V., & Semenov, V. A. (2010). A link between reduced Barents-Kara sea ice and cold winter extremes over northern continents. *Journal of Geophysical Research Atmospheres*, *115*(21). https://doi.org/10.1029/2009JD013568

Raible, C. C., & Blender, R. (2004). Northern Hemisphere midlatitude cyclone variability in GCM simulations with different ocean representations. *Climate Dynamics*, *22*(2). https://doi.org/10.1007/s00382-003-0380-y

Riahi, K., Rao, S., Krey, V., Cho, C., Chirkov, V., Fischer, G., … Rafaj, P. (2011). RCP 8.5—A scenario of comparatively high greenhouse gas emissions. *Climatic Change*, *109*(1–2), 33. https://doi.org/10.1007/s10584-011-0149-y

Rigor, I. G., Wallace, J. M., & Colony, R. L. (2002). Response of Sea Ice to the Arctic Oscillation. *Journal of Climate*, *15*(18), 2648–2663. https://doi.org/10.1175/1520-0442(2002)015<2648:ROSITT>2.0.CO;2

Rodwell, M. J., Drévillon, M., Frankignoul, C., Hurrell, J. W., Pohlmann, H., Stendel, M., & Sutton, R. T. (2004). North Atlantic forcing of climate and its uncertainty from a multi-model experiment. *Quarterly Journal of the Royal Meteorological Society*, *130*(601), 2013–2032. https://doi.org/10.1256/qj.03.207

Rondeau-Genesse, G., & Braun, M. (2019). Impact of internal variability on climate change for the upcoming decades: analysis of the CanESM2-LE and CESM-LE large ensembles. *Climatic Change*, 1–16. https://doi.org/10.1007/s10584-019-02550-2

Samset, B. H., Stjern, C. W., Lund, M. T., Mohr, C. W., Sand, M., & Daloz, A. S. (2019). How daily temperature and precipitation distributions evolve with global surface temperature. *Earth's Future*. https://doi.org/10.1029/2019EF001160

Serreze, M. C., & Barry, R. G. (2011). Processes and impacts of Arctic amplification: A research synthesis. *Global and Planetary Change*, *77*(1–2), 85–96. https://doi.org/10.1016/J.GLOPLACHA.2011.03.004

Sillmann, J., Thorarinsdottir, T., Keenlyside, N., Schaller, N., Alexander, L. V., Hegerl, G., … Zwiers, F. W. (2017). Understanding, modeling and predicting weather and climate extremes: Challenges and opportunities. *Weather and Climate Extremes*, *18*, 65–74. https://doi.org/10.1016/J.WACE.2017.10.003

Stroeve, J., Holland, M. M., Meier, W., Scambos, T., & Serreze, M. (2007). Arctic sea ice decline: Faster than forecast. *Geophysical Research Letters*, *34*(9). https://doi.org/10.1029/2007GL029703

Suarez-Gutierrez, L., Li, C., Müller, W. A., & Marotzke, J. (2018). Internal variability in European summer temperatures at 1.5 °c and 2 °c of global warming. *Environmental Research Letters*, *13*(6). https://doi.org/10.1088/1748-9326/aaba58

Sutton, R., & Mathieu, P.-P. (2002). Response of the atmosphere–ocean mixed-layer system to anomalous ocean heat-flux convergence. *Quarterly Journal of the Royal Meteorological Society*, *128*(582), 1259–1275. https://doi.org/10.1256/003590002320373283

Taylor, K. E., Stouffer, R. J., & Meehl, G. A. (2009). *A Summary of the CMIP5 Experiment Design*. Retrieved from https://pcmdi.llnl.gov/mips/cmip5/docs/Taylor_CMIP5_design.pdf?id=14

Trouet, V., Babst, F., & Meko, M. (2018). Recent enhanced high-summer North Atlantic Jet variability emerges from three-century context. *Nature Communications*, *9*(1), 180. https://doi.org/10.1038/s41467-017-02699-3

Vogel, M. M., Zscheischler, J., & Seneviratne, S. I. (2018). Varying soil moisture-atmosphere feedbacks explain divergent temperature extremes and precipitation projections in central Europe. *Earth Syst. Dynam*, *9*, 1107–1125. https://doi.org/10.5194/esd-9-1107-2018

Wilcox, L. J., Dunstone, N., Lewinschal, A., Bollasina, M., Ekman, A. M. L., & Highwood, E. J.

(2019). Mechanisms for a remote response to Asian anthropogenic aerosol in boreal winter. *Atmospheric Chemistry and Physics*, *19*(14), 9081–9095. https://doi.org/10.5194/acp-19-9081-2019

Williams, P. D., Alexander, M. J., Barnes, E. A., Butler, A. H., Davies, H. C., Garfinkel, C. I., … Zhang, C. (2017). A Census of Atmospheric Variability From Seconds to Decades. *Geophysical Research Letters*, *44*(21), 11,201-11,211. https://doi.org/10.1002/2017GL075483

Wills, R. C., Schneider, T., Wallace, J. M., Battisti, D. S., & Hartmann, D. L. (2018). Disentangling Global Warming, Multidecadal Variability, and El Niño in Pacific Temperatures. *Geophysical Research Letters*, *45*(5), 2487–2496. https://doi.org/10.1002/2017GL076327

Xie, S.-P., Deser, C., Vecchi, G. A., Collins, M., Delworth, T. L., Hall, A., … Watanabe, M. (2015). Towards predictive understanding of regional climate change. *Nature Climate Change*, *5*(10), 921–930. https://doi.org/10.1038/nclimate2689

Årthun, M., Eldevik, T., Viste, E., Drange, H., Furevik, T., Johnson, H. L., & Keenlyside, N. S. (2017). Skillful prediction of northern climate provided by the ocean. *Nature Communications*, *8*(1). https://doi.org/10.1038/ncomms15875

Appendix A

A.1 September daily temperatures and September Sea Ice (5-95%)

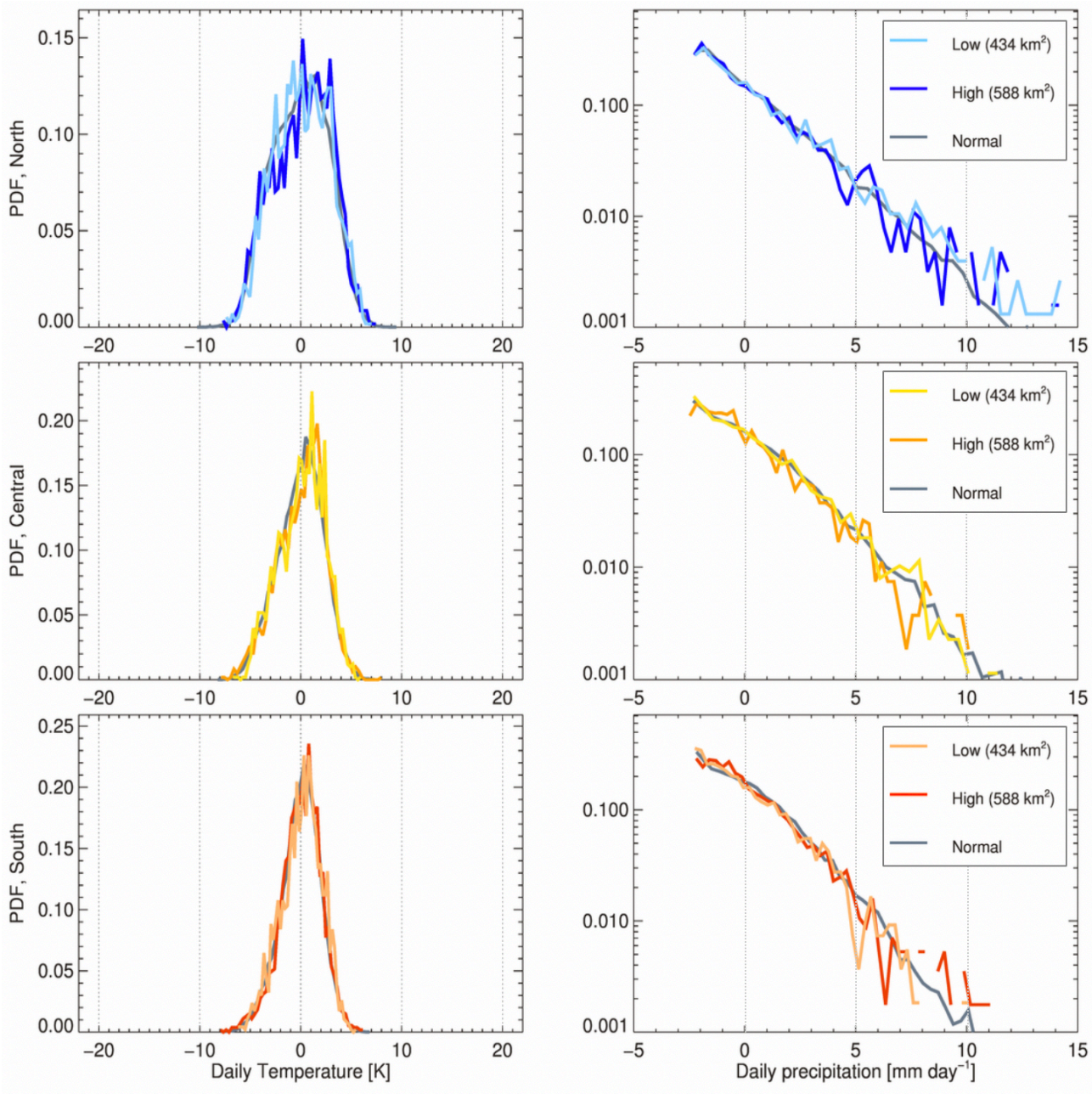

A.2 March Daily Temperatures and March Sea Ice (5-95%)

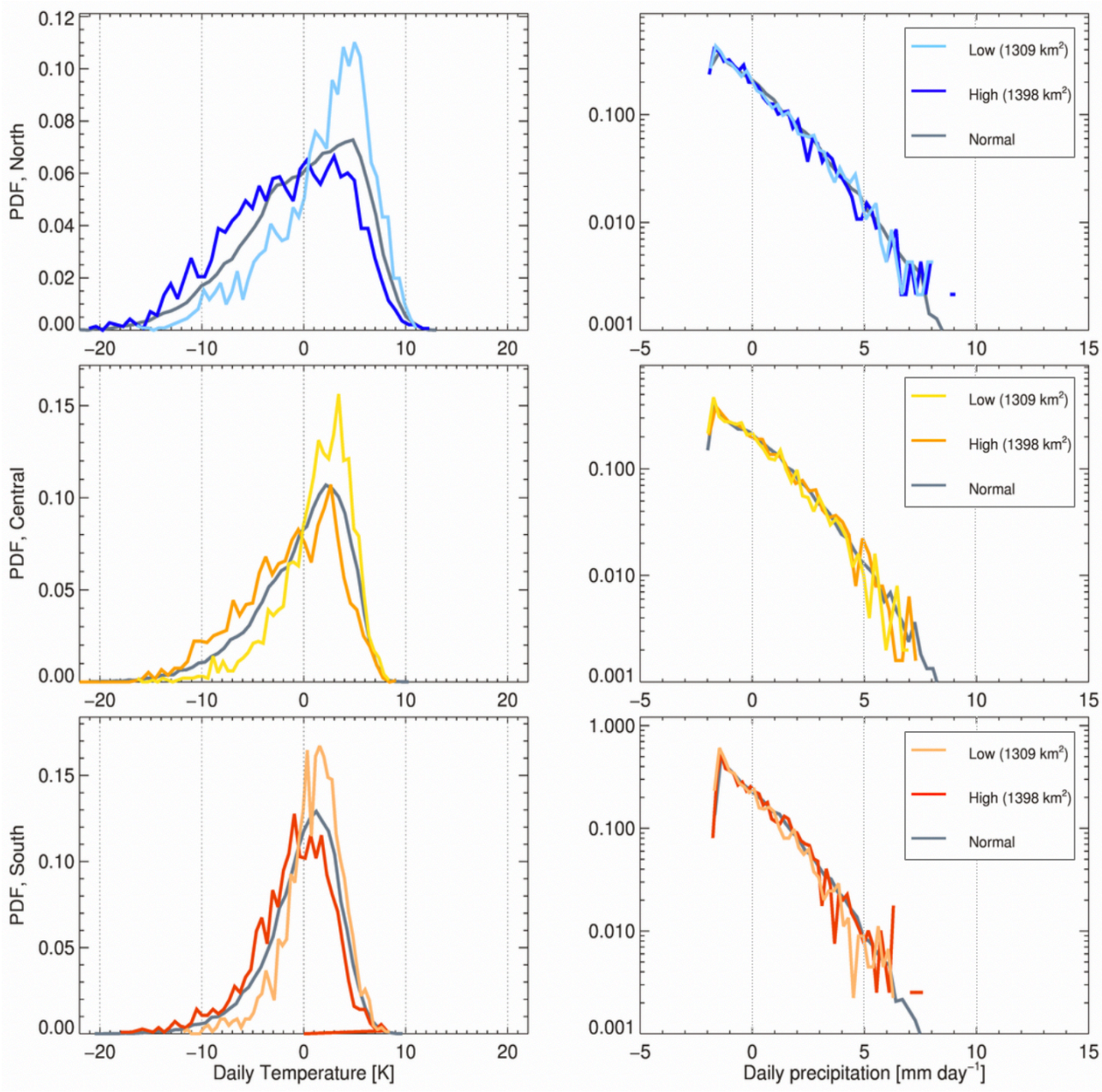

A.3 Temperatures for Northern Scandinavia (all months) and March Sea Ice (5-95%)

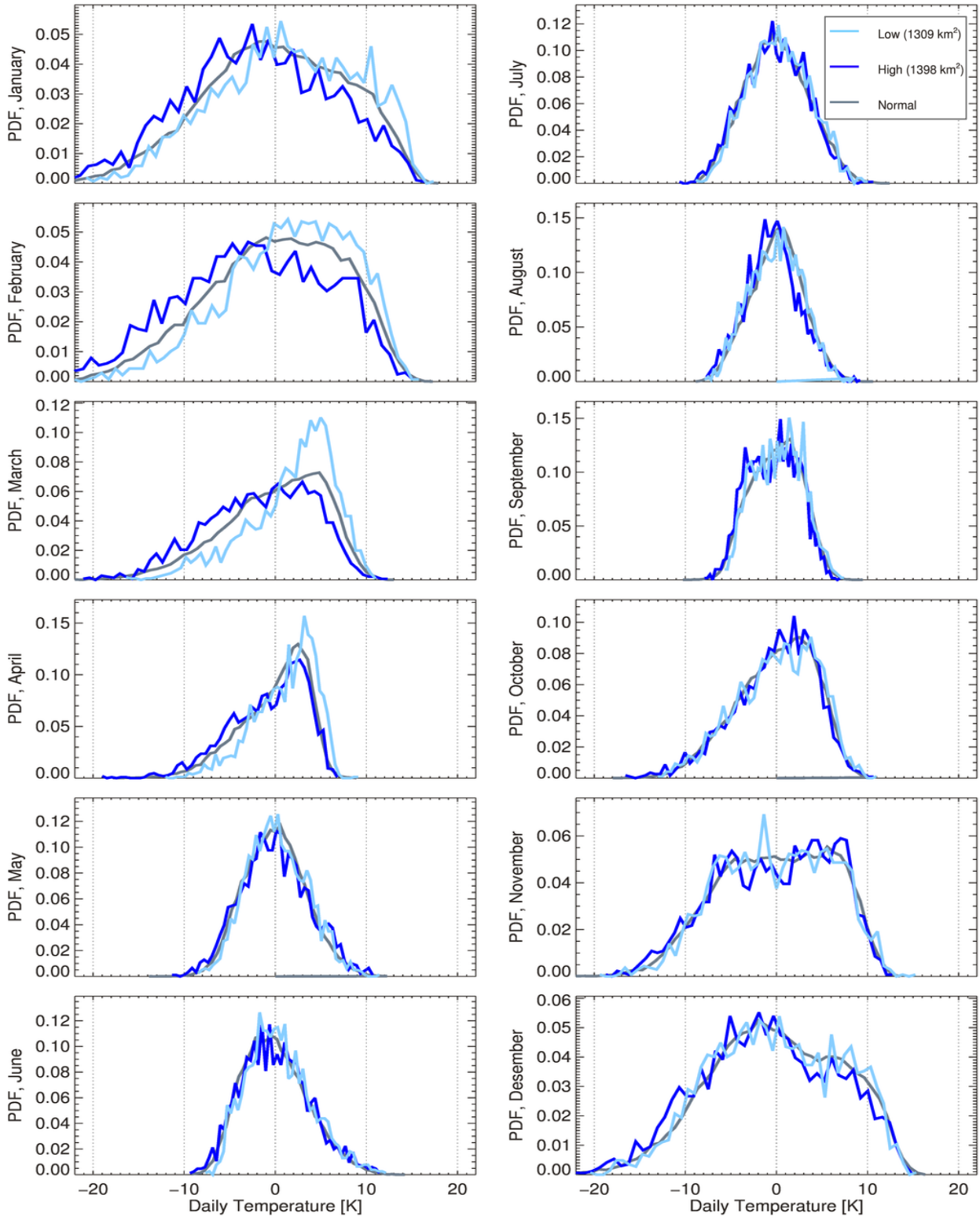

A.4 Temperatures for Northern Scandinavia (all months) and March Sea Ice (1std)

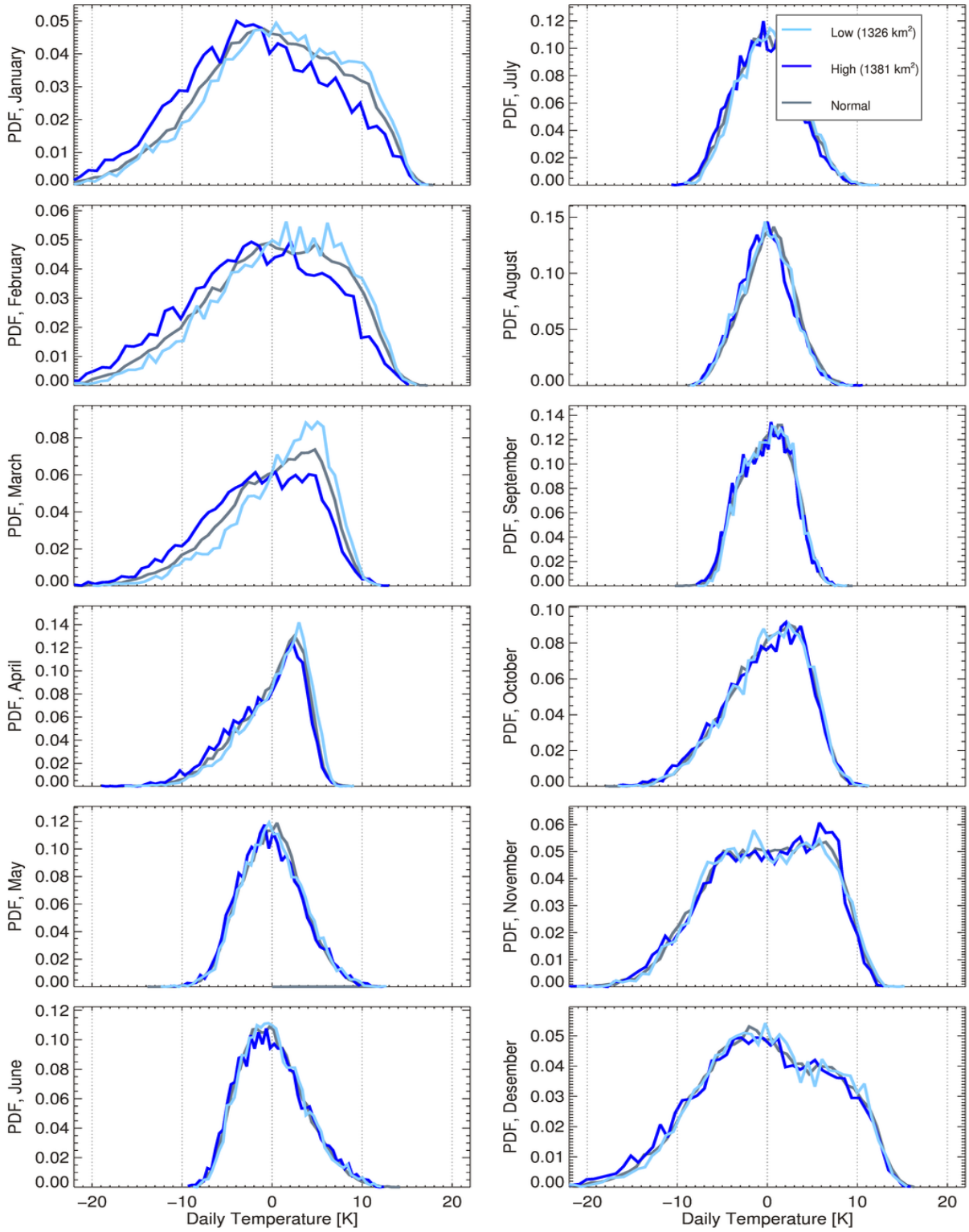

A.5 Temperatures for Central Scandinavia (all months) and March Sea Ice (5-95%)

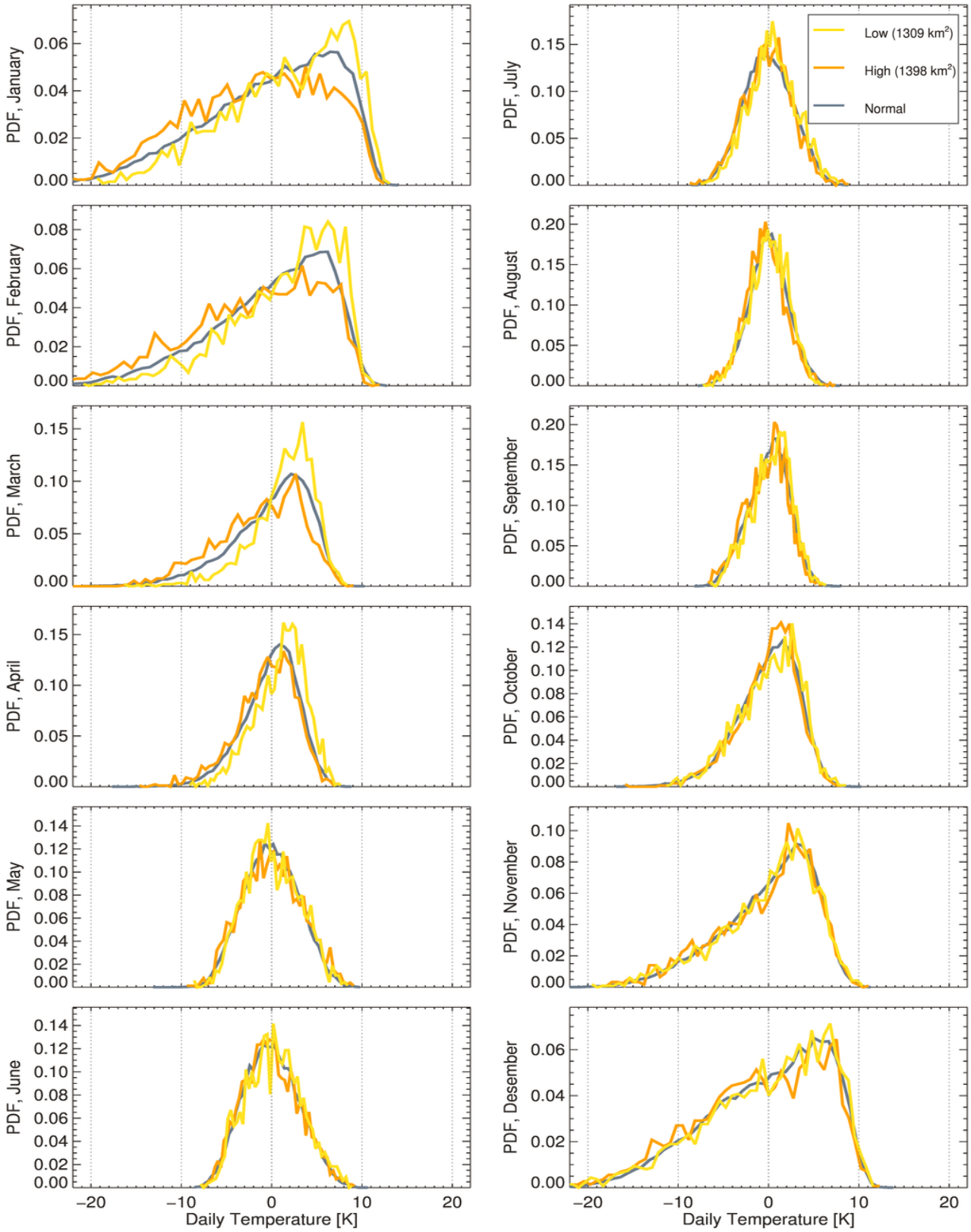

A.6 Temperatures for Central Scandinavia (all months) and March Sea Ice (1std)

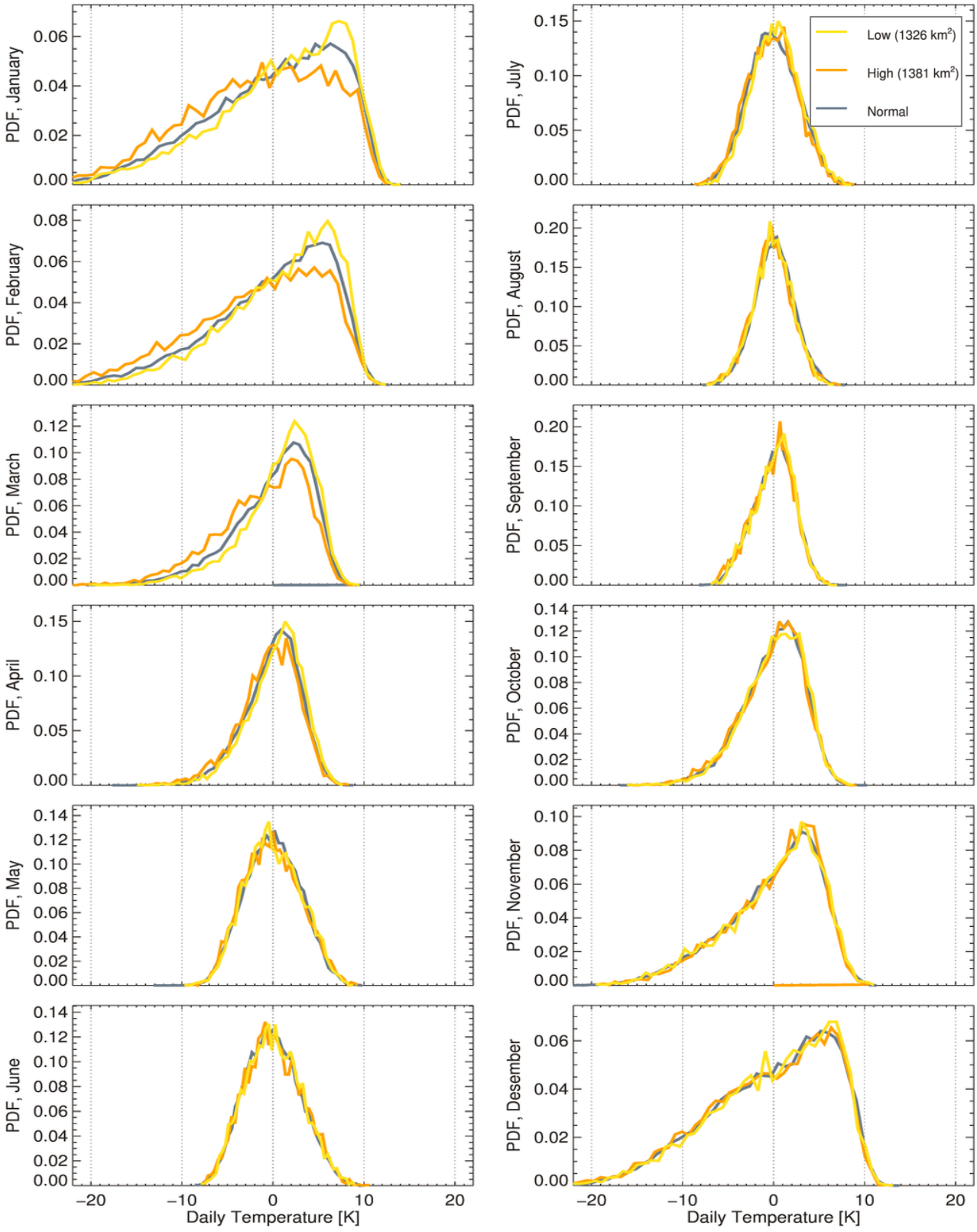

A.7 Temperatures for Southern Scandinavia (all months) and March Sea Ice (5-95%)

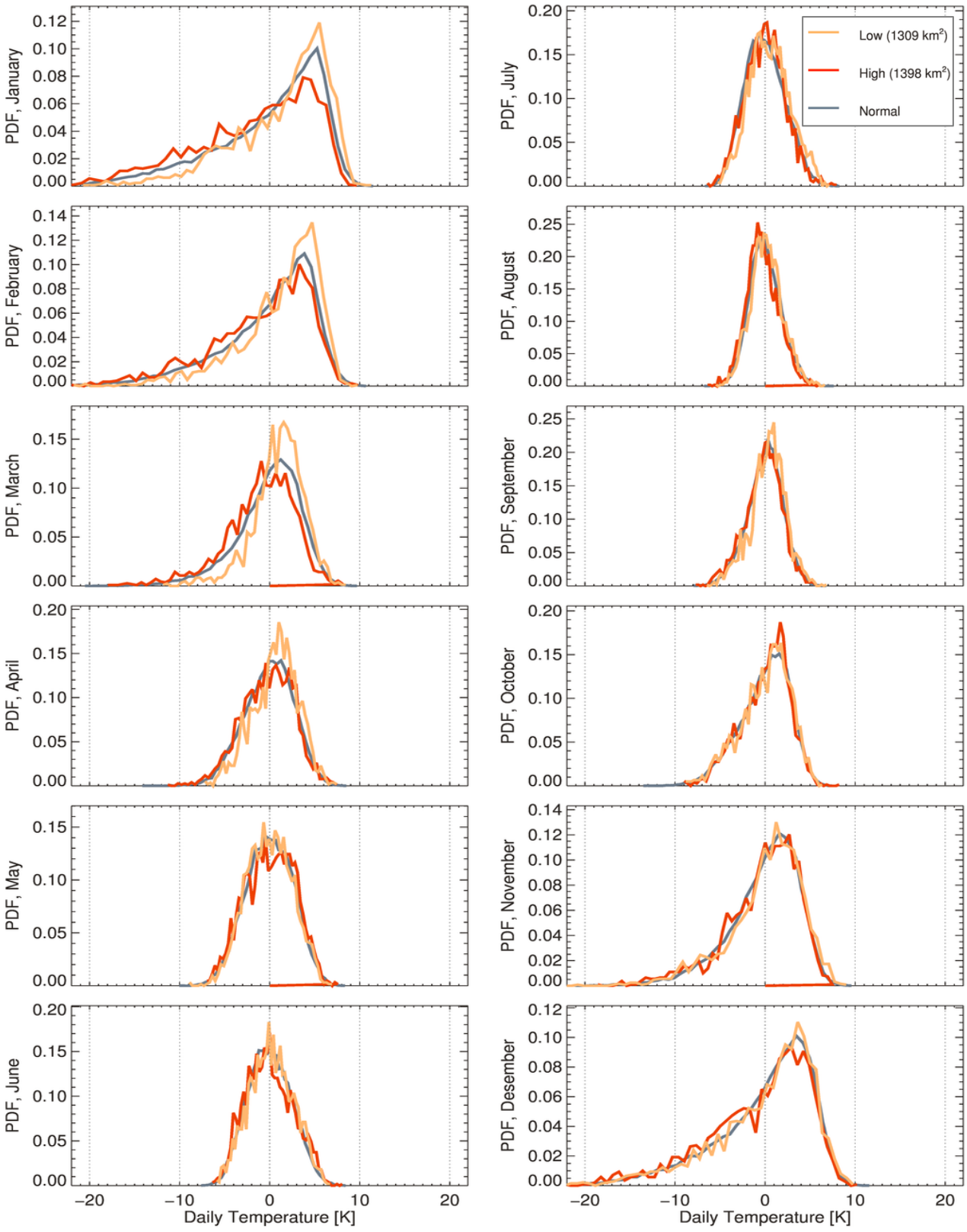

A.8 Temperatures for Southern Scandinavia (all months) and March Sea Ice (1std)

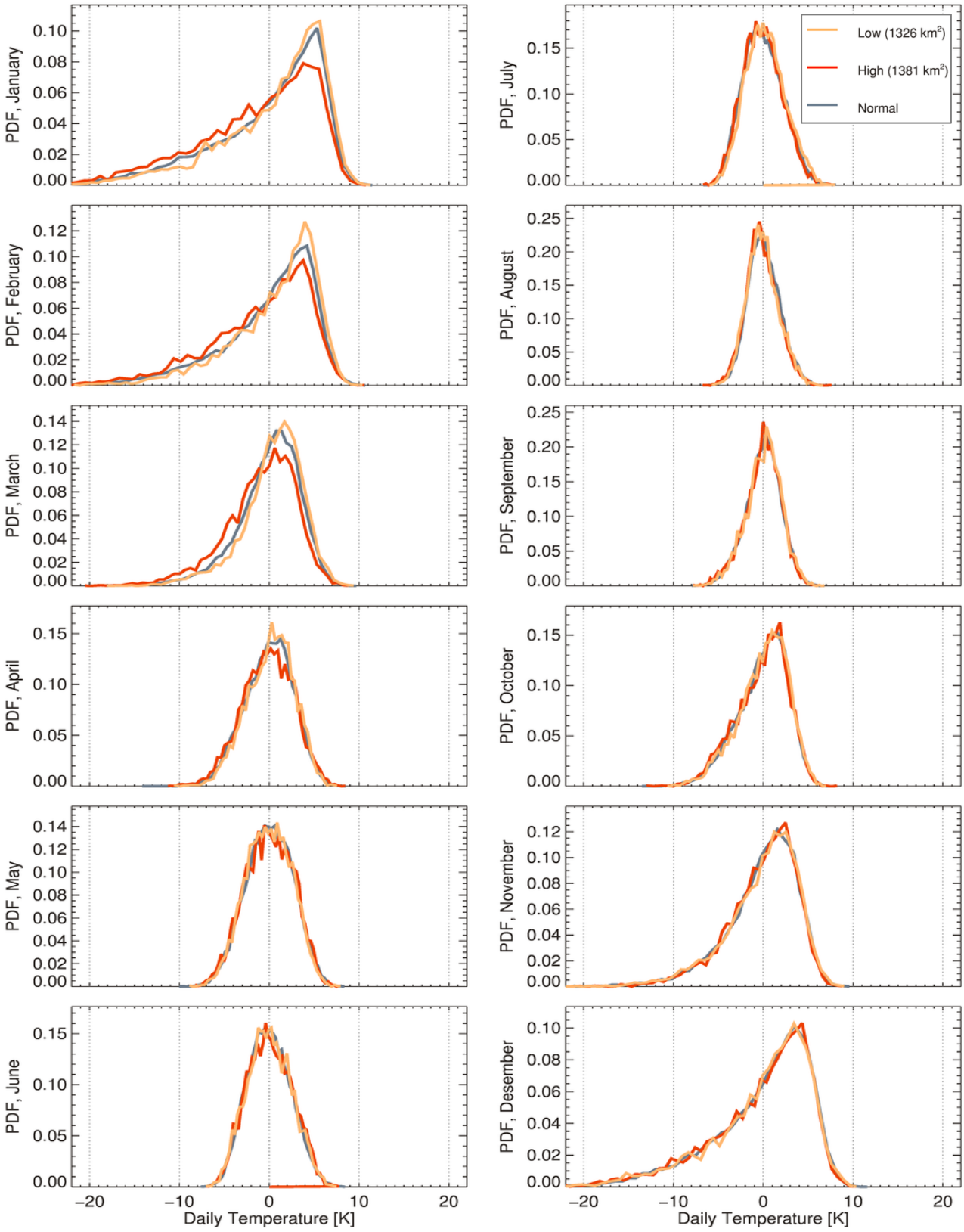

A.9 Temperatures for Northern Scandinavia (all months) and September Sea Ice (5-95%)

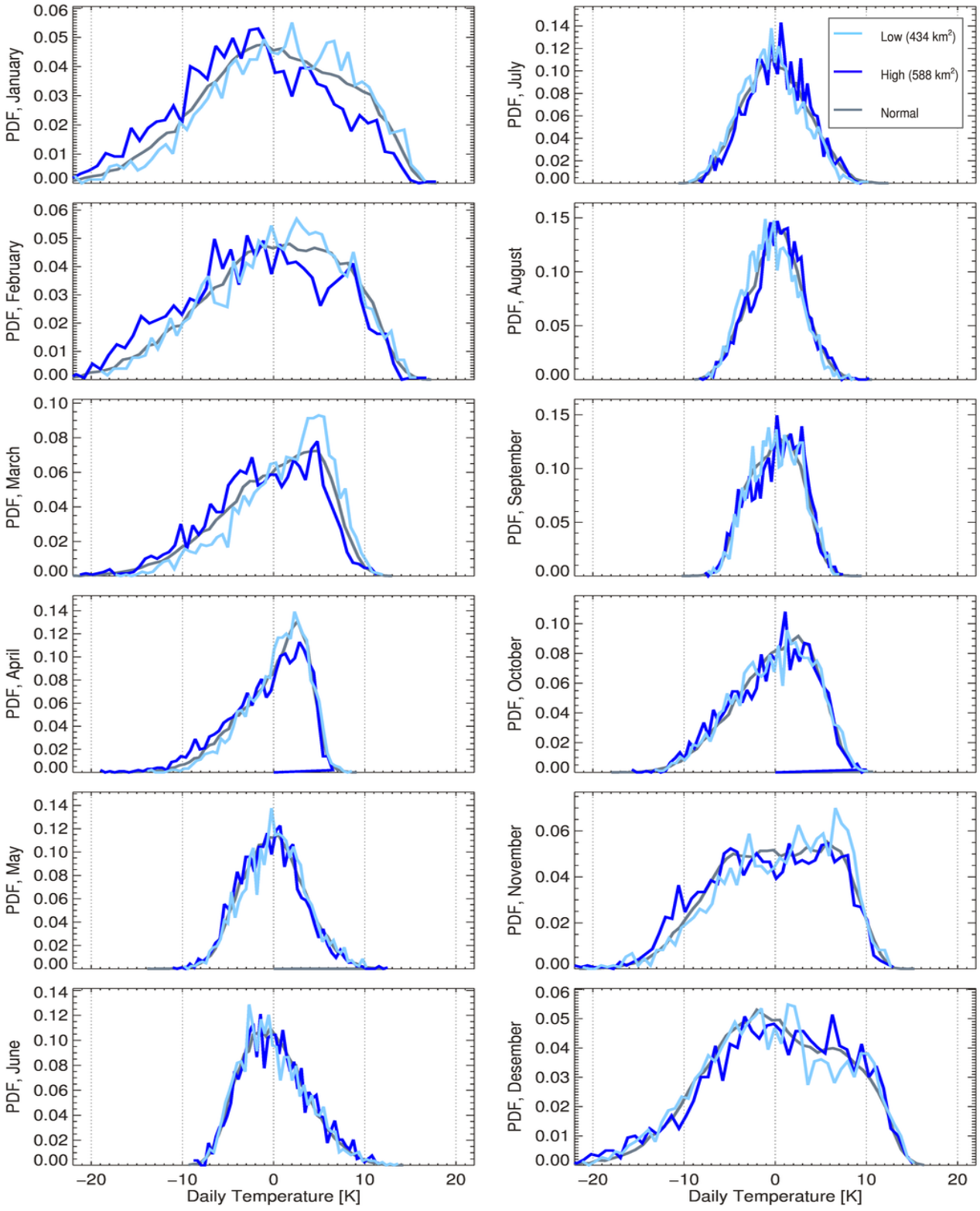

A.10 Temperatures for Northern Scandinavia (all months) and September Sea Ice (1std)

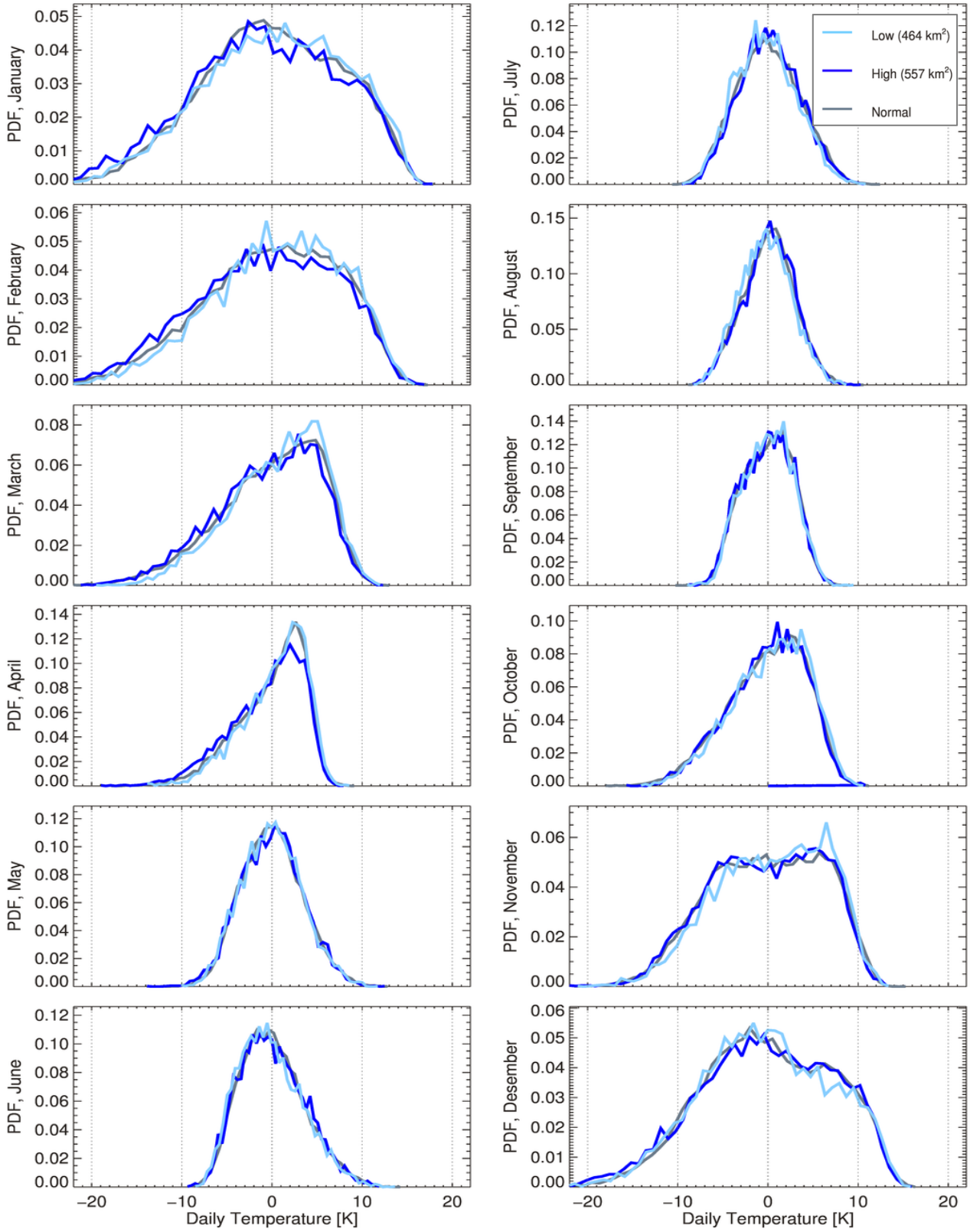

A.11 Temperatures for Central Scandinavia (all months) and September Sea Ice (5-95%)

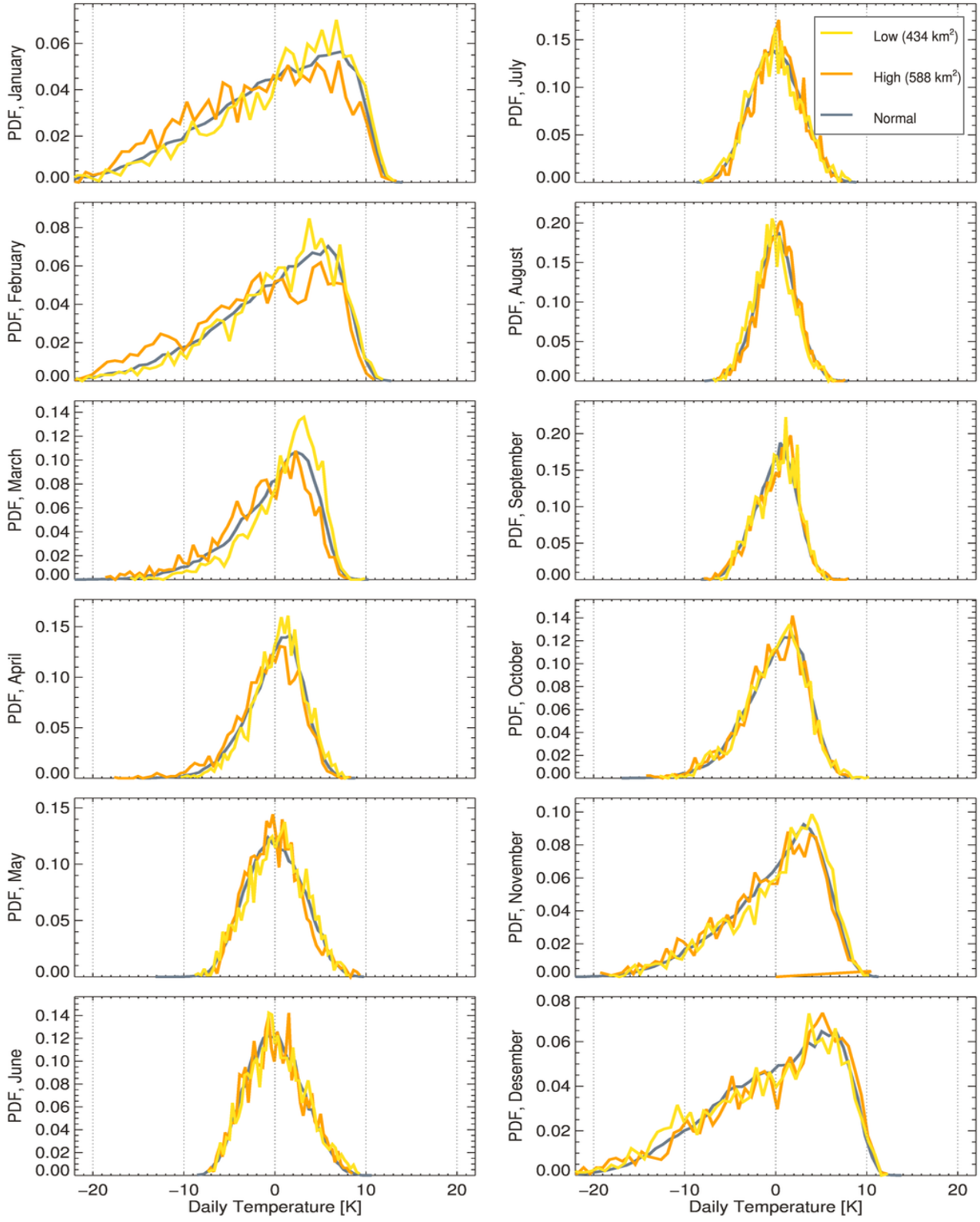

A.12 Temperatures for Central Scandinavia (all months) and September Sea Ice (1std)

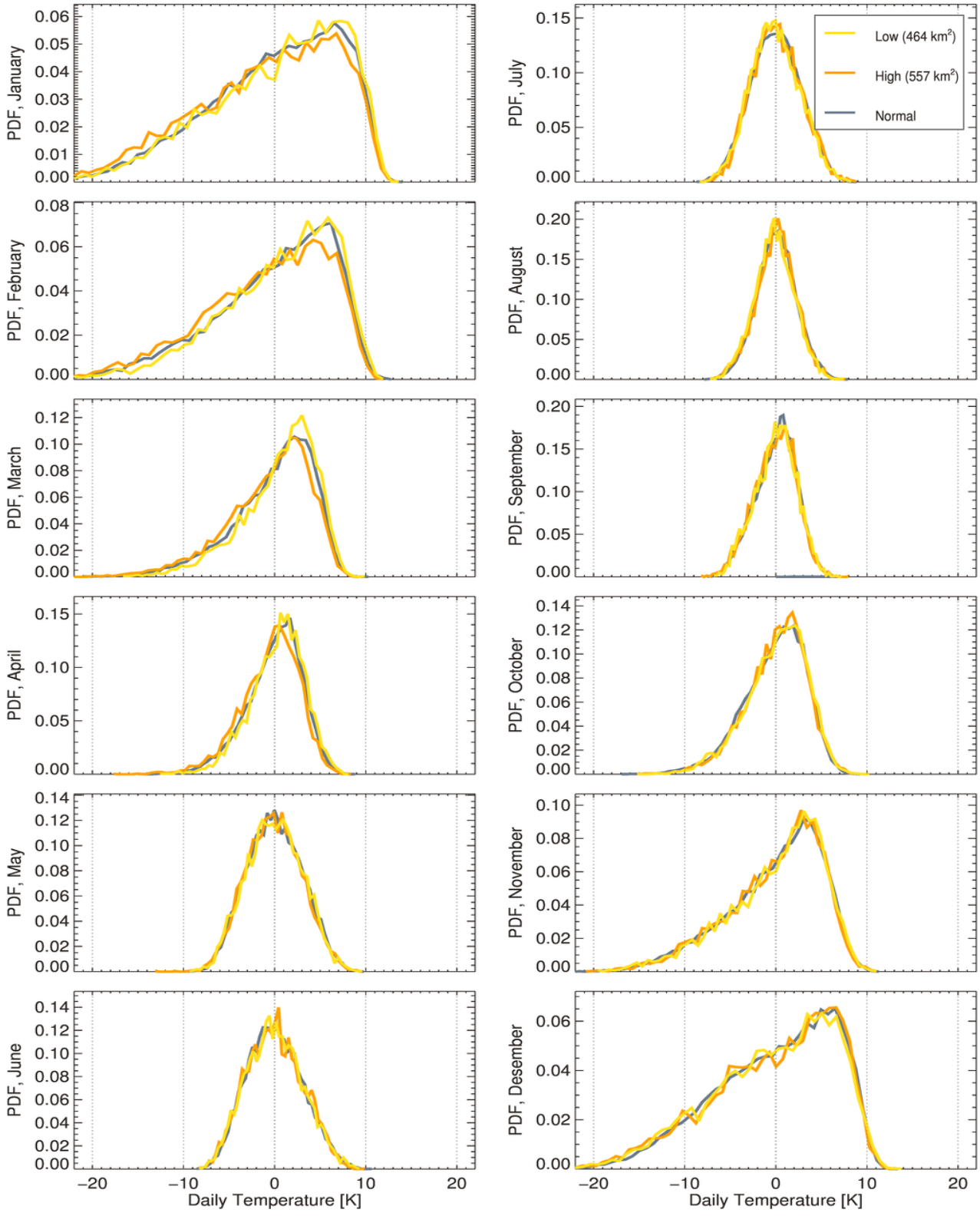

A.13 Temperatures for Southern Scandinavia (all months) and September Sea Ice (5-95%)

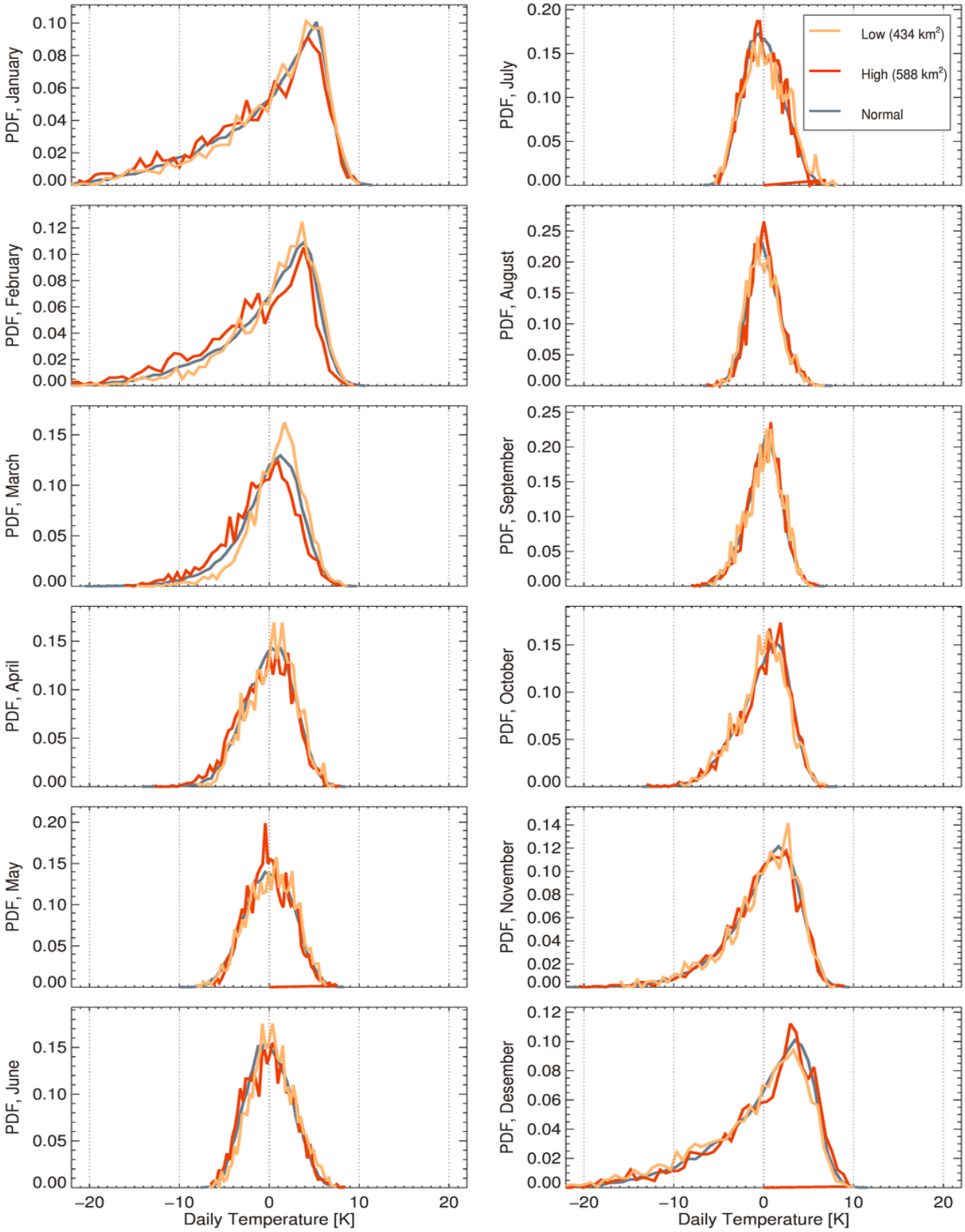

A.14 Temperatures for Southern Scandinavia (all months) and September Sea Ice (1std)

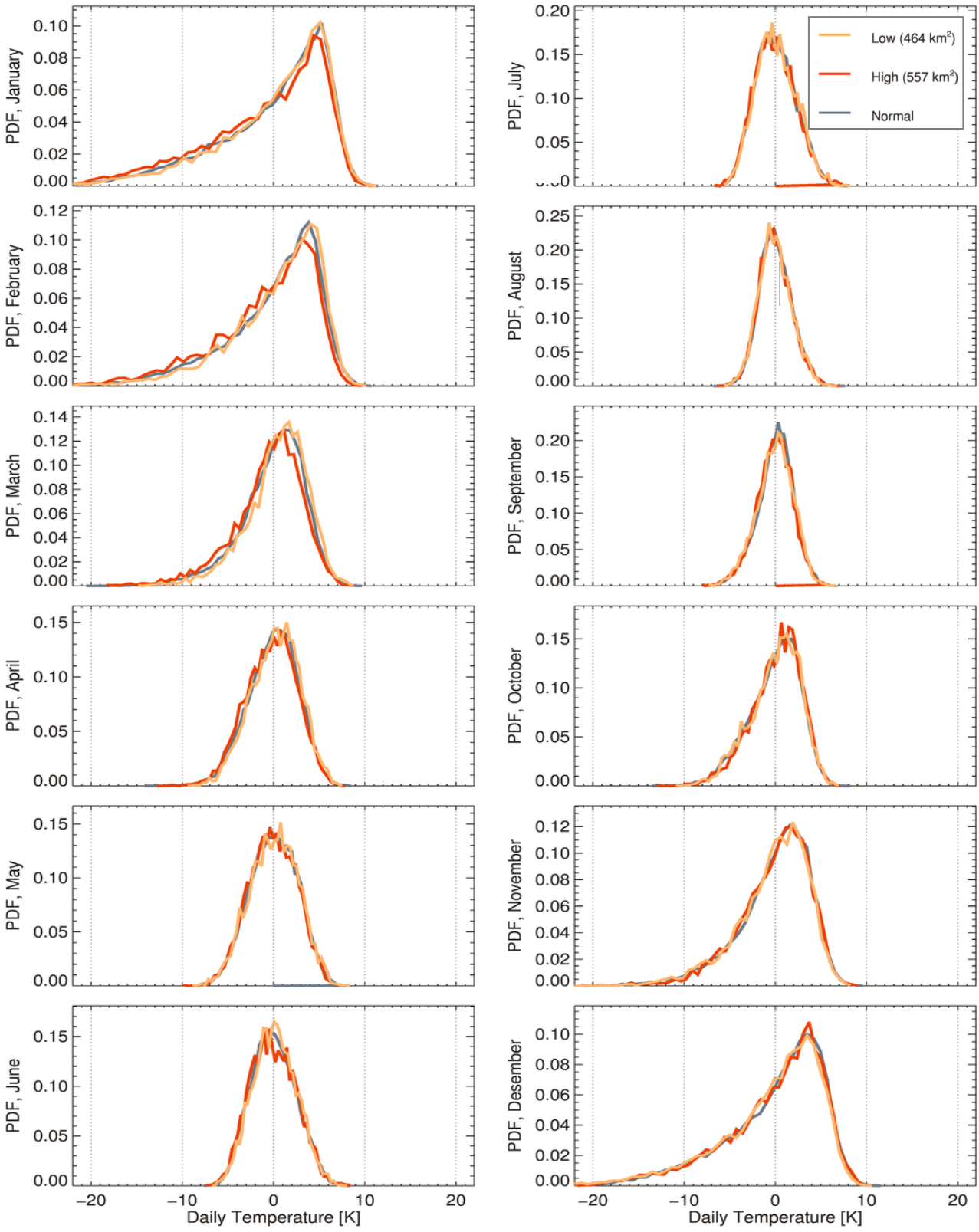

Norges miljø- og biovitenskapelige universitet
Noregs miljø- og biovitskapelege universitet
Norwegian University of Life Sciences

Postboks 5003
NO-1432 Ås
Norway